INNOVATIVE TOOL FOR OPTIMIZING HOLE CLEANING EFFICIENCY IN DEVIATED AND EXTENDED REACH WELLS

A Dissertation

by

MOHAMED SHAFIK ABD ELALIM KHALED

Submitted to the Graduate and Professional School of
Texas A&M University
in partial fulfillment of the requirements for the degree of

DOCTOR OF PHILOSOPHY

Chair of Committee,	A. Rashid Hasan
Co-Chair of Committee,	Mohammad Rahman
Committee Members,	Samuel F. Noynaert
	M. M. Farque Hasan
Head of Department,	Jeff Spath

August 2021

Major Subject: Petroleum Engineering

ABSTRACT

Poor cuttings transport in deviated wells is considered a main factor limiting drill rate; inducing excessive torque and drag; or in severe cases, resulting in stuck pipes. This study presents a computational fluid dynamics (CFD) model for investigating cuttings transport phenomena in deviated wells under different conditions. Moreover, data-driven models utilizing statistical techniques were developed for optimizing hole cleaning efficiency in deviated and extended reach well.

A CFD model was developed and validated with our experiments conducted in the TAMUQ horizontal flow loop and open literature to study the impact of Herschel Bulkley fluids on cuttings transport at various drilling conditions. The Eulerian-Eulerian approach is used to simulate solid-liquid laminar flow in annular geometry utilizing hexahedral and polyhedral mesh under transient conditions. Finally, the developed data-driven models' utilized dimensionless parameters to estimate cuttings concentration and stationary bed height in deviated wells.

Results show that the developed CFD model is a robust tool for evaluating hole cleaning efficiency during the drilling planning phase, while the developed data-driven models are reliable tools for real-time hole cleaning optimization. It is advisable to use drilling motors with less bend angle and a shorter bit to bend distance for efficient cuttings transport in lateral sections. The best approach to cleanout horizontal wells flowing under a turbulent flow regime is to keep n⁄K value high and for the laminar flow to increase YP/PV ratio. The most critical range for efficient hole cleaning in straight

and spiral holes is from 0-200 RPM and increasing RPM above 200 will have a marginal impact on improving hole cleaning. Cuttings size of 0.004 m for straight holes and 0.006-0.008 m for spiral profiles was determined to be the critical particle size for solid particle removal. Finally, the developed data-driven models show good accuracy in estimating cuttings concentration and bed height ratio with a ±20% error margin in most cases. These models prove to be robust tools for simulating cuttings transport in real-time, monitoring cuttings accumulation, improving drilling efficiency, and avoiding Non-Productive Time (NPT) related to hole cleaning issues in deviated and horizontal wells.

DEDICATION

This work is dedicated only and foremost to God Almighty. I would like to praise and thank God, the almighty, who has granted countless blessings, knowledge, and opportunity to the author. It was with God's help that I was able to finish my work and get to where I am today.

ACKNOWLEDGEMENTS

I owe so much to my mother Faten and father Shafik for their love, care and encouragement, and my wife Sarah for her patience, support and love during this long journey. The continuous support, scarifies, and love I received from all my family members were tremendous and I am grateful to them.

I would like to express my gratitude and appreciation to my advisor/mentor Dr. A.Rashid Hasan, a unique professor for allowing me to work in his research group, his guidance, and patience contributed much to the success of this thesis.

A very special thanks to Dr. Muhammad Azizur Rahman for his guidance, help, and allocating resources during the work. I would like also to thank my committee members Dr. Sam Noynaert and Dr. Farque Hasan for their valuable suggestions to improve research quality.

A special thanks to our research group in Qatar, Dr. Muhammad Sami from ANSYS Inc., and Prof. Fred Dupriest for their help and suggestion to improve the quality of my research.

Thanks also go to my friends, colleagues, and the department faculty and staff for making my time at Texas A&M University a great experience.

Finally, thanks to everyone (I did not mention his name) who helped me to accomplish this work

CONTRIBUTORS AND FUNDING SOURCES

Contributors

This work was supervised by a dissertation committee consisting of Professor A.Rahsid Hasan [advisor], Professor Muhammad Azizur Rahman (co-advisor) and prof. Samuel Noynaert of the Department of Petroleum Engineering, and Professor Faraque Hasan of the Department of Chemical Engineering.

The data analyzed from the Texas A&M University at Qatar (TAMUQ) flow loop for Chapter 3 was provided by Dr. Saad Khan and Abinash Barooh.

Funding Sources

Graduate study was supported by the grant NPRP10-0101-170091 from Qatar National Research Fund (a member of the Qatar Foundation.

NOMENCLATURE

Nomenclature

A_{hole}	Area of hole or casing (m^2)
A_{pipe}	Area of inner pipe (m^2)
BHA	Bottom hole assembly
BUR	Wellbore build up rates
C	Cuttings feed concentration (%)
CVF	Cuttings concentration (solid average volume fraction)
C_l	Lift coefficient
D_{hole}	Hole inside diameter (m)
D_{pipe}	Drillpipe outside diameter (m)
D_h	Hole hydraulic parameters (m)
Dc	Cuttings diameter (m)
DLS	Wellbore dogleg severity (degree/m)
E	Hole eccentricity
e	Distance between outer and inner pipe (m)
$\vec{F}_q$	External body force (N)
$\vec{F}_{lift,q}$	Lift force (N)
$\vec{F}_{vm,q}$	Virtual mass force (N)
k	Wellbore curvature
LWD	Logging while drilling (N)

MWD	Measurement while drilling (N)
MD	Measured depth (m)
$\dot{m}_{pq}$	Mass transfer between phases
r	Radius of spiral (m)
RANS	Reynold averaged Navier-Stokes simulation
RSM	Reynold stress model
RSS	Rotary steerable system
Re	Reynold number
N	Total number of phases
P	Pressure shared by all phases (Pa)
p	Spiral pitch length (m)
P_s	Solid pressure, consists of the kinetic term and the term due to particle collisions (Pa)
RPM	Revolution per minute
ROP	Rate of penetration (m/sec)
Vcut	Cuttings velocity (m/sec)
y	Distance from wall to the cell center (m)

Greek Letters

φ	Wellbore inclination (degree)
ϑ	Wellbore azimuth (degree)
γ	Shear rate (sec^{-1})

η	Flow behavior index
α_q	Phase volume fraction
$\bar{\bar{\tau}}_q$	Qth stress-strain tensor
ν	Liquid velocity (m/sec)
ω	Drillstring rotation (sec^{-1})
Φ	Rock porosity
$\dot{m}_{pq}$	Mass transfer between phases
v_q	Phase q velocity (m/sec)
λ_q	Bulk viscosity of phase q (Pa.sec)
μ_q	Shear viscosity of phase q (Pa.sec)
ρ	Density (Kg/m^3)
ρl	Liquid density (Kg/m^3)
ρc	Cuttings density (Kg/m^3)
μ	Dynamic viscosity (Pa.sec)
η_l	Reference viscosity for power law fluids (Pa.sec)
μ_q	Shear viscosity of phase q (Pa.sec)
k	Consistency index (Pa.sec)
K	Turbulent kinetic energy (kg/m^1sec^3)
K_{pq}	Interphase momentum exchange coefficient (-)
K_{ls}	Momentum exchange coefficient between liquid & solid phase (-)
K_{sl}	Momentum exchange coefficient between solid & liquid phase (-)

ε	Turbulent dissipation energy ($kg/m^1.sec^3$)
v_{pq}	Interphase velocity (m/s)

TABLE OF CONTENTS

Page

LIST OF FIGURES

Page

LIST OF TABLES

Page

CHAPTER I

INTRODUCTION

Drilling fluids are used to circulate rock fragments (cuttings) to the surface. The operational effect of poor cuttings transport is to limit drill rate, or in severe cases to resulting in a stuck pipe. The flow rates and fluid properties normally used by industry in a given hole size allow for relatively high drill rates with very little risk or restriction. When these do occur, the root cause is usually hole enlargement due to inadequate fluid density for hole stability. The fluid velocity falls in the enlarged section and cuttings concentrate. Reduced drill rate or stuck pipe may also occur if conditions, such as lost returns, do not allow normal flow or fluid properties. If borehole enlargement or lost returns occur, the drill team will continue to attempt to compensate by adjusting flow rate, fluid properties, or operational practices. It is in these situations where the potential effect of different operational, hydrodynamic and geometric conditions need to be understood. This study presents a computational fluid dynamics (CFD) model validated with our experimental data and literature to investigate cuttings transport phenomena with Herschel Bulkley drilling fluids in deviated wells under different conditions. Moreover, data-driven models based on dimensionless parameters were developed to shift results from lab scale to field-scale applications.

Different experimental and numerical studies had been conducted to investigate various parameters affecting cuttings transport phenomena while drilling. Iyoho (1980), and Tomren et al. (1986) conducted their experiments on 12.2 m long flow loop to

investigate different parameters that can impact cuttings transport in wellbore. They concluded that hole inclination and fluid circulation are the main parameters that could enhance or aggravate cuttings accumulations. Further experimental work was done to study the effect of mud rheology and fluid type on improving cuttings circulations on deviated wells (Okrajni and Azar, 1986; Prioozian et al., 2012; Ford et al., 1990; Rasul et al., 2020; Terry et al., 1996). Moreover, Ozbayoglu et al. (2008), and Sorgun (2010) showed that drillpipe rotation improves hole cleaning and decreases the critical velocity required to remove the stationary bed at high angle wells (>60 degrees). The impact of drillpipe eccentricity and hole inclination on cuttings transport was studied by Peden et al. (1990). Although many experimental and numerical studies were carried out to investigate the effect of changing operating, hydrodynamic and geometric conditions on cuttings transport in deviated and horizontal wells, very limited researches were published to study the fundamentals of cuttings transport utilizing Herschel Bulkley fluids at different conditions Up to this date, there is an unresolved question regarding the selection of the favorable fluid rheology while drilling and how one can evaluate the quality of mud rheology. Moreover, the question of wellbore tortuosity impact cutting transport arises does the flow pattern created by spiral geometry reduce or increase the concentration of cuttings in a given foot of hole, and what is the magnitude of this effect relative to other design or operating factors. In addition, there is no standard tool available for the industry to optimize and evaluate hole cleaning efficiency in deviated and extended reach wells in real-time or during the planning phase. Because established

correlations and mechanistic models are extremely limited to their experimental data range and setup, the models can not be applied to all drilling situations

This research aims:

1- To contribute to the understanding of the drill cuttings transport under various forces such as drag force, centrifugal force, and lift force by developing a computational fluid dynamics (CFD) model validated by our experiments conducted in Texas A&M (TAMU) Tower Lab and Texas A&M at Qatar (TAMUQ) horizontal flow loop.

2- To provide some insight into the dynamics of solid-liquid flows in inclined wellbores by Herschel Bulkley drilling fluids at different ranges of operating conditions (flow rate, penetration rate, drillstring rotation, and eccentricity), wellbore configuration (Hole size, wellbore inclination, pipe size, and wellbore tortuosity), fluid parameters (density, and rheology) and cuttings parameters (cuttings density, size, and shape).

3- There are many design choices the engineer can make, as well as operational practices, that may reduce the amplitude of spiraling, but awareness is low and practices vary greatly. So the study of how spiraling tortuosity affects cuttings transport it relevant to a great deal of industry footage today. The results may help inspire engineers to cost-justify more of the changes needed to reduce the period length and amplitudes, and operations to change more practices to manage them in real-time.

4- To present a reliable model/tool for optimizing hole cleaning efficiency in deviated and horizontal wells and minimizing cuttings deposition in real-time during drilling daily operations.

C**hapter II** serves as a detailed literature review about cuttings (solid) transport in oil wells and computational fluids dynamics (CFD) modeling of solid-liquid interactions. In addition, the impact of fluid rheology and wellbore spiral tortuosity on cuttings removal; and hole cleaning evaluation models are also discussed as well. In **chapter III,** the CFD mathematical model, boundary conditions, and mesh setup are described. Moreover, the CFD model validation with our experiments conducted in TAMUQ Horizontal Flow loop and open literature experimental data. **Chapter IV** demonstrates the impact of drilling flow rate, hole enlargement, fluid rheology, drillstring rotation, drilling rate of penetration, annular eccentricity, wellbore inclination, cuttings size, cuttings density, and wellbore tortuosity on cuttings accumulation and annular pressure loss for optimum hole cleaning. **Chapter V** proposes data-driven models (regression) to estimate cuttings accumulation and bed height thickness applicable to wide ranges of drilling conditions by utilizing dimensionless parameters to shift model results from lab scale to field-scale application. Finally, **Chapter VI** highlights the main outcomes and summary from this research and presents the author's recommendation for future work.

CHAPTER II

LITERATURE REVIEW

Drilling fluids (drilling mud) are used in rotary drilling to control wellbore formation pressure, remove cutting outside the annulus, cool and lubricate the bit and maintain wellbore stability. Cuttings transport is the process of circulating rock fragments cut by the bit from bottomhole through the annulus between drillstring and wellbore to the surface. In vertical or near-vertical wells, cuttings transport is assessed by settling velocity. Rock fragments will be transported outside the hole as long as the fluid axial velocity is greater than cutting slip velocity. However, cuttings transport is more complex and challenging in deviated and horizontal wells than vertical wells, because liquid axial force is perpendicular to gravity and thus cuttings will be circulated to the surface by rolling effect rather than dynamic drag as in vertical wells. This why Dupriest et al. (2010) reported that borehole cleaning was identified as one of the drilling limiters that could limit drilling performance and footage per day Poor hole cleaning can lead to high torque and drag, fast bit wears, and poor cement jobs.

Cuttings Transport becomes a major challenge in extended reach wells with a long horizontal section nowadays. Poor hole cleaning can lead to high torque and drag, fast bit wears, poor cement jobs and slow rate of penetrations; and can end up in stuck pipe, and loss of the well. Different drilling parameters affects cutting transport in directional wells such as: drilling flow rates, fluid rheology, wellbore inclination, drilling

fluid (mud) weight, mud type, hole size, drillstring rotation, annular eccentricity, drilling penetration rate, cuttings size, cuttings density, and well profile.

1. Fluid Dynamics (CFD)

Computational fluid dynamics (CFD) is a numerical modeling technique that is used to understand downhole multiphase flow interactions in virtual annular geometry. It is widely employed to handle problems in petroleum engineering due to the growth of computer processing speed and high available memory (Ferroudji et al., 2020). CFD is used to simulate liquid loading in gas wells and predict the critical gas flow rate that allows liquid to flow back in the wellbore (Adaze et al., 2018; Hussein et al., 2019) Khaled et al. (2020) also showed the capability of the CFD model to simulate liquid loading in gas wells. He concluded that the liquid film flow reversal mechanism is the root cause of liquid loading in gas wells. Moreover, Bilgesu et al. (2007) developed a CFD model showing that high flow rate and drillpipe rotation has more cleaning effect for smaller particles compared to larger particles in the horizontal wellbore. Han et al. (2010) also examined the impact of annulus inclination and drillpipe rotation on particle rise velocity, pressure drop, and drilling fluid carrying capacity by performing different experiments and numerical tests. They concluded that particle rise velocity was misleading to evaluate cutting transport phenomena due to bed formation and flow area reduction. Sun et al. (2014) conducted a numerical study on solid-liquid transport phenomena at different wellbore inclination, rotational speed, and flow rate. They noted that pipe rotation significantly increases drilling fluid tangential velocity, leading to generate drag force that helps in cutting suspension. In addition, he proposed the

empirical correlation for pressure drop and cuttings concentration. The impact of different drilling conditions on cuttings transport was evaluated by Yan et al. (2014) where they found that angular speed should be selected carefully to enhance the hole cleaning process. But after a certain rotation speed, this effect degrades, at high flow rates. Ofei et al. (2014) investigated the influence of flow rate, diameter ratio, fluid rheology, and rotation speed on the behavior of pressure drop and cuttings concentration in the eccentric horizontal annulus. The Discrete Element Method (DEM) was coupled to CFD by Akhshik et al. (2015) to investigate the cuttings transport process through an eccentric annulus. They concluded that rotation of the inner pipe resulted in a non-symmetrical distribution of the cuttings, as well as, playing a key role in cuttings carrying for medium and high flow rates. He successfully showed on his model particle suspension at low inclinations and rolling behavior at a high inclination. The effect of the inner pipe rotation was investigated by Ofei and Alhemyari (2015) using the CFD approach where they found that the increment of the inner pipe rotation from 0 to 120 rpm is the most critical range to carry out efficient transportation of cuttings. Moreover, they noticed that the inner pipe rotation has a marginal effect at high flow rates. In addition, an increase in solid particles' diameter results in a decrease in carrying capacity. Kamyab and Rasouli (2016) used both experimental and numerical approaches to evaluate cuttings transport in coiled tubing drilling technology, taking into consideration the inclination of the well, drilling fluid properties, and solid particle size. They found that the angles from 30 to 60 degrees are the most critical to transport the solid cuttings. Dewangan and Sinha (2016) utilize the Eulerian-Eulerian approach to

model cuttings transport behavior in a concentric annulus with inner cylinder rotation. They found that amount of the turbulence was least at the middle of the borehole wall and maximum at some distance from the inner and outer cylinder. He also noted there is a strong relation between slip velocity and mixture total kinetic energy. Omid et al. (2017) developed a CFD model to study the effect of eccentric annuluses on cutting accumulation. They found that drillpipe eccentricity can aggravate cutting accumulation due to the reduction of the flow area available for the cuttings, leading to its settlement. Moreover, they noticed that drillstring rotation impact on improving hole cleaning is more effective with high eccentric annulus due to drag force effect and dispersion of the cutting. Solid-liquid flow in annular space was also investigated numerically by Epelle and Gerogiorgis (2017). Their simulation outputs are cuttings concentration, pressure drop, and axial velocity of both phases as considering the rotation of the inner pipe, ROP, eccentricity, and inclination as well as fluid properties. They deduced that rotation of the inner pipe affects cuttings transport positively; however, this effect is followed by an increase of drilling fluid pressure drop. In addition, with the increase of the eccentricity, cuttings removal becomes more difficult. The low density of polypropylene beads was introduced in the flow of water-based mud (WBM) by Yeu et al. (2019) to investigate the transport capacity in terms of cuttings transport ratio (weight of collected cuttings by fluid divided by initial introduced weight). They were focusing on the effect of the inner pipe rotation on the cuttings transport ratio for various solid particle sizes, wellbore inclination, and different concentrations of polypropylene beads. The authors observed an enhancement of 16.57% and 15.73% of cuttings transport ratio for vertical

and horizontal wellbores, respectively. Moreover, larger solid particles seem to be more effectively transported than smaller ones for all ranges of polypropylene concentrations and the inner pipe rotation speeds. Epelle and Dimitrious (2018) conducted a numerical study to investigate cutting transport phenomena in the steady-state and the transient condition under turbulent conditions.

2. Fluid Rheology

The impact of fluid rheology on the cuttings transport was investigated in different papers; Yu et al. (2004) showed that four forces are acting on the cuttings while circulating in the annulus: downward gravitational force, upward buoyant force, drag force parallel to the flow and lift force perpendicular to the flow. They performed his tests on a beaker to examine the effect of chemical surfactant, particle size, and fluid PH on cutting transport. They found that adding chemical surfactant helped in circulating cuttings through the entire length of the loop scale cutting transport in horizontal pipe. Duan et al. (2006) reported that smaller cuttings are difficult to circulate out of the hole compared to larger ones when water was used as the circulating fluid. They also showed that pipe rotation and mud rheology were major factors for cutting transport in a horizontal wells. Okrajni and Azar (1986) studied the effect of mud rheological properties on cuttings transport in directional wells. Experiments were conducted on water and bentonite/polymer mud at a different inclination from 0 to 90 degrees. They examined the effect of drilling fluid plastic viscosity (PV), yield point (YP), and apparent viscosity (AV) on hole cleaning. He concluded that using a high ratio of (YP/PV) provides efficient hole cleaning only when the flow is laminar. While in

turbulent flow, mud rheological properties were insignificant for hole cleaning. Luo et al. (1992) developed a physical model based on the different forces acting on the solid particles and four dimensionless groups. They validated his model by data from 8-1/2", 12-1/4", and 17-1/2" holes from the field. They concluded that decreasing fluid viscosity in turbulent flow improves cutting removal in deviated wells. Terry et al. (1996) conducted a comparative study on the capability of water and oil-based mud on hole cleaning. They conducted several experiments on 5-inch flow loop with 2-3/8 inch inner diameter with 0.62 eccentricity. They used limestone cuttings and different type's oil and water base mud and showed that flow diversion from under the pipe in high angle wells is controlled by the fluid's flow index n and flow diversion is less affected at low and intermediate angles. They also showed that water base and oil base muds clean the well similarly under the same rheological properties and velocity.

On the other hand, Tomren et al. (1986) reported that low viscosity in turbulent flow regime performs similarly to high viscosity fluid in turbulent flow in inclined annuli. Their study was very important because they used long test section (40 ft) to ensure establishment of steady flow and cover wide ranges of inclination from 0 to 90 degrees. Ford et al. (1990) performed a comprehensive study on different drilling parameters required to ensure good hole cleaning. A laboratory setup of 21 feet with an inner tube size 3.5-inch and 2.4-inch diameter that can be orientated at any angle was used for this purpose. They found that increasing fluid viscosity improves cutting removal for cutting rolling and suspension mechanisms when using high or medium fluid viscosity. They also reported that drillstring rotation did not improve cutting

transport when using water. Moreover, Pedan et al. (1990) showed the bad performance of medium viscosity fluid on cutting removal when compared to low viscosity and high viscosity fluids. This was opposed to what was observed by Piroozian et al. (2011) that medium viscosity fluid perform much better in cutting removal than high viscosity mud in directional wells.

There are many contradicting results reported from literature on the effect of fluid rheology on hole cleaning of horizontal wells. In addition, the limited number of papers were published using numerical models to study fluid rheology effect on cutting transport. Up to date, there is an unresolved question regarding the selection of the favorable fluid rheology while drilling and how one can evaluate the quality of mud rheology while drilling if it's efficient for hole cleaning or not?

3. Wellbore Tortuosity

Directional wells were being drilled for different reasons: maximize reservoir contact area, controlling blowout, sidetracking around a fish, and exploiting reservoirs located beneath seas from rigs on land. Directional wells position is evaluated by inclination (angle between vertical and the wellbore), and azimuth (angle between projections of the wellbore onto a horizontal plane and geographic north). The change in wellbore position is expressed by dogleg severity (DLS) value that is expressed by Lubinski et al. (1953), **Eq. 1**. There are two dominant types of steering systems, the bent housing motor, and rotary steerable system. The bent motor is less expensive and is used in most unconventional horizontal wells or low-angle directional wells. The bit is mounted on a motor with a small bend in the body (0.5 – 3 degrees) so the bit face is

tilted and cutting slightly to the side of the hole at all times. When the pipe is rotated the side-cut occurs equally on all sides so the bit drill smoothly ahead. When the driller wishes to steer pipe rotation is stopped so the bend is pointed in a specific direction. Fluid is still being circulated so the motor is turning the bit, but it only drills in the direction it is pointed. The loss of pipe rotation while steering does not affect cuttings transport greatly at lower angles, but at a high angle where we form an equilibrium bed it results in a higher cuttings bed and a thicker transportable layer. The higher bed creates more axial drag on tool joints and in longer high angle wells it becomes impossible to transfer weight to the bit. Also, if there are any sections of the enlarged hole due to inadequate mud weight (MW), the increasing bed height with no rotation is more likely to result in a stuck pipe. The rotary steerable systems (RSS) differ in that they are capable of steering without stopping drill string rotation. A tool just above the bit uses push pads that are timed to extend and retract with each rotation so bit side force is maintained on the same side of the hole, and the bit cuts preferentially in that direction. Other RSS may achieve the same effect by synchronizing a flexure or bent shaft within the body of the RSS to maintain side force on the bit at a constant azimuth. RSS are more expensive than bent motors so they tend to be used in long extended reach wells where a bent motor can no longer slide to steer due to the higher axial drag and increases bed height when not rotating to steer. Bent motors dominate the drilling of lower cost wells, like unconventional horizontals. The other major difference in the systems that's relevant to this paper is that bent motors have a much greater tendency to create a poor wellbore quality with more severe spiral tortuosity (**Fig. 1**).

$$\mathrm{DLS} = 2\arcsin\sqrt{\sin^2\left(\frac{\varphi_2-\varphi_1}{2}\right)+\sin\varphi_1\sin\varphi_2\sin^2\left(\frac{\vartheta_2-\vartheta_1}{2}\right)} \quad (1)$$

Where DLS is the wellbore dogleg severity, φ is the wellbore inclination, and ϑ is the wellbore azimuth between points 1 and 2.

Wellbore quality is mainly related to the smoothness of the drilled hole and is considered a major factor for successful drilling. Poor hole quality can lead to many problems while drilling such as tight borehole, stuck pipe, drillstring vibration, high torque and drag, and difficulties in directional control and casing. Dupriest et al. (2010) reported that borehole quality was identified as one of the drilling limiters that could limit drilling performance and footage per day. Borehole limiters include wellbore instability limits, hole cleaning limits, and vibration-induced patterns. Mason et al. (2005) discussed different elements that can improve hole quality and lead to the construction of a perfect hole. These elements include minimum tortuosity, no wellbore spiraling, no cuttings beds accumulations, no ledges, hole in gauges (no wellbore breakout), and run casing easily in hole. Similar observations were reported by Chen et al. (2002) that the quality of a good hole is measured by hole gauge, wellbore smoothness, and wellbore tortuosity. Directional wells are designed to be a smooth well path where the curved section with constant curvature. But, the actual drilled path is usually suffered from unwanted undulations from the planned well trajectory. This unwanted deviation is known as wellbore tortuosity (Gaynor et al., 2001; Mitchell and Miska, 2010; Menad, 2013). Wellbore tortuosity was first defined by MacDonald and Lubiniski (1951) when they presented the definition of a smooth, vertical, and crooked

hole. They showed the concept of a crooked hole in vertical wells even before the invention of any sophisticated measuring tools. Their conclusions about hole spiraling were confirmed later by the images captured by the logging tools.

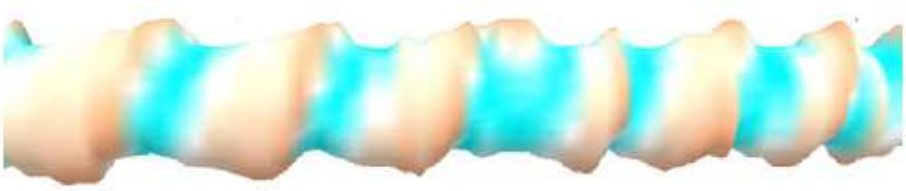

Figure 1 –Spiral hole with 3 foot pitch (period) length (Dupriest et al., 2010)

Wellbore tortuosity phenomena occurred while drilling due to different reasons: changes in formation lithology (rock type, formation dip angles, and faults), drillstring vibration, bit gauge deflection, and directional drilling deflection tools (Mitchell and Miska, 2010). Spiral tortuosity can impact the drilling phase by reducing hole size, aggravating drillstring buckling, intensifying drillstring vibration, slowing drilling rate of penetration (ROP), increasing torque and drag; aggravating logging tool reliability; and complicate casing and cement job (Chen et al., 2002; Stuart et al., 2003; Menad, 2013). It can also affect the completion and production phase by reducing the effective diameter of the wellbore that causes equipment stuck and high bending moments acting on it (Bang et al., 2015). It can even lead to wrong calculations of well position that will require a borehole trajectory model for correcting well position (Abughaban, 2017). The spiral shown in **Fig. 1** is due to an interaction between the bit and the first hard contact point above it in the bottom hole assembly. This hard contact is usually a stabilizer. The distance between peaks in the spiral will be equal to the distance from the bit to the hard

contact point. In motors that are usually 2-4 ft. The height of the spiral is due to a variety of factors but the dominant one is the amount of continuous side force on the bit. Bent motors have enough mass eccentricity due to the bend that when the string is rotated there is a high side force. Also, they tend to develop lateral vibration which greatly amplifies that force. In **Fig. 1**, the centerline of the wellbore is moving off-center by 2 inches every three feet. Other researchers (Gaynor et al., 2001; Chen et al., 2002; Mark, 2015) reported that a spiral period between 2 and 10 ft. can occur while drilling. A spiral hole with 5 feet period and 0.5 inch amplitude can cause 12 DLS/1m in the wellbore as observed by Gaynor et al. (2001). An RSS will also create a spiral but the first hard contact is usually a stabilizer around 20 ft from the bit so the period is much longer. There is also no significant mass eccentricity or tilt to the bit face so side cutting and the amplitude of the spiral tend to be low. **Fig. 2** Shows the main difference between a horizontal well with a smooth profile and another well with a spiral tortuous profile (2D View).

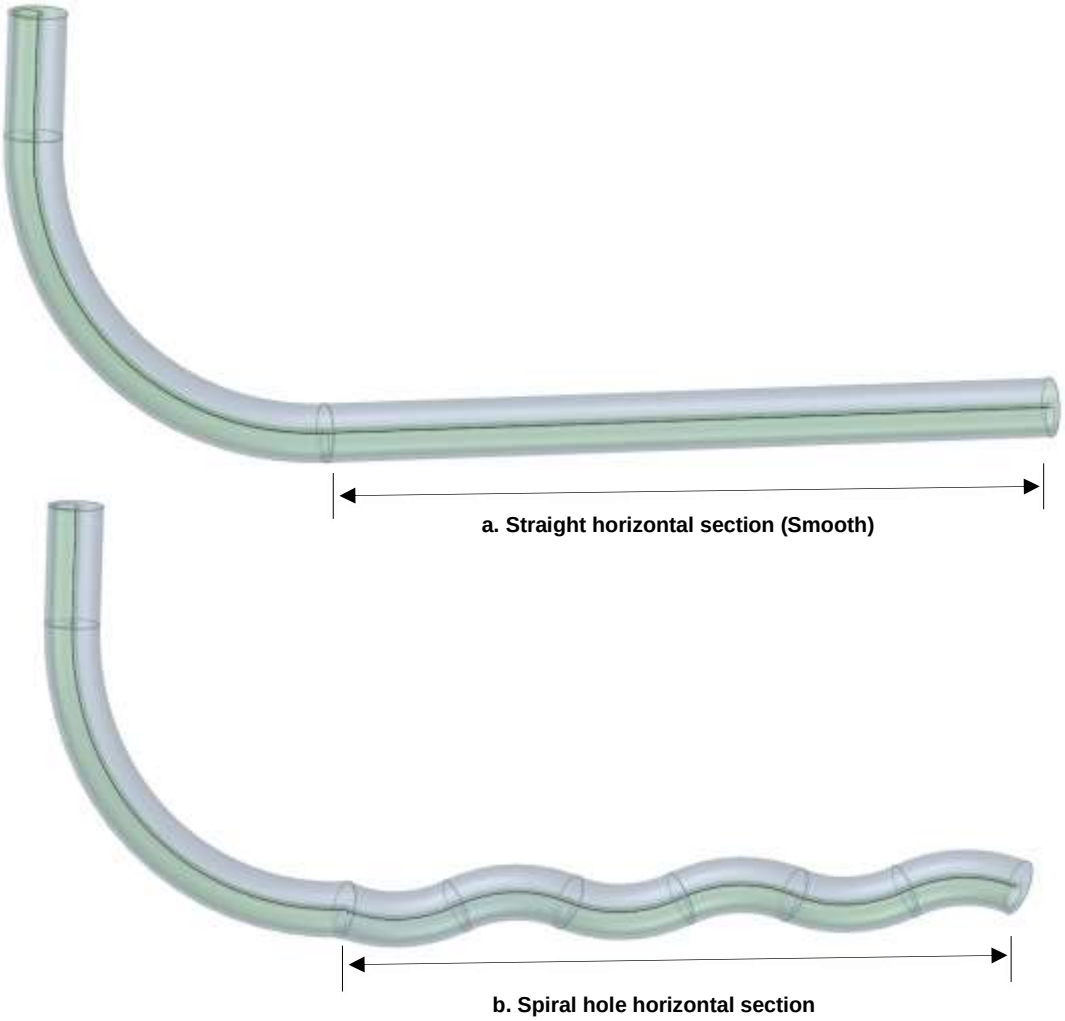

Figure 2 –Horizontal Flow Geometry (2D View) (a) horizontal well with a smooth profile; and (b) horizontal well with a spiral hole profile

4. Hole cleaning Evaluation models

Among factors that can induce a Non-Productive Time (NPT) during the evolution of a drilling operation is inefficient cuttings (solid) transportation from a drilled rock at a certain depth to the surface or so-called “poor hole cleaning”. In addition, this effect can be credited to other mechanical issues such as the collapse of the casing, shape of the drilled wellbore, …etc. Moreover, similar consequences might be

caused by formation characteristics, including moving, unconsolidated, geo-pressured, and reactive formations. For instance, Amoco found that around 70% of Non-Productive-Time was induced by unexpected perturbations in which pipe stuck was the principal cause of time lost and increased drilling operation costs (Massie et al. 1995). Such issues are mostly encountered in recent drilling technology like extended reach wells, coiled tubing, directional, and horizontal drilling. For that, a reliable predictive tool that takes into account different drilling parameters that impact the accumulation of cuttings in the real cases are required to reduce the possibility of occurrence of such obstacles during drilling phase in oil and gas fields and avoid NPT.

From the literature review, both real measurements of field scale and experiment results of the lab scale indicated that borehole cleaning is still the major issue for horizontal and vertical explored boreholes (Li and Luft, 2014). Through the last three decades, hole cleaning has been a subject of various types of investigations, including mechanistic modeling, lab-scale experimentation, field-scale analysis, and numerical modeling through Computational Fluid Dynamics (CFD), where basic drilling parameters were considered (drill pipe angular speed, drilling fluid flow rate, fluid properties, cuttings properties, and annulus geometry). Some interesting investigations can be cited as follows: Sanchez et al. (1997); Duan et al. (2006); Chen et al. (2007); Bilgesu et al. (2007); Mohammadzadeh et al. (2016); Epelle and Gerogiorgis (2017); Hakim et al. (2018); Rasul et al. (2020); Qureshi et al. (2021). The authors studied the effects of these parameters on cuttings accumulation, pressure drop, cuttings transport ratio, velocity distribution, flow pattern, etc. These investigations led to the development

of various tools to accurately predict the flow of drilling fluid behaviour under different operation conditions through developing empirical correlations for cuttings accumulation, pressure drop, critical velocity to prevent the appearance of cuttings bed, as well as, the establishment of flow charts for identifying flow regime of multiphase flow in the annulus. Although, a lot of work was conducted to understand the influence of drilling parameters on the cuttings transport phenomena and to optimize drilling operations, as well as, to comprehend the relationship between various drilling parameters. However, Most of the developed correlations and mechanistic models are limited in their application because they were developed based on their experimental conditions, setup, and did not take in account all drilling parameters affect cuttings accumulation while drilling. Therefore, these models cannot apply to different drilling cases and a generalized data driven model (global correlation) for better analysis and real-time assessment of the hole cleaning process is still required.

Martins and Santana (1992) modeled non-Newtonian flow flowing in an eccentric annular geometry in the presence of cuttings using a mechanistic model where they assumed that the upper and lower layers consist of cuttings in suspension and cuttings bed, respectively. In addition, their model considered several configurations of flow that represented mixtures of solid and liquid through the horizontal annulus. The authors developed a dimensionless method to evaluate the hole cleaning process. Later, Kamp and Rivero (1999) considered the same representation of a solid-liquid flow via a horizontal and inclined annulus where their model allowed to estimate transport velocity for various flow rates, pressure annulus of the mixture, and bed deposition height.

Similarly, a mechanistic model is considered in the study of Cho et al. (2000) but the flow of solid-liquid mixture is modeled employing three layers: suspension layer, moving bed layer, and cuttings bed layer. The authors proposed a method to determine the carrying capacity, and they established empirical correlations and charts for each layer taking into account the influence of geometry parameters of the annulus, fluid flow rate, fluid rheology, and cuttings size. It was found that the drilling fluid has a primordial effect on hole cleaning in horizontal and deviated wells in addition to other parameters. Li et al. (2004) numerically solved a transient model for cuttings transportation in a horizontal annular geometry utilizing a mechanistic model to estimate the height of solid deposition in the lower zone of the annulus as a function of annular geometry parameters and drilling fluid characteristics. Their model was validated against experimental data, and a good coincidence was found. Also, it was exhibited that the thick drilling mud presents better carrying capacity at moderate flow rates.

From an experimental setup, and based on the Buckingham-π theorem, Ozbayoglu et al. (2008) suggested empirical correlations to predict solid particles volume fraction and annular pressure drop of Water-Based Mud (WBM) in horizontal and inclined wells. In addition, their experimental data showed that rotation of the inner pipe has an important influence on the erosion of cuttings deposition, where this effect leads to a reduction in pressure drop due to the enlargement in the cross-section flow area. Also, it was noticed that the drill pipe has more impact on hole cleaning when it makes an orbital motion. Sun et al. (2014) carried out a numerical work in which the effect of the drill pipe rotation on hole cleaning for inclined and horizontal annulus was

addressed. Then, the authors performed extensive simulation runs in order to develop a relationship for estimation of pressure drop and solid particles accumulation in the entire annulus. Moreover, it was noticed that rotation of the drill pipe may enhance hole cleaning until a certain value of angular speed where this effect becomes marginal, particularly at low flow rates of drilling mud. Another experimental work (Song et al. 2017) discussed the wellbore cleaning issue for horizontal microhole cases. The concentration of the secondary phase of the mixture (solid phase) and height of cuttings deposition were estimated via suggested correlations considering drilling parameters that have an essential effect on carrying capacity. For applicability purposes, they compared the results of the developed correlations with experimental data. Pandya et al. (2020) also considered the same way as Song et al. (2017), in which they carried out a dimensionless analysis through non-linear regression to suggest relationships for field utilization.

Erge and van Oort (2020) assessed the effects of some drilling factors (Angular speed of the drill string, eccentricity, and blockage of the annular geometry) on hole cleaning efficiency. A novel model was suggested for carrying capacity analysis in terms of critical velocity. Besides, it was concluded that drilling fluid flow rate is not the only principal parameter for inclined wells to improve carrying capacity, but the rotation of the drill pipe may also play a primordial role. To improve hole cleaning efficiency, pulsed drilling fluids were evaluated experimentally and numerically by Zhu et al. (2021), considering various drilling parameters. Moreover, they characterized the pulse by amplitude, varied period, and duty cycle of the pulsed drilling fluid. They concluded

that with the utilization of pulsed drilling mud, the motion of the cuttings bed was improved by around 19% as compared to traditional drilling fluids. Yeo et al. (2021) performed a numerical study using appropriate Computational Fluid Dynamics (CFD) software to optimize drilling parameters. They generated correlations in terms of critical velocity and critical pressure drop where they stated the pipe roughness induced a progressive rise of the critical pressure drop. Recently, Ozbayoglu et al. (2021) attempted to develop a data-driven tool for optimization of the angular speed of the drill pipe and drilling fluid flow rate based on a wide interval of drilling parameters (fluid properties, annular geometry characteristics, rate of penetration, etc.).

CHAPTER III

MODEL DEVELOPMENT AND VALIDATION

1. Mathematical Model and Governing Equations

A three-dimensional model is developed to study the effect of different drilling parameters on cuttings transport in horizontal pipe based on computational fluid dynamics (CFD). Two-phase flow (solid and liquid) model is considered to simulate flow in the annular space of a well. For that, the governing equations are presented in the Eulerian-Eulerian framework in which both phases are assumed as continuous phases. The continuous phase and dispersed phase are assumed to be interpenetrating continua in the Eulerian approach. The Eulerian approach was selected because the solid volume fraction in this analysis was expected to be higher than 0.1; and the particle-particle interactions and particle volume fraction on the continuous cannot be neglected. Therefore using Eulerian-La grange discrete phase model (DPM) was being omitted. The behavior of the liquid phase (drilling mud) and the solid phase (cuttings) can be predicted by solving the governing equations in the cylindrical coordinate system. Continuity and the momentum equations presented by Van Wachem and Almsted (2003) can be written as follow.

The equation of continuity for phase q can be defined as follow:

$$\frac{\partial(\alpha_q \rho_q)}{\partial t} + \nabla \cdot \left(\alpha_q \rho_q \vec{v}_q\right) = \sum_{p=1}^{N} \dot{m}_{pq} \quad \text{..... (2)}$$

where α_q is the phase volume fraction, ρ_q is the phase q density velocity, v_q represents the phase q velocity, and $\dot{m}_{pq}$ stands for the mass transfer between phases.

The equation momentum balance the liquid phase q is given by:

$$\frac{\partial(\alpha_q\rho_q\vec{v}_q)}{\partial t} + \nabla\cdot(\alpha_q\rho_q\vec{v}_q\vec{v}_q) = -\alpha_q\nabla P + \nabla\cdot\bar{\bar{\tau}}_q + \alpha_q\rho_q\vec{g}_g + \sum_{p=1}^{N}\left(K_{pq}(\vec{v}_p - \vec{v}_q) + \dot{m}_{pq}\vec{v}_{pq}\right) + \alpha_q\rho_q\left(\vec{F}_q + \vec{F}_{lift,q} + \vec{F}_{vm,q}\right). \quad (3)$$

where $\bar{\bar{\tau}}_q$represents the qth stress-strain tensor and can be written as follows:

$$\bar{\bar{\tau}}_q = \alpha_q\mu_q\left(\nabla\vec{v}_p - \nabla\vec{v}_q^{\,T}\right) + \alpha_q\left(\lambda_q - \frac{2}{3}\mu_q\right)\nabla\cdot\vec{v}_p\bar{I} \quad (4)$$

where λ_q and μ_q represent the bulk and the shear viscosity of the phase q, $\vec{F}_q$ represents the external body force, $\vec{F}_{lift,q}$ is the lift force, $\vec{F}_{vm,q}$ is the virtual mass force, K_{pq} is the interphase momentum exchange coefficient, P stands for the pressure shared by all phases, and v_{pq} is the interphase velocity.

The equation of momentum for the solid phase is written as follow:

$$\frac{\partial(\alpha_s\rho_s\vec{v}_s)}{\partial t} + \nabla\cdot(\alpha_s\rho_s\vec{v}_s\vec{v}_s) = \alpha_s\nabla P - \nabla P_s + \nabla\cdot\bar{\bar{\tau}}_q + \alpha_s\rho_s\vec{g}\sum_{p=1}^{N}\left(K_{ls}(\vec{v}_l - \vec{v}_s) + \dot{m}_{lq}\vec{v}_{ls}\right) + \alpha_s\rho_s\left(\vec{F}_s + \vec{F}_{lift,s} + \vec{F}_{vm,s}\right). \quad (5)$$

where P_s represents the solid pressure, consists of the kinetic term and the term due to particle collisions, $K_{ls} = K_{sl}$ stands for the momentum exchange coefficient between liquid and solid phases shown as l and s respectively, N represents the total number of phases, and $\vec{F}_s$, $\vec{F}_{lift,s}$ and $\vec{F}_{vm,s}$ are the different forces exerted on the solids as defined previously for the liquid phase.

In the previous equations α is the volume fraction and can be written as follow:

$v = \int_V^0 \alpha dV$. …….. (6)

The turbulent regime in the present report is modelled using $K - \varepsilon$ model (Shih and Liou, 1995) where the effective viscosities in the case of slurry flow type have been calculated considering this model. Therefore, the effective viscosity relationship for the liquid phase is evaluated as:

$\mu_{eff} = \mu + \mu_{tl}$. …….. (7)

$\mu_{tl} = \frac{C_\mu \rho_l {K_l}^2}{\varepsilon_l}$. …….. (8)

$C_\mu = 0.09$. …….. (9)

While, the effective for the solid phase is calculated as:

$\mu_{eff} = \mu + \mu_{ts}$. ……... (10)

$\mu_{tl} = \frac{C_\mu \rho_s {K_s}^2}{\varepsilon_s}$. ……. (11)

$C_\mu = 0.09$. ……. (12)

where μ stands for the dynamic viscosity, C_μ represents a constant considered to be 0.09, ρ is the density, K is the turbulent kinetic energy and ε is the turbulent dissipation energy.

While circulating cuttings outside the wellbore, different forces are acting on solid particles during hole cleaning such as drag force (Fd), Lift force (Fl), Gravitational force (Fg), and Buonacy force (Fb) These different forces acting on solid particles are shown in **Fig. 3**

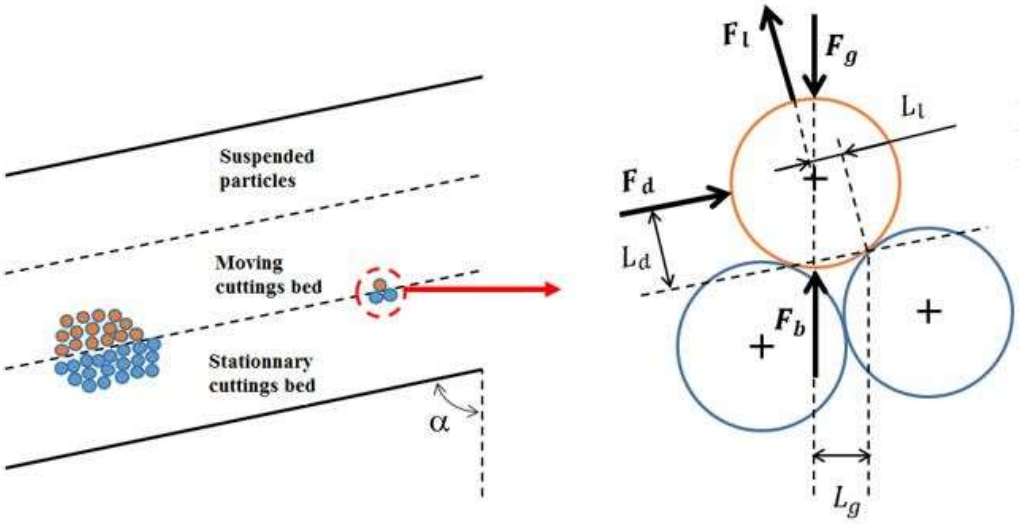

Figure 3 –Forces acting on solid particles adapted from Hyun et al., 2000

Where Lg is the distance influencing on drag, buoyancy and gravity, L_d is the distance impacting the drag force and L_l is the distance affecting the lift force.

For the drag force (F_d), the formulation suggested by Gidaspow (1994) is employed since it would provide accurate results even for high cuttings concentrations. When the cuttings concentration $\alpha_s \leq 0.2$, the fluid-solid coefficient of exchange, K_{sl}, is computed using the following relationship:

$$K_{sl} = \frac{3}{4} C_D \frac{\alpha_s \alpha_l \rho_l |\vec{v}_s - \vec{v}_l|}{d_s} \alpha_l - 2.65 \quad \text{..... (13)}$$

Where $C_D = \frac{24}{\alpha_l Re_s}[1 + 0.15(\alpha_l Re_s)^{0.687}]$. ……..… (14)

When $\alpha_s > 0.2$, the fluid-solid coefficient of exchange, K_{sl}, can be determined using the following expression:

$K_{sl} = \frac{150\alpha_s(1-\alpha_l)\mu_f}{\alpha_l {d_s}^2} + 1.75\frac{\alpha_s \rho_l |\vec{v}_s - \vec{v}_l|}{d_s}$. …… (15)

Saffman-Mei lift force formulation Fl (Saffman, 1965; Mei and Klausner, 1994) is considered in this study. This model can be applied to spherical and slightly deformed which makes it widely used as compared to the Moraga et al. (1999) model. The lift coefficient can be defined as:

$C_l = \frac{3}{2\pi\sqrt{Re_\omega}} {C'}_l$ ….…… (16)

With ${C'}_l = 6.46$ and $0 \le Re_p \le Re_\omega \le 1$. …… (17)

Mei and Klausner (1994) developed the formulation of this model to take into account high values of the particle Reynold numbers. Thus, the correlation of Saffman–Mei can be written as:

$C_l = \frac{3}{2\pi\sqrt{Re_\omega}} {C'}_l$. …… (18)

With ${C'}_l = \begin{cases} 6.46 \times f(Re_p, Re_\omega) & Re_p \le 40 \\ 6.46 \times 0.0524(\tilde{\beta} Re_p)^{1/2} & 40 < Re_p < 100 \end{cases}$ …… (19)

Where

$\tilde{\beta} = 0.5\left(\frac{Re_\omega}{Re_p}\right)$. ……..…… (20)

$$f\left(Re_p, Re_\omega\right) = \left(1 - 0.3314\tilde{\beta}^{0.5}\right)e^{-0.1Re_p} + 0.3314\tilde{\beta}^{0.5} \quad \text{..... (21)}$$

$$Re_p = \frac{\rho_q|\vec{\nabla}_q - \vec{\nabla}_p|d_p}{\mu_q}. \quad \text{..... (22)}$$

$$\mathrm{Re}_\omega = \frac{\rho_p|\nabla\times\vec{\nabla}_p|{d_p}^2}{\mu_q}. \quad \text{..... (23)}$$

The previous partial differential equations are nonlinear, and only numerical methods can handle such kinds of equations. For that, CFD Software is employed to solve the governing partial differential equations of slurry flow applied to the cuttings transport in an annular geometry of a wellbore. These equations were solved numerically using the finite volume formulation in ANSYS Fluent solver

(version 2019 R3) on each cell throughout the drilling annulus. The simulations were executed in the pressure-based explicit solver and the semi-implicit method for pressure-linked equations (SIMPLE) algorithm developed by Patankar and Spalding (1972). The second-order implicit scheme was utilized to solve the momentum equation and the transient flow behavior was adopted with a time step size from 10^{-4} to 5 x 10^{-4} to avoid any numerical divergence and nonphysical flow patterns. The convergence criterion for all simulations was set to be equal10^{-4} for the root mean square of the normalized residual errors. The simulation was run for a total flow times equals 5-8 seconds for each run and Computations were done by using the Texas A&M high performance research computing (TAMU HPRC) with 64 GB and 18 cores (Ada Cluster - Intel x86-64 Linux). Each data point takes a computational time from TAMU HPRC equals 1-8 days.

2. Geometric domain and boundary conditions

The annular geometric domain (**Fig. 4**) consists of two horizontal cylindrical bodies of 2m length to ensure that the selected period length is longer than hydrodynamic entrance length in all flow conditions and configurations based on the equations proposed by Yunus and Cimbala (2006) in **Eqs 27-28**. The outer wall is always kept stationary, while the inner wall is either kept stationary or had a clockwise rotation to simulate drillstring rotation while drilling. An eccentric annulus E is considered between these two cylinders to represent the effect of gravity on the drillstring in deviated holes.

$$E = \frac{2e}{D_{hole} - D_{pipe}}. \quad \text{..... (24)}$$

where E is the annular eccentricity, e is the offset distance between the centers of the inner and outer pipes, D_{hole} is the hole or casing inner dimeter, and D_{pipe} is the outer diameter of the inner pipe.

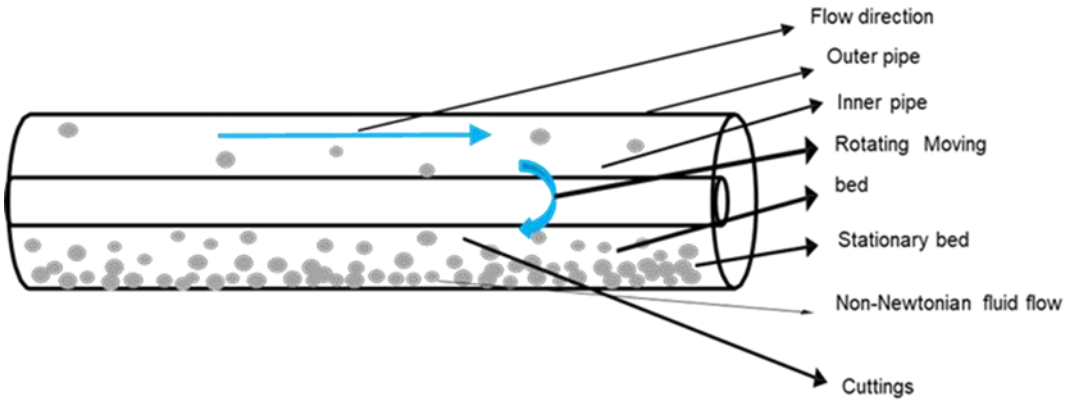

Figure 4 –Annular geometric domain (flow domain)

Drilling fluid adopted in this model is a non-Newtonian fluid of Herschel Bulkley type that is a mixture of water, carboxymethyl cellulose (CMC) and Flowzan inspired from TAMUQ flow loop and Abu-Jdayil and M. Ghannam, 2014 (**Eq. 25**); and Power Low Fluid (**Eq. 26**) for fluid rheology and wellbore tortuosity analysis that is a mixture of water and bentonite inspired from Iyoho dissertation(1980).

$$\tau = \tau_0 + K\,\gamma^n \quad \text{(25)}$$

$$\tau = \mathrm{K}\,\gamma^n. \quad \text{(26)}$$

Where τ is the fluid shear stress, τ_0 is the Herschel Bulkley yield stress, γ is the fluid shear rate, K is fluid consistency index, n is either Herschel Bulkley or Power Low constant based on the fluid rheology model used. Simulation data for cuttings fluid flow is summarized in **Table 1** including geometry, drilling parameters and fluid rheological properties.

Table 1 –Simulation input data

Geometry	
Wellbore Length (m)	2
Hole diameter (m)	0.0739
Pipe diameter (m)	0.047
Wellbore inclination (degrees)	0-90
Annular eccentricity, E	0 – 0.8
Fluid rheological properties	
Fluid density (kg/m^3)	1018.5
Flow behavior index, n	0.88
Consistency index, K ($Pasec^n$)	0.0429
Fluid yield stress, τ_0 (Pa.sec^n)	3.8
Drilling parameters	
Drilling fluid velocity (m/sec)	0.8 – 1.5
Rate of penetration ROP – m/sec / (ft/hr)	0.0004 (50) – 0.013 (150)
Drillpipe rotation (RPM)	0 - 500
Particle properties	
Cutting density (kg/m^3)	2761.4
Cutting diameter (m)	0.00201
Porosity	0.36

Drilling fluid is considered to flow in a laminar and turbulent flow regime, if the drilling fluid Reynold number Re ≤ 3250-1150η, while fluid flow is considered in turbulent regime when Re ≥ 4150-1150η (Mitchell and Miska (2010)). Reynolds number calculations in **Eqs. 30-32** used in this simulation are proposed by A.Busch et al. (2019). These equations were selected, because it takes in account the effect of rotational velocity (drillstring rotation) on Reynold number calculations beside the fluid flow linear velocity.

$$L_{h,lamianr} = 0.05\left(D_{hole} - D_{pipe}\right)N_{RE}. \quad (27)$$

$$L_{h,turbulent} = 1.359\left(D_{hole} - D_{pipe}\right)(N_{RE})^{\frac{1}{4}}. \quad (28)$$

$$Re = \frac{\rho_f D_h \nu}{\eta_o}. \quad (29)$$

$$\eta_o = k\left(\frac{2n+1}{3n}\right)^n (\dot{\gamma})^{n-1}. \quad (30)$$

$$u_r = \frac{\pi d_i}{2\times 60} RPM. \quad (31)$$

$$\dot{\gamma} = \sqrt{\left(\frac{12\,\nu}{D_h}\right)^2 + \left(\frac{12\,u_{,r}}{D_h}\right)^2}. \quad (32)$$

where Re is the Reynolds number, ν is the fluid velocity, ρ_f is the fluid density, n is the power law flow behavior index, k is the power law consistency index, and D_h is the hydraulic diameter ($D_h = D_{hole} - D_{pipe}$), η_o is the reference apparent viscosity, $\dot{\gamma}$ is the reference shear rate, u_r is the average rotational drilling fluid velocity.

The selection of the appropriate turbulence models depends on the physics of the flow, computational time, and accuracy level. Three main approaches are usually used to calculate a turbulent flow: direct numerical simulation (DNS), large eddy simulation

(LES), and Reynolds average Navier stokes simulation (RANS). RANS approach solves the times average Navier stokes equation and is considered the most acceptable approach for industrial flows. Different turbulence models are based on the RANS approach: k-epsilon (κ-ε), k-omega (κ-ω), SST k-omega, and Reynold stress model (RSM). Different turbulence models were compared and validated with experimental data to determine the optimum turbulence model in this simulation for computing annular pressure loss (**Fig. 5**). Results show that the κ-ε model is the most suitable model for predicting the turbulence flow behavior. Therefore, the κ-ε model was utilized to the model turbulence flow regime in the simulation. The (κ-ε) model is based on model transport equations, dissipation rate (ε), and kinetic energy (κ). Shih (1995) proposed κ-ε realizable model to overcome the deficiency of modeling dissipation rate in the standard model by proposing the new eddy-viscosity equation. Therefore, the κ-ε realizable model was adopted in this simulation for modeling turbulent flow behavior.

It is worth to mention that most wellbore tortuosity are with pitch length between 2-4 ft. and they are the great majority of problematic spiral. This why all wellbore tortuosity analysis was done on spiral pitch length 2-4 ft. and with a total pipe length 2-3m to ensure that the selected period length is longer than hydrodynamic entrance length in all flow conditions and configurations based on the equations proposed by Yunus and Cimbala (2006), since Beger et al. (1983) showed that spiral hydrodynamic length for bending and spiral pipe is less than or equal to what calculated for normal straight pipe. Gaynor et al. (2001) presented a mathematical model to compute the wellbore curvature and dogleg severity for spiral tortuous hole (**Eqs. 34-38**).

Spiral hole geometry can be defined in Cartesian coordinate system (Gaynor et al., 2001)

$X = r.cos\,\theta$. ……..……..... (34)

$Y = r.sin\,\theta$. ……. (35)

$Z = \frac{p.\theta}{2\pi}$. ……. (36)

where p is representing the period (pitch) length of the spiral and r represents the radius of the spiral (amplitude)

$k = \frac{4\pi^2 r}{(P^2+4\pi^2 r^2)}$. ……. (37)

$DLS = \frac{K.360}{2\pi}$. ……. (38)

where k represents wellbore curvature and DLS is the wellbore dogleg severity/m.

A mixture of liquid and solid velocity was specified at the inlet and zero gauge pressure at the outlet. No-slip boundary conditions were considered on both walls for both particles and fluid. The drilling rate of penetration (ROP) was computed based on the equations developed by Ozbayoglu et al. (2010). He correlates the solid feed concentration with ROP and porosity (**Eqs. 39-41**). If rock porosity is not provided, Larsen et al. (1997) is utilized (**Eq. 41**). It was assumed that the annular walls are smooth and particle shape won't change due to particle-particle interactions. A value of 0.9 for friction restitution coefficient between particles and walls was utilized.

$C = \frac{ROP\,(1-\phi)}{\left(1-\frac{D_{pipe}}{D_{hole}}\right)^2 V_{cut}}$. …… (39)

$C = \frac{Net\ volume\ Occupied\ by\ particles}{Total\ volume\ of\ annulus}$. …….. (40)

where ROP represents drilling rate of penetration, ϕ is the rock porosity, C is the cuttings average concentration, and V_{cut} is the cuttings velocity

$$C = \frac{ROP}{\left[1-\left(\frac{A_{pipe}}{A_{hoole}}\right)\right]V_{cut}}. \quad \text{(41)}$$

where A_{pipe} represents the area of inner pipe, and A_{hole} is the area of borehole or casing

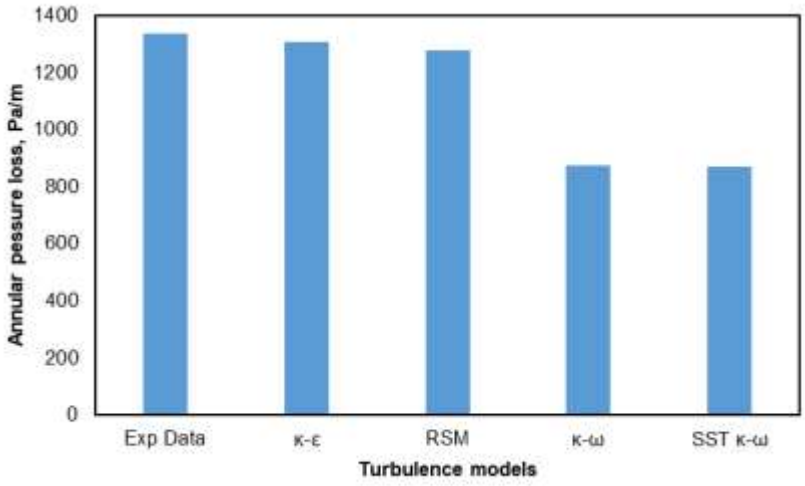

Figure 5 –Turbulence model comparison

3. Grid Setup

Khaled et al. (2020a) showed that hexahedral grid (mesh) is an efficient meshing technique for two phase-flow inside the annular geometry of cylindrical bodies because of the fewer cells required for the same number of nodes compared with tetrahedron mesh. Thus, structured hexahedral meshes were adopted in most simulations except for spiral geometry where polyhedral mesh was used to achieve good mesh quality. The hexahedral mesh was adopted by implementing the edge sizing, radial division

technique, and face meshing method at the inlet, walls, and outlet boundaries as shown in **Fig. 6**. It represents mesh cross-sectional for concentric and eccentric annuli utilized in these simulations.

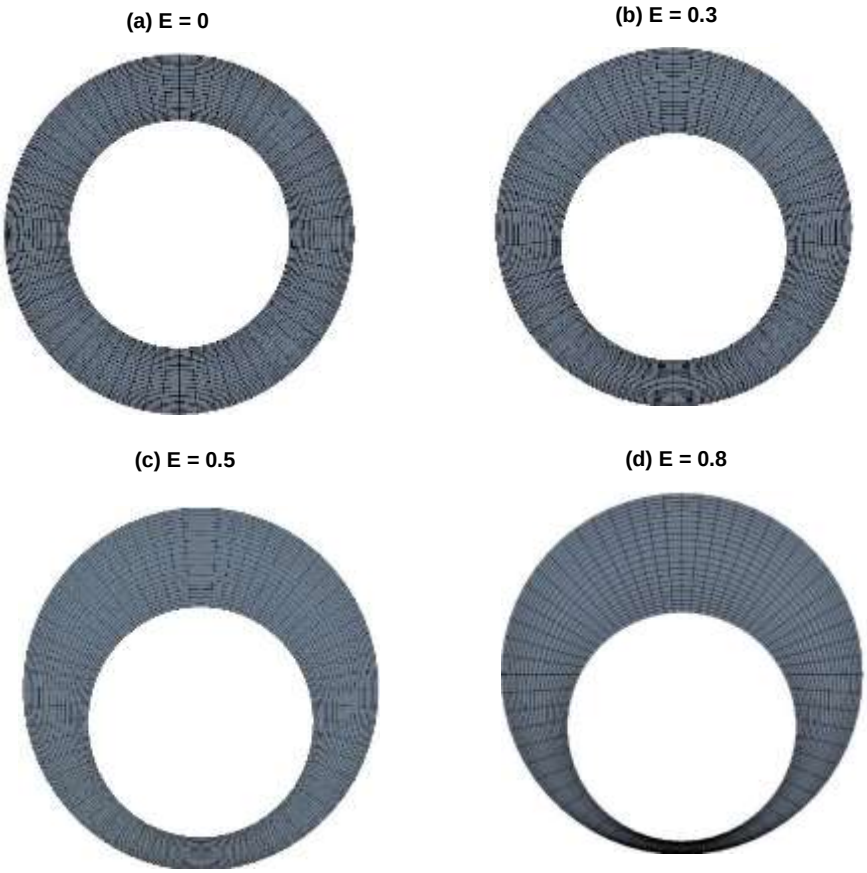

Figure 6 –Mesh cross section of the domain at different annular eccentricity

During turbulent flow, fluid velocity near the wall changes rapidly. Therefore, a good estimation of first layer thickness constant (Y^+) is essential for an accurate computational results (Eq. 40). Y^+ is kept above 30 for the realizable κ-ε model based on the recommendation by ANSYS Fluent (2013). Then, Grid (mesh) sensitivity analysis was done to determine the optimum number of elements for an accurate solution. The

study was conducted by varying radial sizing and edge sizing, then computing the annular pressure loss as shown in table 2. The mesh choice was done based on results that can show stabilization of the annular pressure loss and good mesh properties achieved. It was observed from **Fig. 7** that the annular pressure loss stabilized at mesh size of total number of division = 1200 and the total number of elements equals 435K. This mesh size was adopted in simulation for accurate computation.

$$Y^+ = \frac{y}{\mu}\sqrt{\rho\tau_w}. \quad (40)$$

where y is the first layer thickness (difference between wall and cell center), and τ_w is the wall shear stress.

Table 2 –Grid independence analysis

Edge sizing	Radial sizing	Total division	Total number of elements	Minimum orthogonal quality	Maximum skewness
40	10	400	108400	0.932	0.262
60	10	600	163200	0.941	0.25
60	15	900	244800	0.934	0.249
60	20	1200	326400	0.931	0.249
80	20	1600	435200	0.936	0.243
80	30	2400	652800	0.933	0.262

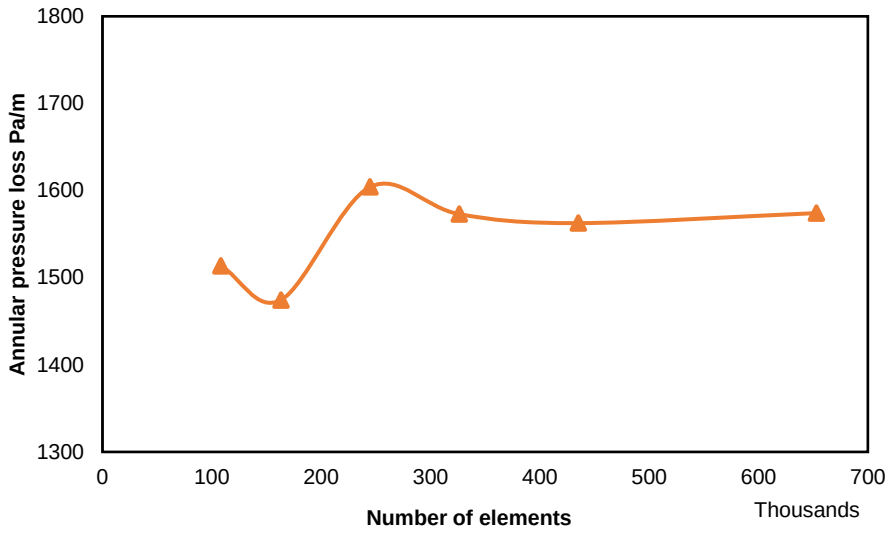

Figure 7 –Mesh independence study

4. Texas A&M at Qatar (TAMUQ) Flow Loop

Extensive hole cleaning experiments were conducted in the horizontal multi-phase flow loop at Texas A&M University at Qatar (TAMUQ). The flow loop (see, **Figure 8** & **9**) consists of an inner (drillpipe) and outer (open hole or casing) diameter of 6.35 cm (2.5 in) and 11.43 cm (4.5 in), respectively with a length of 6.16 m that can be set from a horizontal position (90^o) to 75^o to adjust the inclination of the set-up. The drill pipe can be rotated from 0 -160 rotation per minute (RPM) and its eccentricity can be varied by up to 80% from the concentric position. Experiments were conducted at 140 kpa and with a maximum operating pressure of around 200 kPa. The mixing tank has a total capacity of 1 m^3 (1000 L) and utilized an agitator for appropriate mixing of cuttings (solid) and liquid inside the tank.

Three types of solutions were used as test fluids in our experiments as shown in **Table 3**, freshwater (997 kg/m3) is used as a Newtonian fluid, and a bio-based polymer was used to create non-Newtonian fluids at different concentrations. Fluid rheology was tested in the lab with Grace M3600 rotational viscosity meter and it was observed that the Herschel Bulkley model could represent the rheological behaviour of the non-Newtonian fluid used during experiments. Solid glass beads of density equal 2500-2650 kg/m^3 and average size of the solid particles is 2-3 mm. A centrifugal pump is used to transfer the carrier fluid from the tank to the flow loop system, and Once a steady-state liquid flow is achieved, 4 wt% glass beads were injected into the flow loop system. Different experiments were conducted in TAMUQ flow loop covering wide ranges of different operation, geometric, and hydrodynamic conditions of cuttings transport (see, **Table 4**). One of the objectives of these experiments was to compute the cuttings concentration (average solid volume fraction) in the flow domain utilizing the Electrical Resistance Tomography (ERT) Technique. ERT measurement is done by using two measurement planes (electrode planes) that provide the volumetric concentration profiles across the ERT section. More information about TAMUQ Flow loop experiments can be found by M.M. Huque et al., 2021.

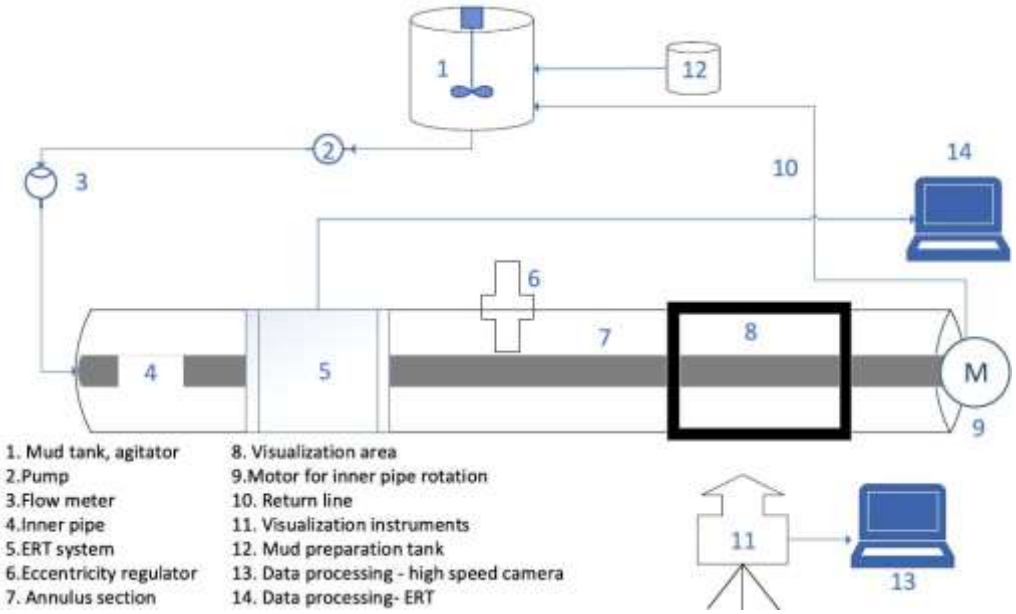

Figure 8 –TAMUQ flow loop schematic, Source: M.M. Huque et al., 2021

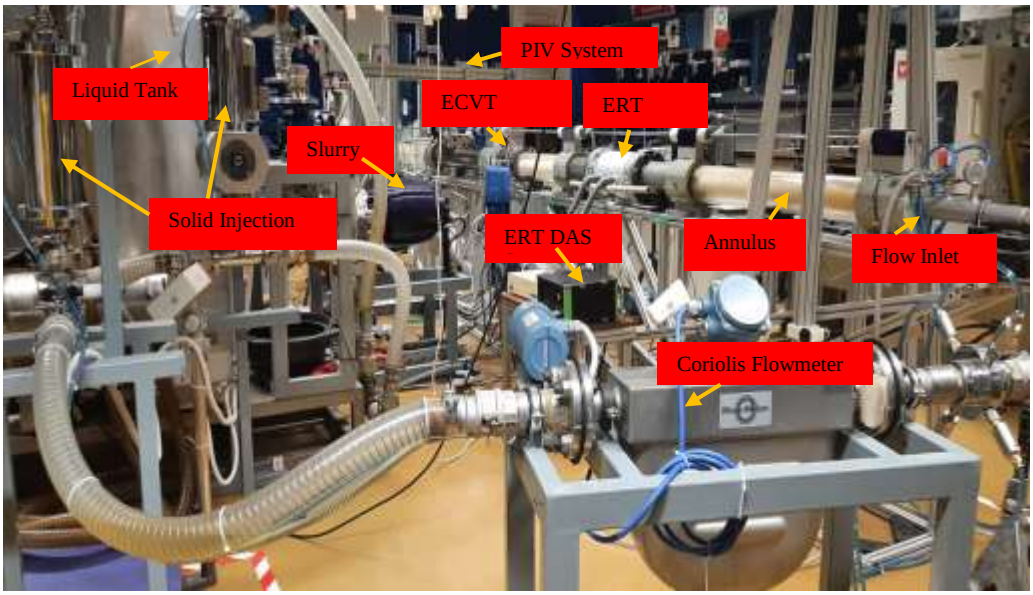

Figure 9 –Real Picture of TAMUQ flow loop during an experiment

Table 3 – Summary of fluid rheological properties

Fluid Properties	**Water**	**0.05 wt.% polymer**	**0.1 wt.% polymer**
Density, Kg/m^3	997	999	1001
Flow behaviour index, n_{HB}	1	0.878	0.557
Consistency index, k_{HB} (Pa.sec^n)	-	0.005	0.064
Yield stress, τ_{HB} (pa)	-	0.229	0.269
Apparent Viscosity, cP	0.889	1.3	1.65

Table 4 – Experiments test matrix

Fluid Type	**Inclination degrees**	**Eccentricity**	**Drillstring rotation RPM**	Mud velocity m/sec
Water Base mud	90	0, 0.3, 0.6	0, 40, 80, 120	0.55, 0.63, 0.72, 0.8
0.05 wt% polymer	90	0, 0.3, 0.6	0, 40, 80, 120	0.39, 0.48, 0.57, 0.64, 0.73, 0.81
0.1 wt% polymer	90	0, 0.3, 0.6	0, 40, 80, 120	0.39, 0.48, 0.59, 0.66, 0.75, 0.84

5. Model Validation

The developed CFD model with all its governing equations were validated with Five experimental data sets from (TAMU Tower Lab - Pedro, 2013; our experiments conducted in TAMUQ horizontal flow loop; Han et al., 2010; Osgouei, 2010; Pedro, 2013; Tang et al., 2016) summarized in **Table 5**.

CFD results show a good agreement with the experimental data on the prediction of annular pressure loss and cuttings concentration with an average absolute error percent (ABE) (1.4 – 8.1%) as shown in **Fig. 10**, **11, 12, 13, 14, and 15.** This proves that our CFD model can be a reliable alternative solution to conventional multiphase flow metering.

Table 5 – CFD Model validation against literature

Geometry	**Tamu Tower Lab**	**Qatar Flow Loop**	**Han et al., (2010)**	**Osgouei (2010)**	**Tang et al., (2016)**
Hole diameter (m)	0.1397	0.1143	0.044	0.0739	0.0614
Pipe diameter (m)	0.06	0.0508	0.03	0.047	Spiral amplitude = 0.665 m
Drillstring Length (m)	43	5	1.8	6.4	Spiral period = 0.075m
Fluid Properties					
Fluid type	Water and air	0.05% Flowzan	0.4% CMC solution	Water	Water
Density (kg/m^3)	997	999	998.5	998.5	998.5
Fluid Yield Stress, $\boldsymbol{\tau_0}$ (Pa.sec^n)	0	0.2287	0	0	0
Flow behavior index, n	1	0.878	0.75	1	1
Consistency index, K (Pas^n)	1	0.00543	0.048	0.001	0.001

Table 5 Cont. –Model validation against literature

Particle properties					
Cutting density (kg/m^3)	-	2550	2550	2761.4	-
Cutting Diameter (m)	-	0.003	0.001	0.00201	-
Porosity	-	-	-	0.36	-
Drilling Parameters					
Drilling fluid velocity (m/sec)	2.71-3.75	0.81	0.41 – 0.66	1.21-1.83	0.56 – 5.6
Rate of penetration ROP (m/s^1) (ft/hr)	-	0.005 (62)	0.00526 (62)	0.00508 (60)	-
Drillpipe Rotation (RPM)	0	0-120	0	100	-
Hole eccentricity, E	0	0	0	0.623	0
Inclination (degrees)	0	90	0 - 60	90	90

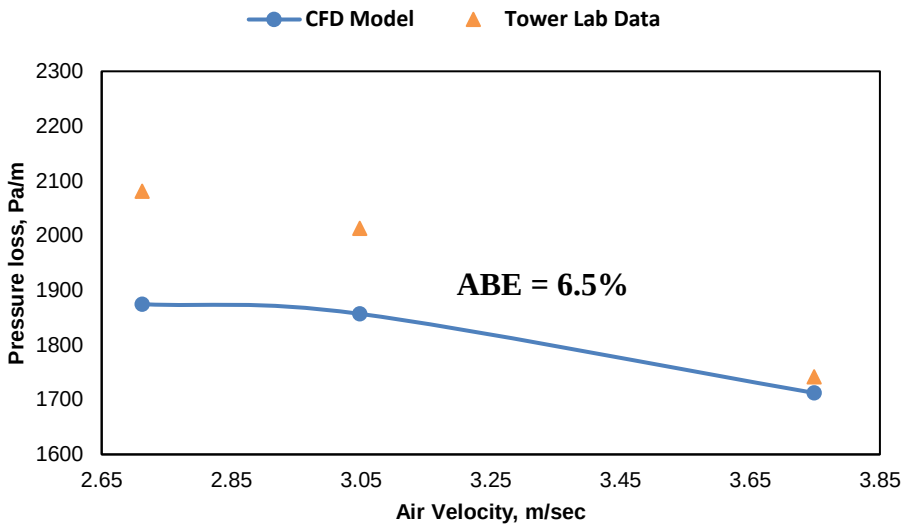

Figure 10 –CFD model vs Tower lab experimental data conducted by Pedro, 2016

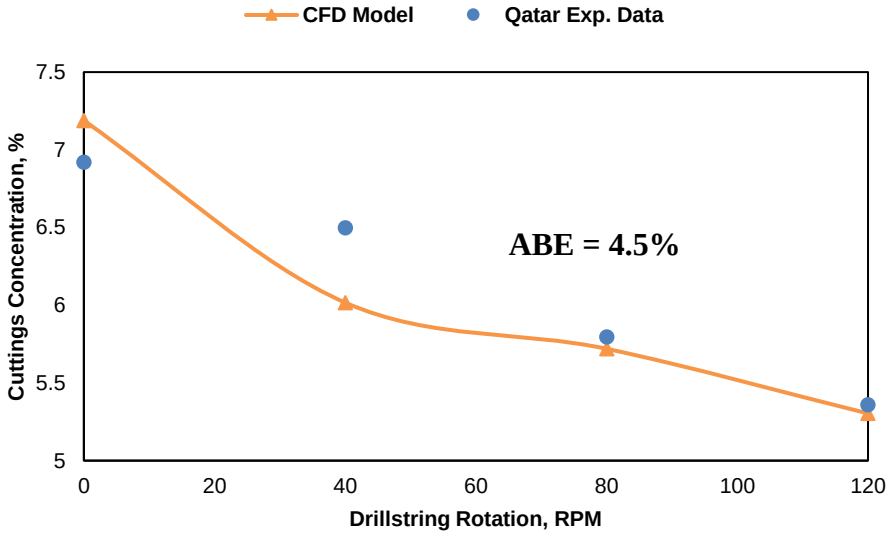

Figure 11 –CFD model vs TAMUQ flow loop

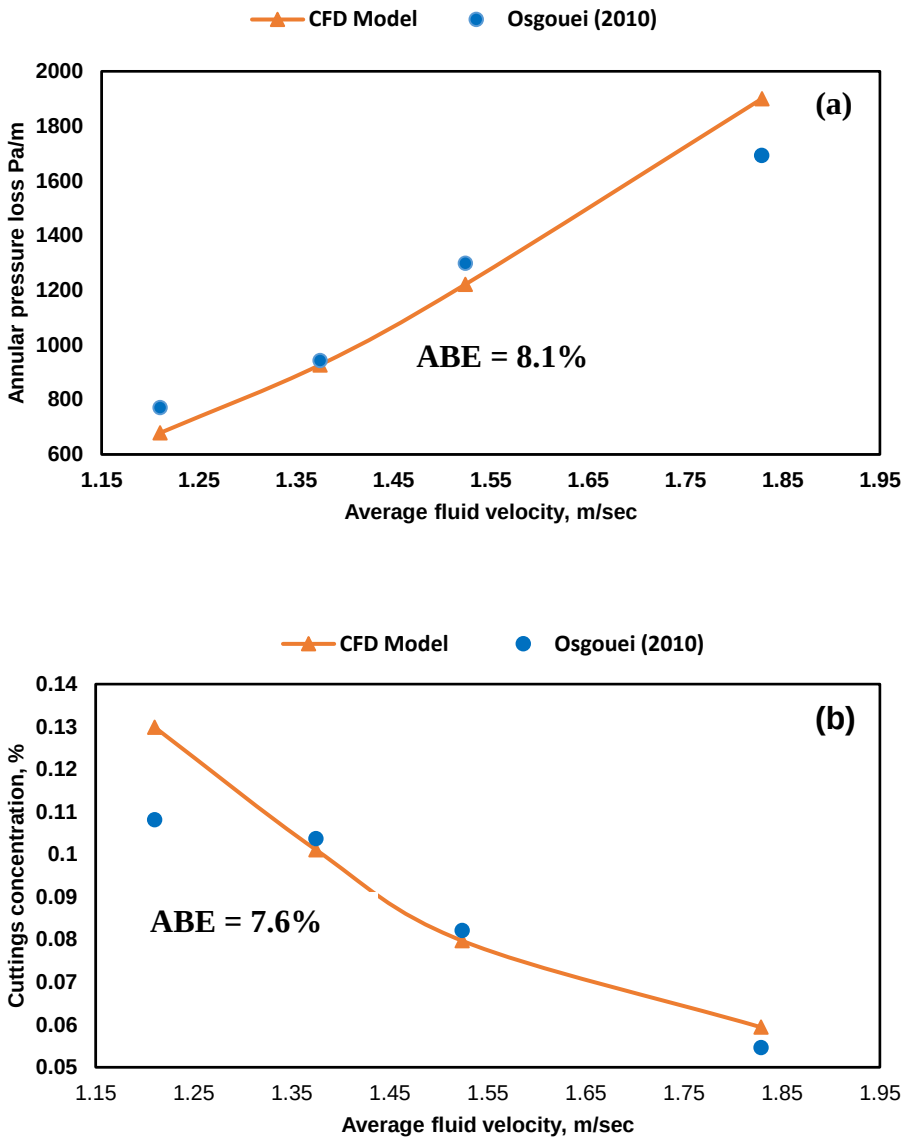

Figure 12 –CFD model vs Osgouei, 2010 at zero RPM and ROP=60 ft/sec: (a) Annular pressure validation; (b) Cuttings concentration validation

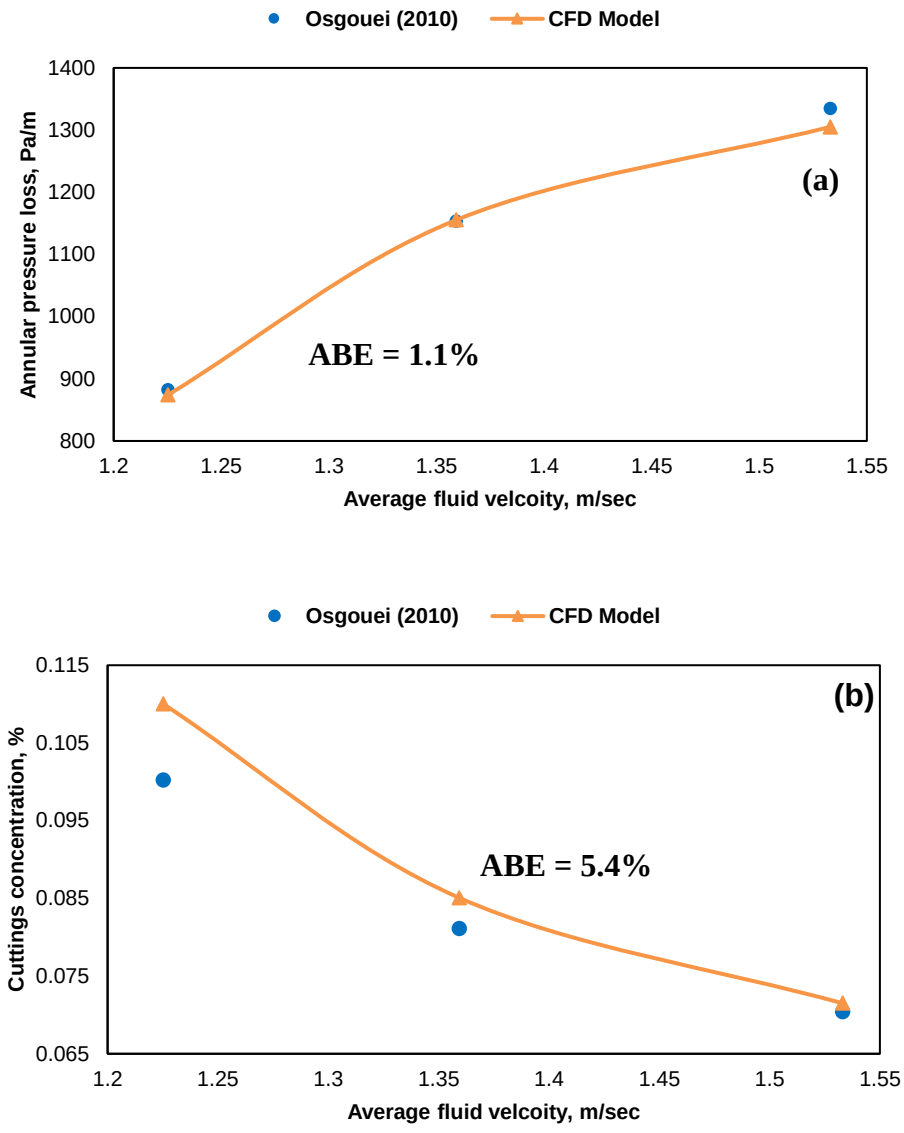

Figure 13 –CFD model vs Osgouei, 2010 at 80 RPM and ROP=60 ft/sec: (a) Annular pressure validation; (b) Cuttings concentration validation

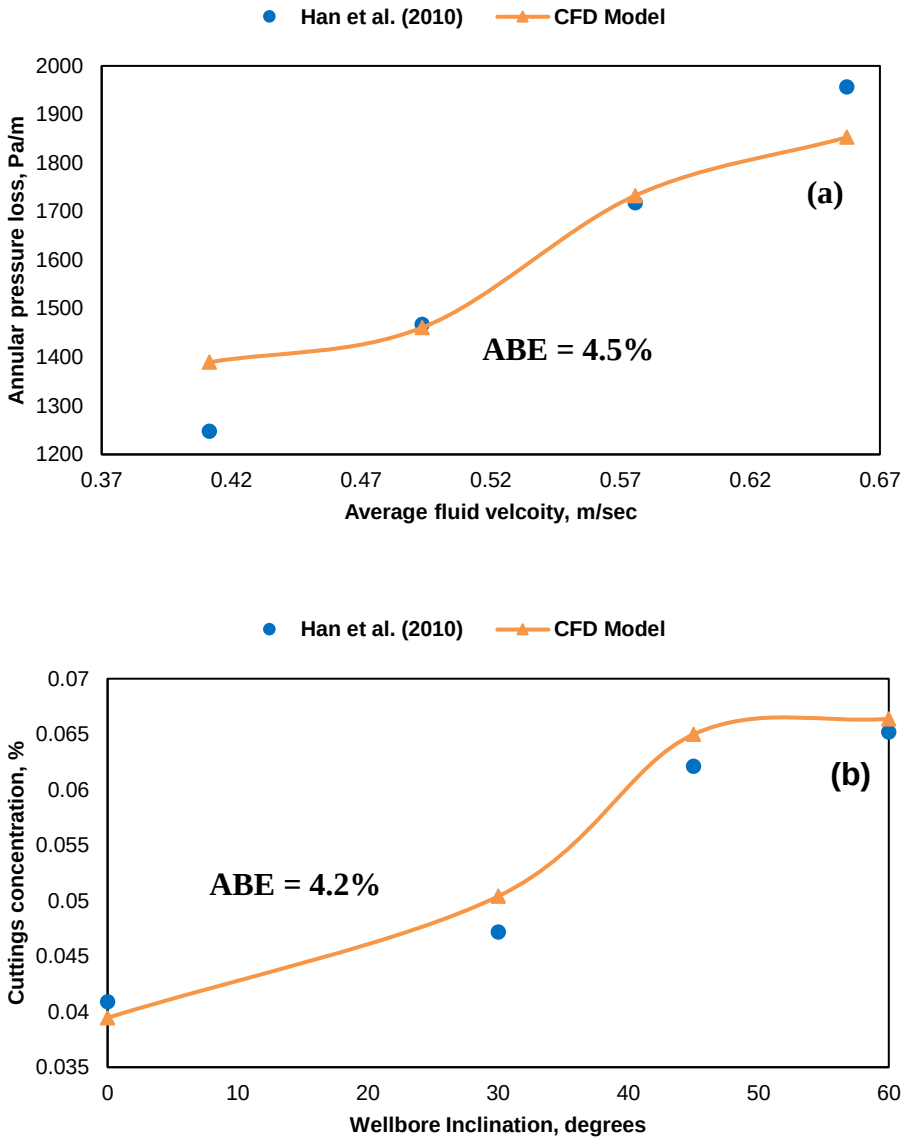

Figure 14 –CFD model vs Han et al., 2010

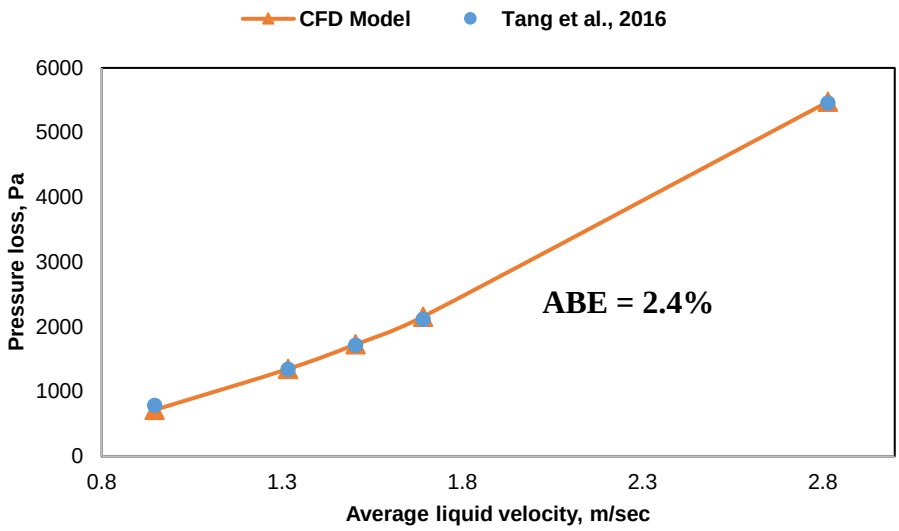

Figure 15 –CFD model vs Tang et al., 2016

CHAPTER IV

RESULTS AND DISCUSSION

The main objective of this study is to investigate the dynamics of solid-liquid flows in inclined wellbores by Herschel Bulkley drilling fluids at different ranges of operating parameters (flow rate, penetration rate, drillstring rotation, and eccentricity), wellbore configuration (hole size, wellbore inclination, and wellbore tortuosity), fluid parameters (density and rheology), and cuttings parameters (cuttings density, and size).

1. Effect of Drilling Flow Rate

Drilling fluids (drilling mud) are used to circulate rock fragments cut by the bit from bottomhole through the annulus between drillstring and wellbore to the surface. The effects of changing drilling flow rates on cuttings concertation and annular pressure loss is shown in **Fig. 16 & 17**. It is clear that as the liquid flow rate increases cuttings concentration decreases. This can be attributed to the enhancement of the cuttings carrying capacity of the fluid and bed erosion when the liquid flow rate is increased. In addition, an increase in the annular pressure drop is observed as the velocity increases, due to the friction between the mixture and the pipe at a higher flow rate.

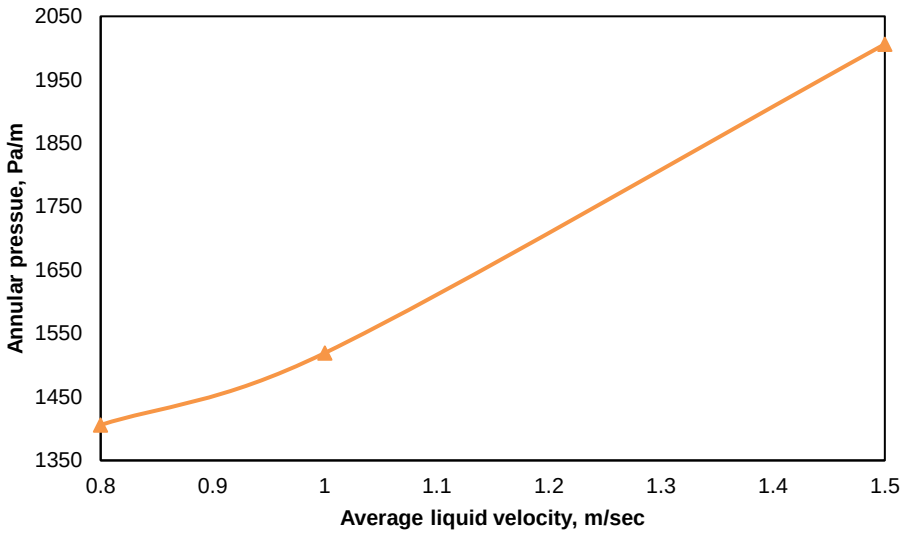

Figure 16 –Effect of drilling flow rate on annular pressure loss

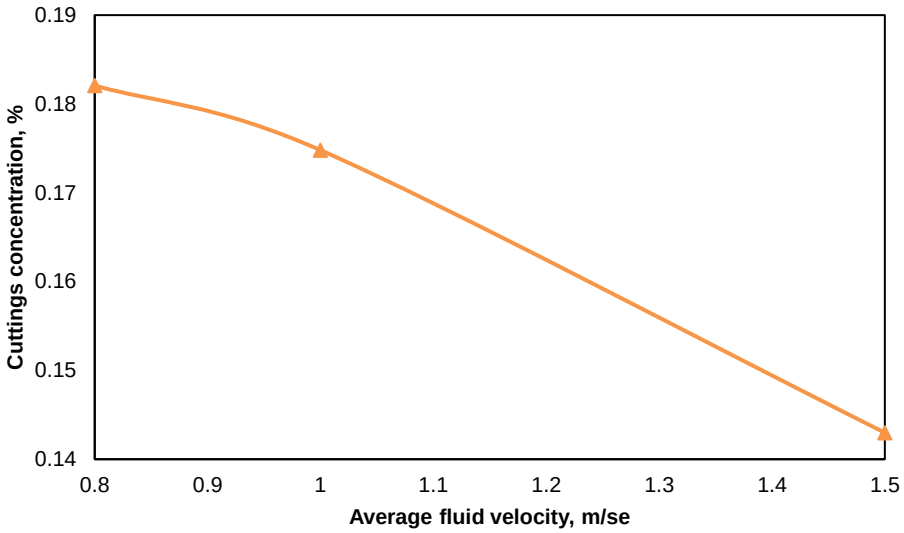

Figure 17 –Effect of drilling flow rate on cuttings concentration

2. Effect of Hole Enlargement

The flow rates and fluid properties normally used by industry in a given hole size allow for relatively high drill rates with very little risk or restriction in drill rate. When these do occur, the root cause is usually hole enlargement due to inadequate fluid density for hole stability. The impact of hole enlargement on cuttings concertation is shown in **Fig. 18**. It is clear from the figure that hole enlargement has a huge adverse effect on the fluid carrying capacity. The fluid velocity falls in the enlarged section and cuttings concentrate.

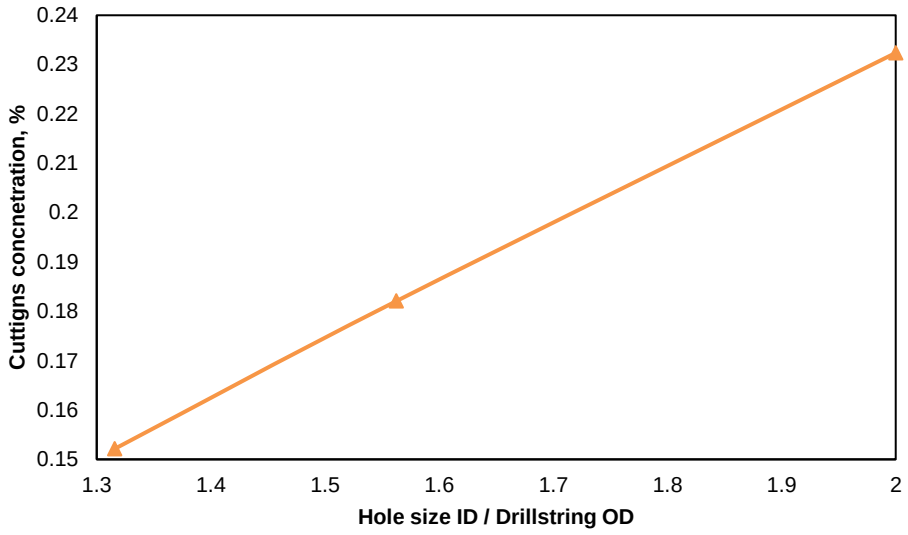

Figure 18 –The impact of hole enlargement on cuttings concentration

3. Effect of Fluid Rheology

The main objective of this study is to investigate the effect of fluid rheology on cuttings transport in horizontal wells. Due to the limited data in the literature for drilling fluid adapted with Herschel-Bulkley rheology model. This study was conducted to with Power Law drilling fluid to investigate the impact of fluid rheology on cuttings concentration.

3.1. Impact of Drilling Fluid Rheology on Cuttings Accumulation

The flow geometry utilized in this study is a horizontal pipe of 2m in length with two walls. The outer wall is stationary and has a diameter (D_o) equals 0.0739m and represents the wellbore. While the inner wall represents the drillstring used while drilling with a diameter (D_i) 0.047m. Inner wall was kept either in stationary or in a rotation mode based on the analysis done. Since drillstring in deviated and horizontal wells have the tendency to lay down on wellbore low side due to gravity. Therefore, annuli eccentricity (E) is assumed to be equal to 0.6. Nine different drilling fluids were adopted in this model inspired from Iyoho (1980) and Okrajni and Azar (1986) to examine the effect of fluid rheology on cutting transport in horizontal well profile. Fluid rheological constants are summarized in **Table 6**. The Power law model was used to describe the non-Newtonian fluid rheology.

Water and low viscosity mud (LVM) used in this analysis are flowing in a turbulent flow regime while circulation. While laminar flow regime was studied by using high viscosity mud (HVM) and Carbopol (CARB). In addition, the medium viscosity mud (MVM) is in transitional flow behavior. The numerical simulation output results are

solid axial velocity and concentration (volume fraction) along the radial distribution of planes 1-4. Solid axial velocity and volume fraction contours are presented for visualization of drillpipe rotation effect on hole cleaning. It is important to point out that the solid axial velocity reported in this study is normalized to the bulk flow velocity.

Table 6 –Mud rheology data extracted from Iyoho, Ph.D. Thesis and Okranji & Azar, SPE-14178-PA

Fluid	**Density, Kgm-3**	n	K (Pas^n)	**Flow regime**
Water	998.7	1	0.001	Turbulent
Low Viscosity Bentonite (LVM)	1006.5	0.68	0.04	Turbulent
Medium Viscosity Mud (MVM)	1006.5	0.61	0.209	Transitional
CARBOPOL (CARB)	1012.5	0.64	0.283	Laminar
High Viscosity Bentonite (HVM)	1018.5	0.61	0.44	Laminar
Fluid 1	1012.5	0.74	0.049	Turbulent
Fluid 2	1012.5	0.59	0.088	Turbulent
Fluid 3	1018.5	0.42	1.044	Laminar
Fluid 4	1018.5	0.74	0.33	Laminar

To investigate solid particle behavior while circulating inside the annulus between the two walls, the designed geometry was divided into four main planes as shown in **Fig. 19**. So that the radial distribution of fluid properties (velocity, and volume fraction) can be observed. Plane 1 represents the wide region between the top of the drillpipe and wellbore, while plane 3 represents the narrow gap between drillpipe and hole.

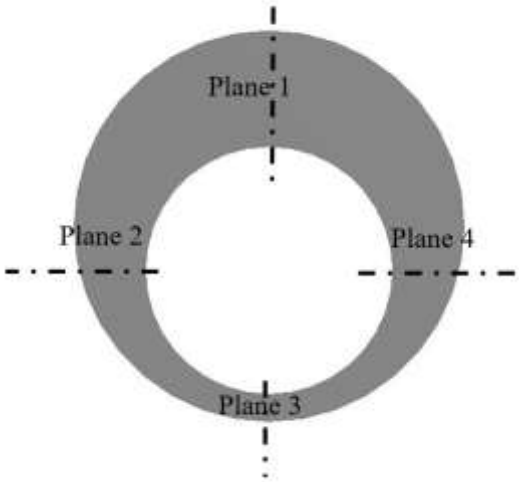

Figure 19 –Geometry set-up with line planes

3.2. Model Geometric Condition

The solid volume fraction across the four planes is presented in **Fig. 20**. It demonstrates that the maximum cuttings (solid) concentration with all drilling fluids is observed on plane 3 (the narrow part of the annulus). This can be related to the gravity impact that aggravates solid slip, phase segregation, and eventually leads to bed accumulation. The maximum cuttings concentration (0.63) was reported when HVM or CARB mud was used as a circulating fluid. On the other hand, water and LVM seem to

be more efficient on hole cleaning and cuttings cleanout operation with a less solid concentration on plane 3. High solid volume fraction on the narrow section can be attributed to pipe eccentricity and fluid flow regime. Pipe eccentricity occurs in high inclination wells because drillstring tends to lay down on the wellbore low side due to the gravity effect. Okrajni and Azar (1986) showed that pipe eccentricity impact is more noticeable at high wellbore inclination (55-90). Pipe eccentricity leads to uneven distribution of velocity profiles across wellbore section. Fluid will flow faster in the wider region than in the narrower part. So cuttings accumulation will increase in the narrower part and cutting bed removal become difficult due to this flow diversion. In addition to pipe eccentricity, fluid flow regime is a very important factor for hole cleaning. Although HVM and CARB flow in a laminar flow regime that is very efficient in cuttings suspension and cuttings removal in vertical wells; this merit reduces and vanishes when wellbore inclination reaches 90 degrees. Because the fluid drag force will be perpendicular to the gravitation force and will have a very small effect to compensate this gravitational force. On the other hand, LVM and water flow in turbulent flow regimes that has a chaotic fluid movement allows the transfer of momentum and velocity distribution more uniformly than laminar. So, drilling fluid will penetrate the narrower part more effectively and decrease the effect of flow diversion resulted from hole eccentricity. In addition to that, fluid in turbulent flow increases frictional pressure loss resulting on inducing more shear stress across the bed surface and eventually helping on cutting bed removal. These findings agree with the experimental results reported from Ozbayoglu et.al (2009) and Mohammad Salehi et.al (2012) that Increasing liquid

viscosity will increase bed area and increase the required flow for hole cleaning. It is observed that there is a slight increase of solid concentration in plane 2 when LVM and water are used as a circulating fluid accompanied by low solid axial velocity in this area. This can be due to the turbulent flow behavior of LVM and water. There is also an asymmetry profile of solid concentration curves between planes 2 and 4 in case of water and LVM. Solid volume fractions in all planes are distinct with off center peaks. Solid particles tends to be lower near the walls and maximum at the center. This proves that solid cuttings tends to travel in the center of the annulus during mud circulation similarly to the fluid flow behavior of non-uniform fluid distribution. It is important to point out that although water is very efficient in cleaning the narrow part (low side) of a horizontal pipe due to its low viscosity and turbulent flow initiation at low flow rates. It is preferable to use low viscosity non-Newtonian fluids than water that had yield stress and thixotropic property for efficient hole cleaning.

Fig. 21 demonstrates solid axial velocity across the four planes. It shows a clear symmetry of axial velocity profiles across planes 2 and 4 for laminar flow that is reflected on solid volume fraction figures. Besides that, a high axial velocity in plane 3 with LVM and water is noticed that is another evidence of hole cleaning enhancements. It is also observed there is a clear asymmetric profiles of axial velocity across all planes of LVM and only on plane 1 and 3 for MVM, HVM, and CARB. This observation supports the previous conclusion on the impact of pipe eccentricity and flow diversion on cuttings accumulation on the narrow side of the wellbore.

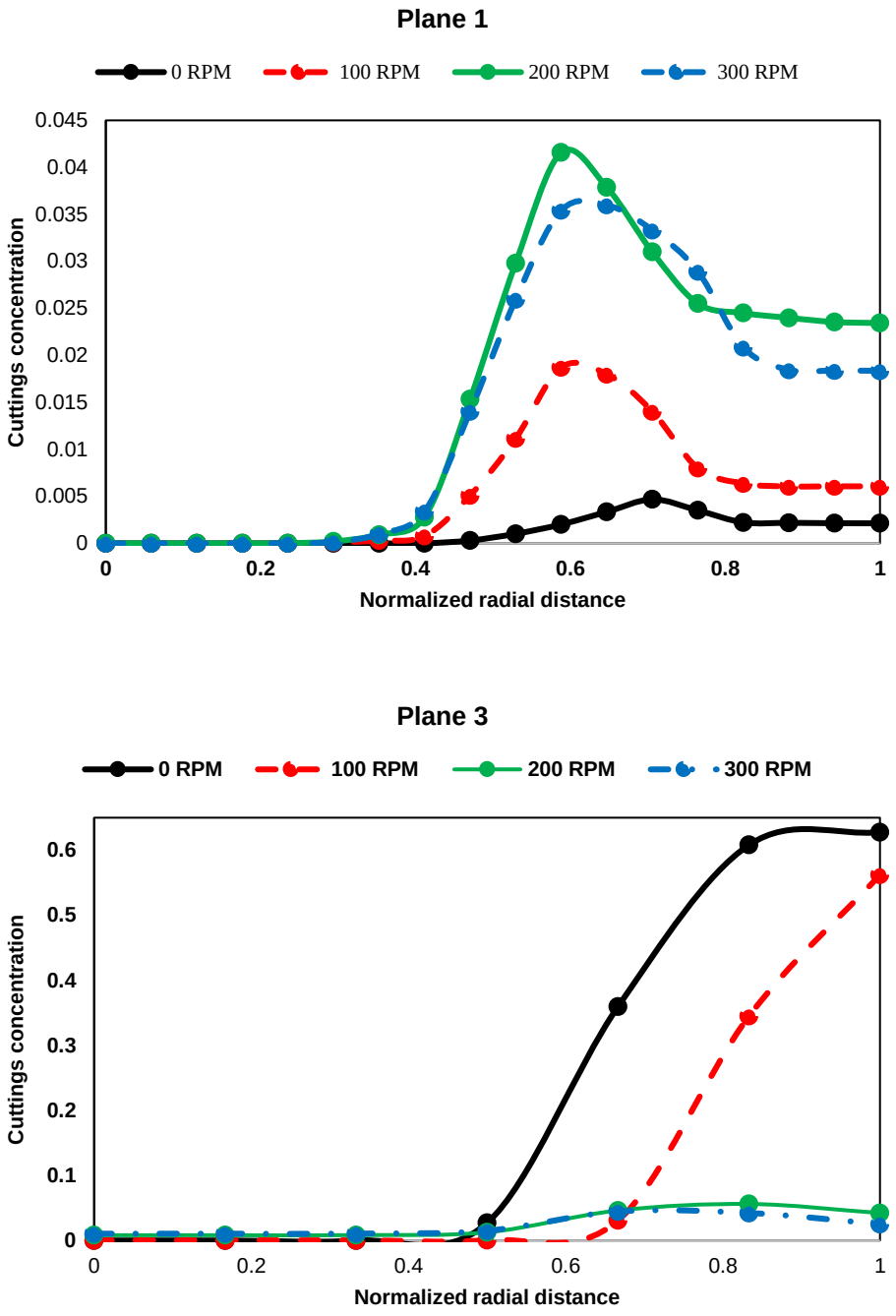

Figure 20 –Cuttings volume concentration profiles

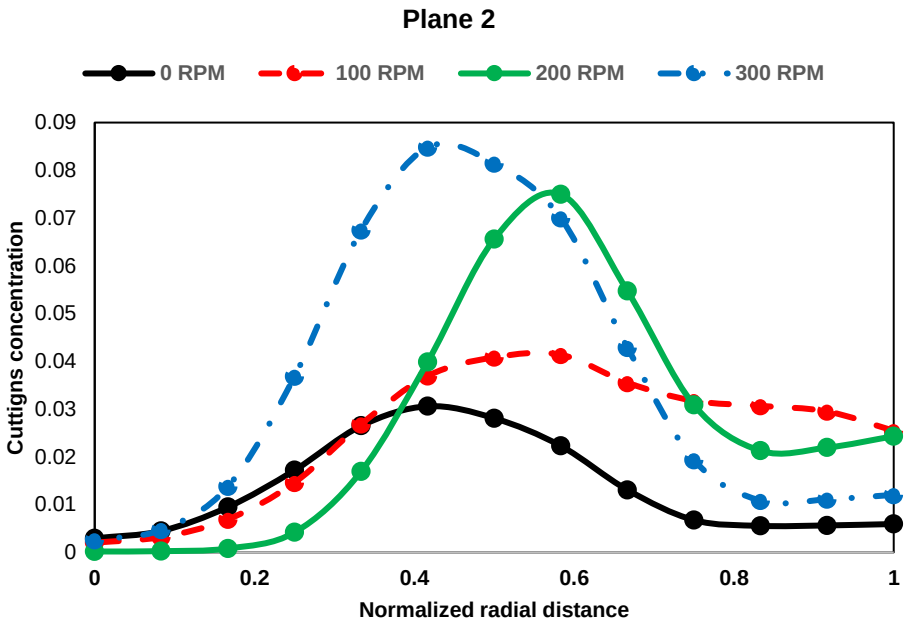

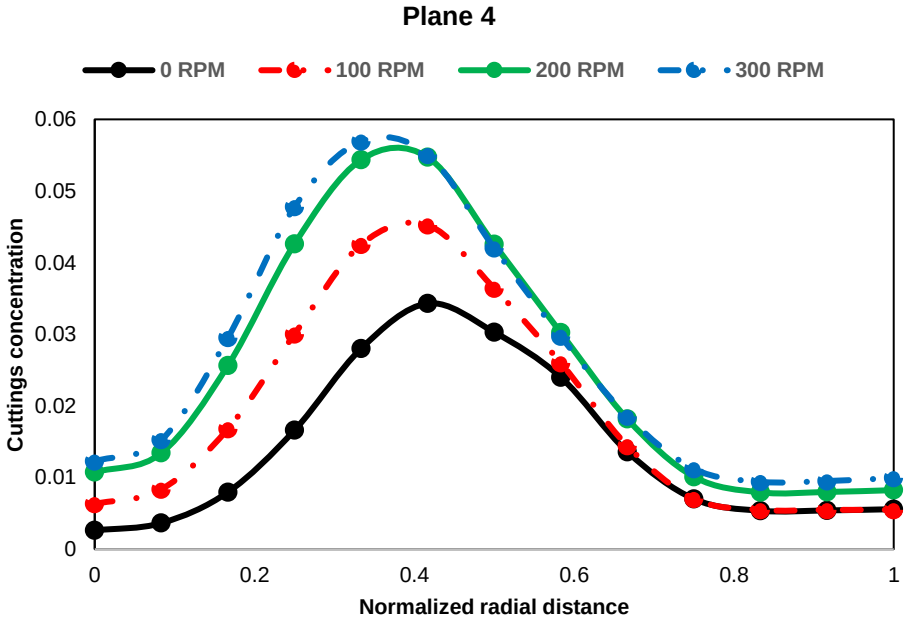

Cont. Figure 20 –Cuttings volume concentration profiles

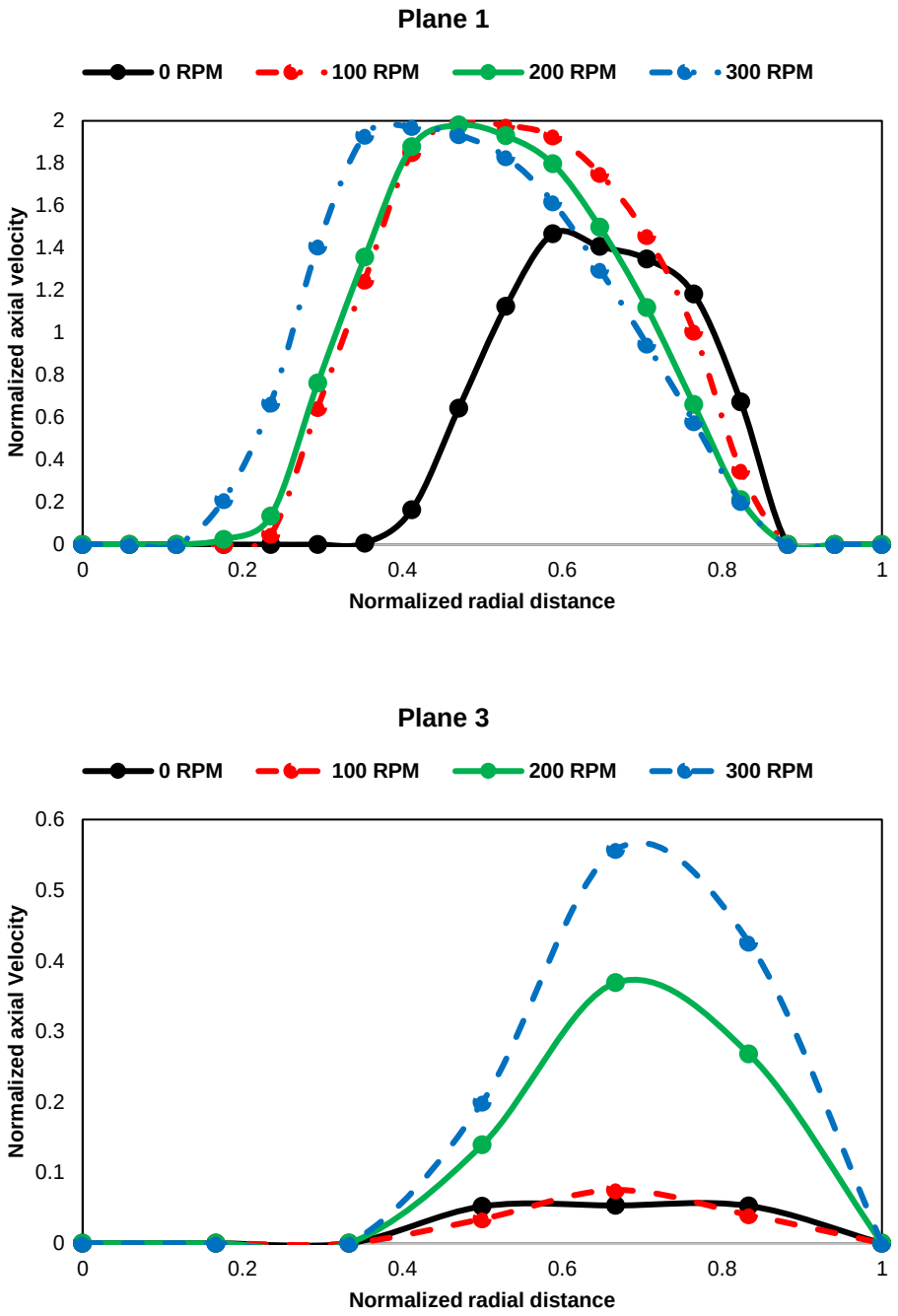

Figure 21 –Normalized axial velocity profiles

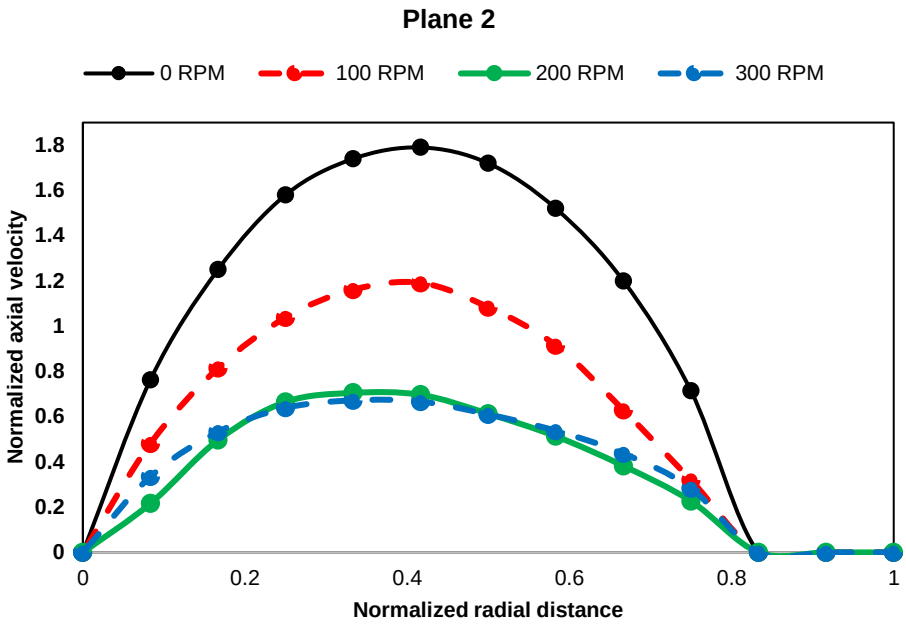

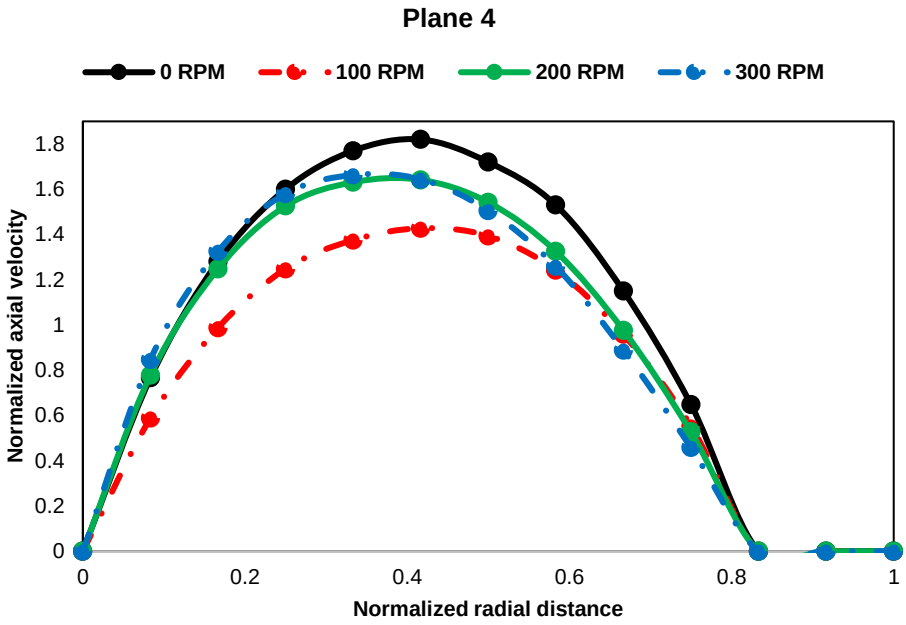

Figure 21 Cont. –Normalized axial velocity profiles

3.3. Drillstring Rotation

Since the HVM study was the worst mud rheology compared to other fluids for cuttings transport as indicated in the previous section. Drillstring rotation effect on enhancing or aggravating HVM performance for cuttings transport was examined. The outer wall is assumed as a stationary wall, while the inner will rotate in a clockwise direction to simulate drillstring rotation in wellbore.

It was noticed that cuttings concentration was dramatically reduced in the narrow part of the eccentric annulus as shown in **Fig. 22** and solid volume fraction contours (cuttings concentration) in **Fig. 22** when inner cylinder rotation increased. This is attributed to the increase of drilling fluid tangential velocity when drillpipe rotates leading to the generation of more drag force on cuttings bed and enhancing cuttings removal. Besides that, Epelle and Dimitrios (2018) showed that drillpipe rotation leads to shear-thinning behavior of the non-Newtonian fluids with viscosity variation around the annulus. This phenomenon can also help in limiting flow diversion occurrence across the eccentric annulus and allow more cuttings transport.

Solid concentration in **Fig. 22** increases in all planes except plane 3 with more drillpipe rotations. This is can be visualized from the area under the curves of all planes. This phenomenon occurs because when drillpipe rotates. It erodes cuttings bed and sways solid particles away against gravity from the narrow part (low side) to the wider areas. So solid concentration decreases on the narrow part of the annulus and increases on the other location. This can be clearly viewed in the solid volume fraction contours in **Fig. 22.** Contours show that solid particles shifted away from the narrow part and

distributed across the whole profile. It can be argued that drillstring rotation aids in keeping homogenous solid concentration around the pipe in the horizontal annulus. Cuttings fraction peaks (maximum value) shift away from the inner pipe axis toward the outer wall due to the rotational effect of mixing solid particles with liquid flow.

These curves also show that as drillstring rotation increases, cuttings concentration decrease until certain value of pipe rotation is reached. Above this value, reduction in solid concentration is negligible with more pipe rotation. This can be viewed from 200 & 300 RPM case, where no improvement in cuttings removal is recorded when rotation increased from 200 to 300 RPM. This observation was also reported from Omid et.al (2017) and Pang et.al (2018) about drillpipe rotation impact for cuttings transport is negligible above a certain point.

Similarly, solid axial velocity increases at plane 3 and decreases in plane 2 and 4 due to an increase in drillstring rotation as shown in **Fig. 21** and axial velocity contours in **Fig. 23**. This matches the previous conclusion about the impact of pipe rotation on applying extra stresses on cuttings bed and divert the solid particles to other locations in the annulus away from the narrow part in the annulus. This is why solid axial velocity in plane 2 was clearly reduced with more pipe rotation due to more solid concentration. It is also noted that as pipe rotation increases, an increase in the asymmetry behavior of axial velocity across all planes.

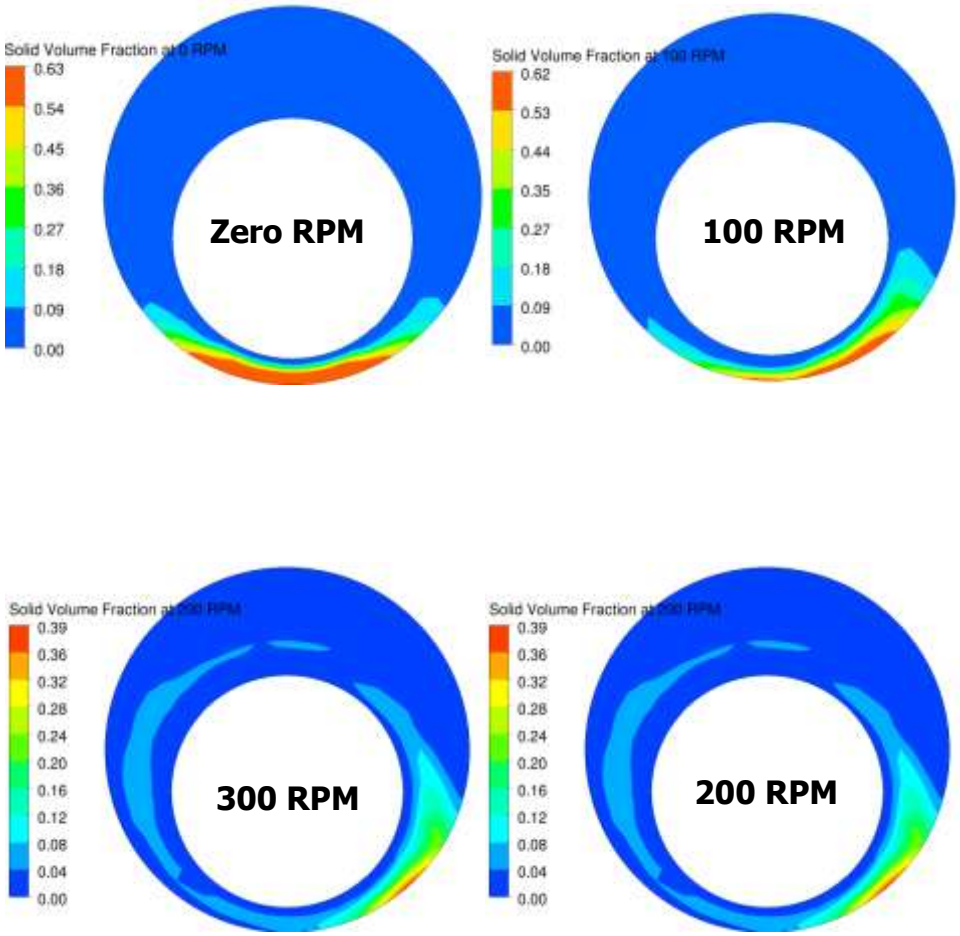

Figure 22 –Cuttings volume fraction contours at different RPM

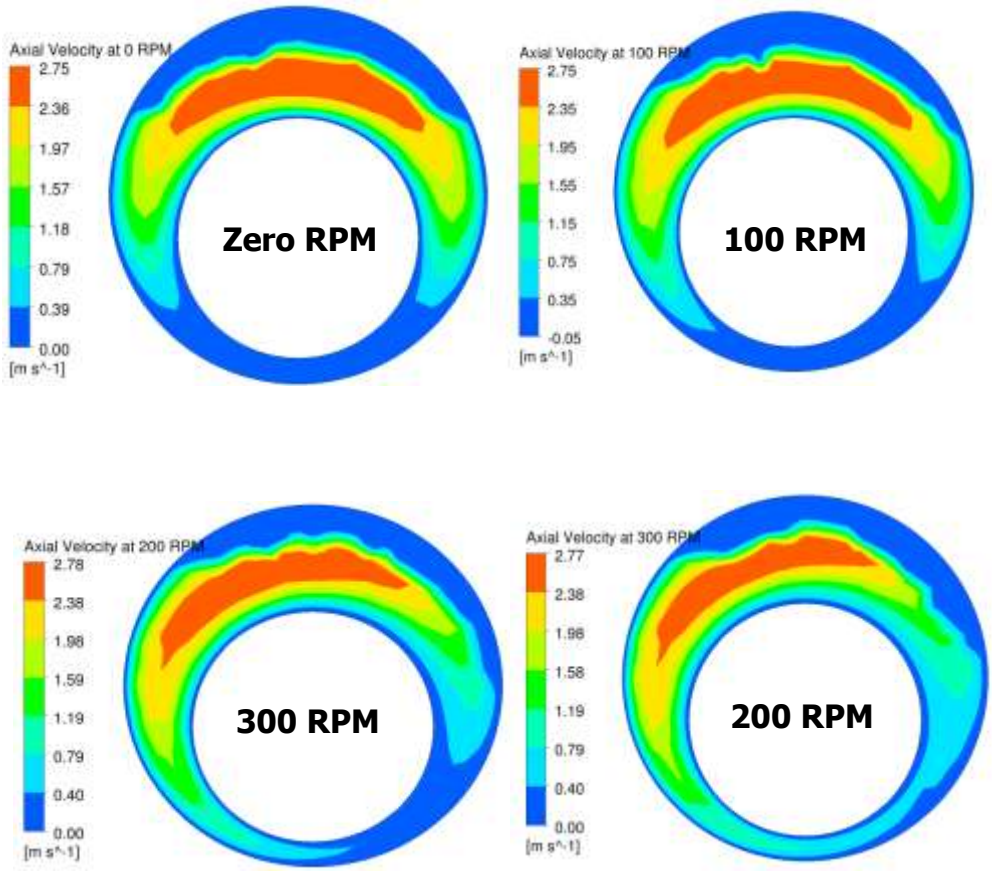

Figure 23 –Axial velocity contours at different RPM

3.4. Cutting Removal and Drilling Fluid Rheology

Based on the previous analysis, low viscosity fluids perform much better than high viscosity mud in cuttings transport on horizontal wells. But, what is the best approach drilling engineers on the oil fields can use to decide the optimum mud properties? or what is the best rheological parameter that can be used to predict the fluid performance in cuttings transport if a hole cleaning problem is encountered? Therefore, different drilling fluid parameters were examined: effective viscosity (U_e), plastic viscosity (PV), yield point/plastic viscosity (YP/PV) ratio, and Power Law flow behavior

index/consistency index (n⁄K) ratio to study their impact on reducing or aggravating cuttings concentration on the well narrow side as shown in **Table 7**.

Table 7 –Drilling fluids with different rheology

Drilling fluid	Flow regime	U_e (Kg/m.s)	PV (CP)	YP/PV	n/K	Bed deposition
1	Turbulent	0.005161	3	0.67	16.9	0.30
2	Turbulent	0.00907	6	0.5	14.9	0.31
3	Turbulent	0.006144	3	1	6.64	0.34
4	Transitional	0.0172	9	0.89	2.93	0.36
5	Laminar	0.0244	8	2	0.4	0.33
6	Laminar	0.030611	19	0.89	1.37	0.39
7	Laminar	0.06064	40	0.5	2.2	0.42

After comparing previous fluid properties with the accumulated bed concentration located on the horizontal wellbore narrow area, it was observed that:

a- the best way to minimize the bed height when the flow is in a turbulent or transitional regime is to keep n⁄K ratio high. n⁄K ratio of 15 or more shows a good cleaning effect in our case study. n⁄K ratio can be interpreted as an inverse function of drilling fluid viscosity as reported by Adari et.al (2000). So high n/K ratio represents low fluid viscosity and strong turbulent flow. **Fig. 24** shows that as n/K ratio decreases, cuttings accumulate and bed height increases in the wellbore low side.

b- **Table 7** and **Fig. 25** show that for laminar flow, cuttings concentration decreases when U_e or PV decreases or YP/PV ratio increases. These three variables can help in optimizing the efficiency of fluid rheology in cuttings transport under a laminar flow regime. A ratio of 2 for YP/PV performs good in hole cleaning and cuttings removal in this study.

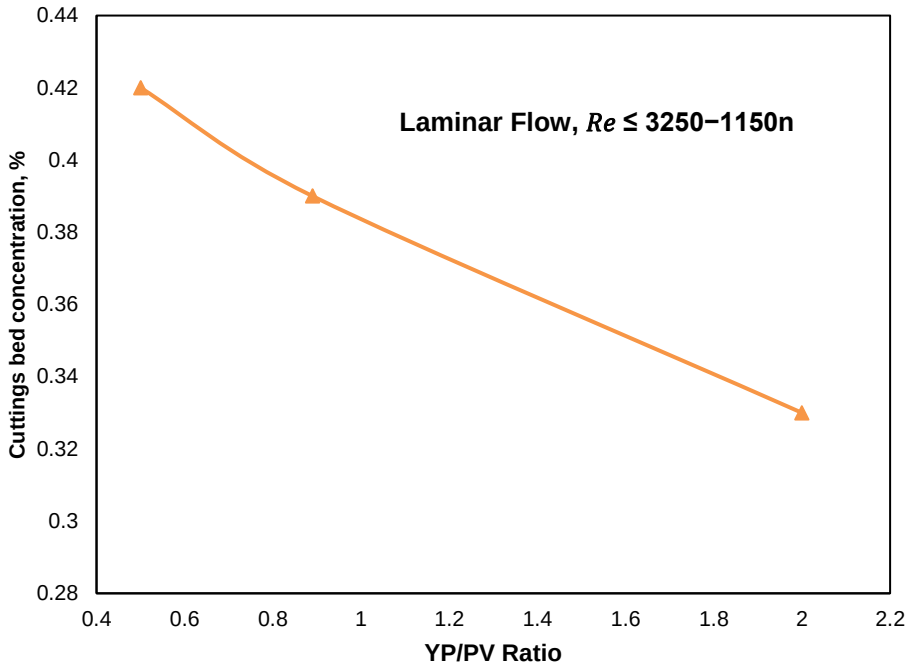

Figure 24 –YP/PV vs cuttings bed concentration for laminar flow

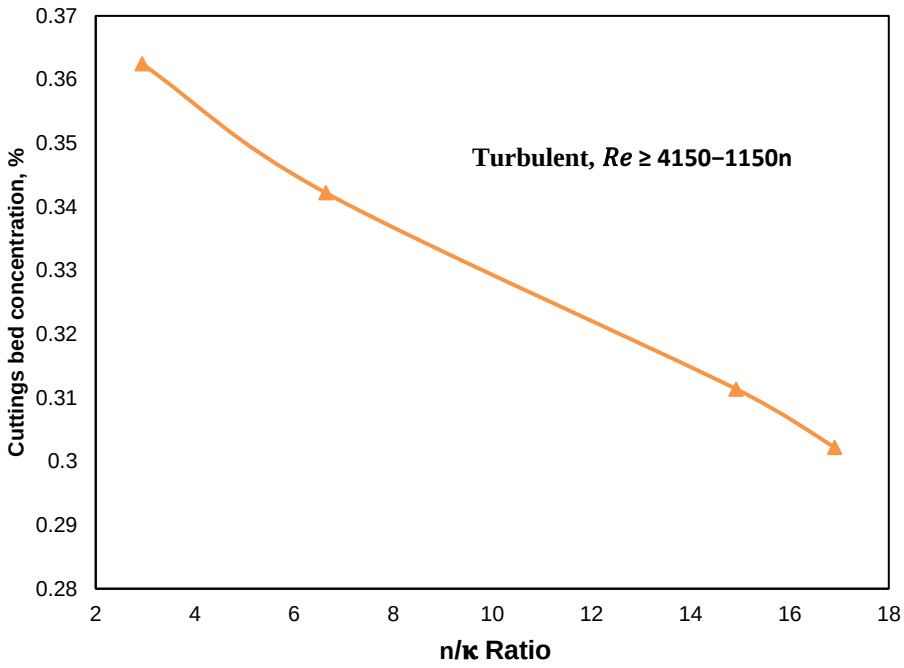

Figure 25 –n/K vs cuttings bed concentration for turbulent flow

4. Drillstring Rotation

Fig. 26 shows the impact of the different drillstring rotation per minute (RPM) from 0 to 500 RPM on cuttings concentration and annular pressure loss. As the drillstring rotates, cuttings volume fraction decreases significantly even at slow drillstring rotation. This can be related to the increase of fluid tangential velocity, and centrifugal force acting on the cuttings during rotation which enhances the erosion effect of the cuttings bed. When drillstring rotates, cuttings are swept from the narrow part to the widest part in the annulus. This helps the cuttings in the lower side of the annulus to be agitated into the liquid and eventually improves the cutting transport to the surface. In

addition, the friction between the rotating pipe and fluid causes some additional transverse flow that is added to the axial velocity. It gives the fluid more velocity, which allows it to erode the bed to a lower height, which opens up more flow area above. This proves the necessity for drillstring rotation for efficient cuttings transport in deviated and horizontal wells to prevent cuttings deposition. In addition, there is no much improvement in cuttings concentration when drillstring rotates above 200 RPM. This coincides with observations reported by Omid et al. (2017); Pang et al. (2018) that drillpipe rotation improves cuttings transport till a certain point. When drillstring rotates above this point, its impact on cuttings removal will be marginal.

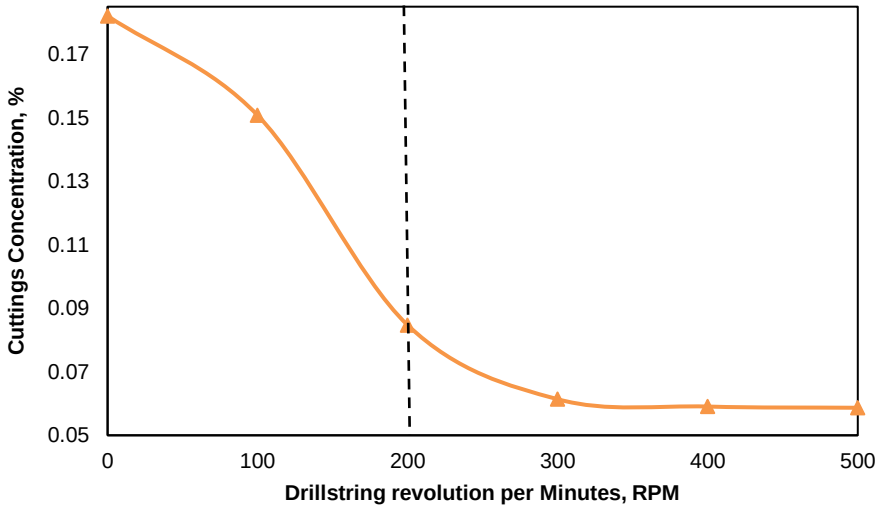

Figure 26 –Effect of drillstring rotation on cuttings concentration

5. Drilling Rate of Penetration

Fig. 27 depicts the impact of drilling rate of penetration (ROP) from 50 to 150 ft./s (0.00423-0.0127 m/s) on cuttings concentration. As the drilling rate increases, more cuttings will be generated by drill bits, and frictional forces between the solid particles

increases, Thus, drilled cuttings will lose some energy due to collision between each other's & walls, and cuttings kinetic energy will decrease. So cuttings concentration increases with a high drilling rate.

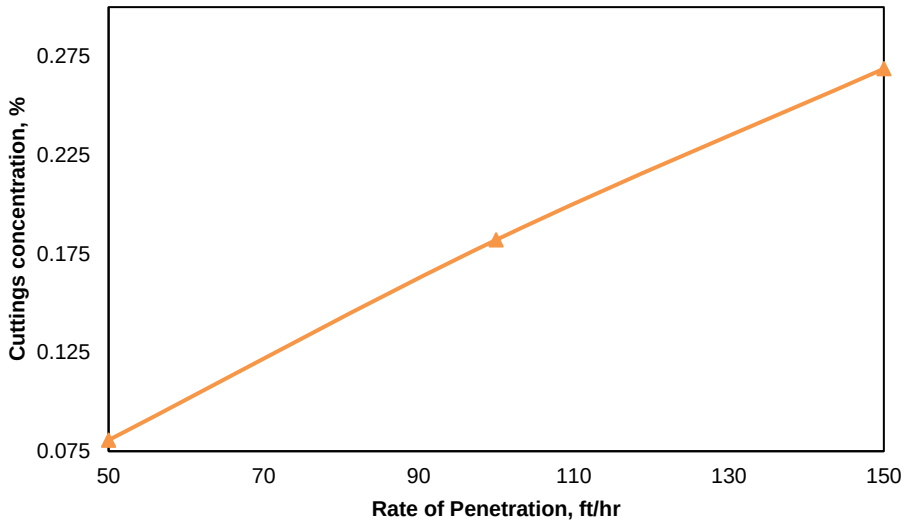

Figure 27 –Effect of drilling rate of penetration on cuttings concentration

6. Annular Eccentricity

Since the drillstring in deviated wells have the tendency to lay down on wellbore low side due to gravity, the cuttings concentration and annular pressure gradient at different annular eccentricities is demonstrated on **Fig. 28 & 29**. It shows that annular eccentricity aggravates cutting deposition and bed height. As the drillstring leans downward more (eccentricity increase), it will reduce the flow area available for the cuttings on wellbore low side, and eventually cuttings accumulation increase. It is shown that eccentric annulus yields a lower annular pressure loss than concentric annulus. This can be attributed to the reduction in the annular mixture velocity in the narrow part and

the larger suspended layer area that have lower resistance to flow. This observation was also reported by Epelle and Gerogiorgris (2017) in an eccentric smooth hole.

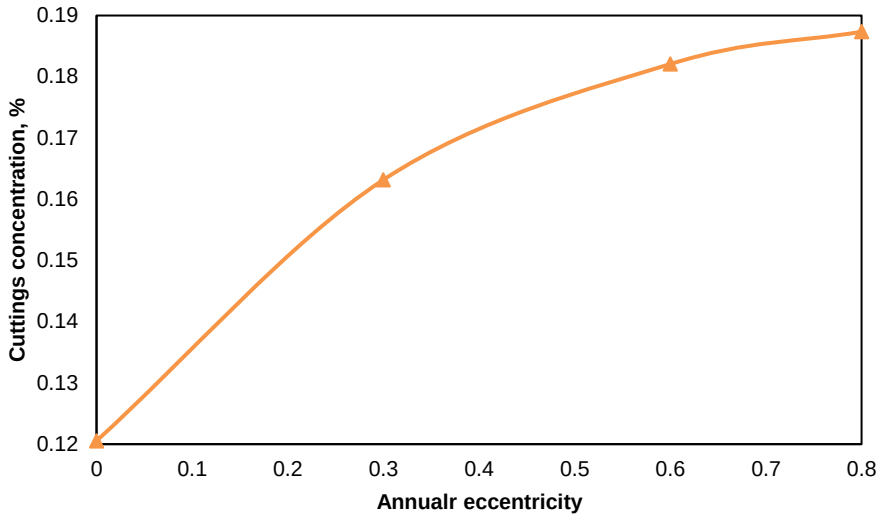

Figure 28 –Effect of annular eccentricity on cuttings concentration

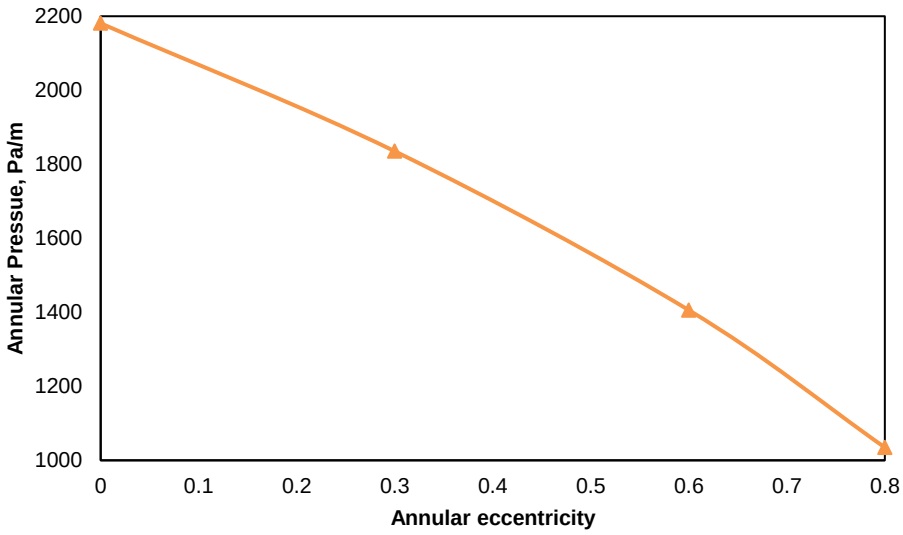

Figure 29 –Effect of annular eccentricity on pressure gradient

7. Wellbore Inclination

The impact of wellbore inclination on cuttings concentration of Herschel Bulkley fluid is investigated as shown in **Fig. 30**. It can be seen that the cuttings concentration does not change much from vertical to 30 degrees wellbore inclination due to the dominance of fluid lift force and preventing particles tendency to settle in the lower side of the annulus induced by gravity. Thus the symmetrical distribution of the solid particles in the annulus occurred (suspended solid particles without formation of a cuttings bed). However with the increase of wellbore inclination beyond 30 degrees, cuttings accumulation aggravates due to the reduction in the impact of drilling fluid lift force as the wellbore inclination increases, and cuttings transportation shifted from the lifting mechanism to the rolling mechanism. Moreover, the inclination angles from 45 to 60 degrees is the hardest interval for hole cleaning. This can be attributed to the reduction of liquid drag force on particles for inclination range 45-60 degrees, while cuttings transport in horizontal is easier through different mechanisms such as rolling. This conclusion matches with Li and Walker (2001) finding that wellbore inclination of 60 degrees is the hardest to clean out.

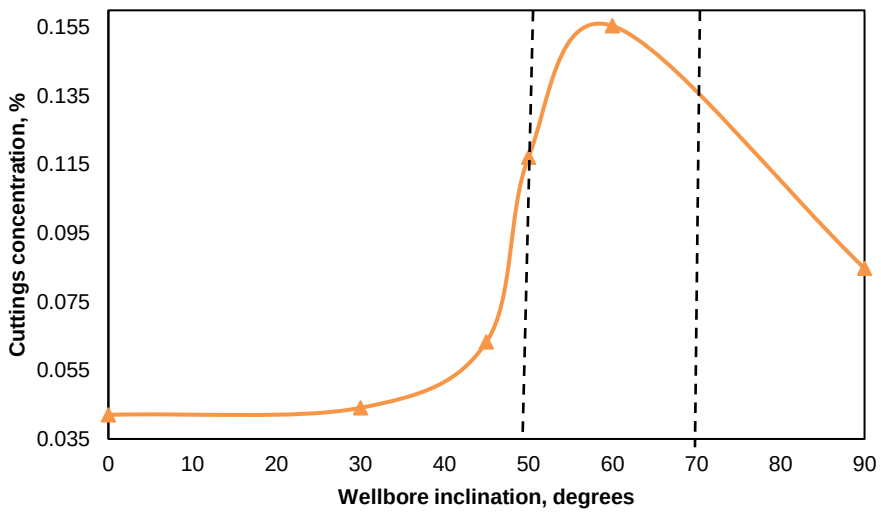

Figure 30 –Influence of wellbore inclination on cuttings accumulation

8. Cuttings (Particle) Size

Cuttings density can be determined by measuring rock specific-gravity obtained on shale shakers. On the other hand, cuttings shape and size are related to formation lithology and bit type used while drilling. The effect of particle sizes on cuttings removal is very contradicting in the literature because most of these studies focus on specific particle size ranges. Martins et al. (1996) and Epelle and Gerogiorgis (2018) showed that larger particles are harder to transport than smaller ones. However, Azar et al. (1990) and Larsen et al. (1990) observed smaller particles are harder to clean out.

Therefore to study the effect of particle size on cuttings transport, a wide range of particle sizes were tested from 0.002 to 0.008 m. and presented in **Fig. 31.** It shows that the cuttings size of 0.004 m is considered the critical particle size that is the hardest to be cleaned out. Below this critical particle size, the smaller particle size is easier for clean out than the larger one. On the other hand particles sizes above the critical size, fine

particles are harder to be transported. These finding matches with Wilson and Judge (1978) conclusion for slurry flow in a single pipe, Walker and Li (2000) for solids transport for coiled tubing. Ramadan et al. (2003) divided cuttings beds into three layers: viscous sublayer, buffer zone, and logarithmic layer. They concluded that when the particle size is large and not fully submerged in the viscous layer, it becomes easier for the fluid to drag and lift solid particles, and eventually improve cuttings removal with bigger particles. On the other hand, when the particle sizes are less than the particle critical size and fully submerged in the cuttings viscous layer, the smaller particles will be easier to remove. Because less drag force and shearing action will be required to remove these tiny particles.

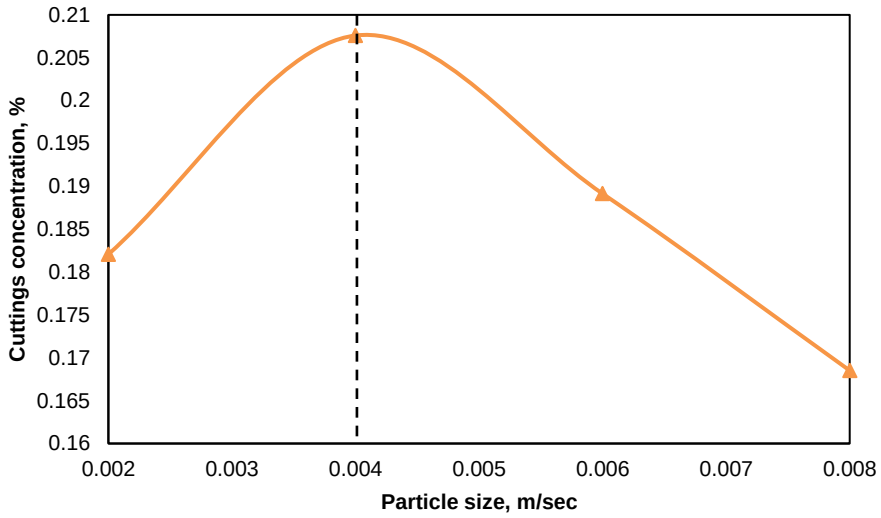

Figure 31 –Impact of particle size on cuttings concentration

9. Cuttings (Particle) Density

The impact of cuttings density on hole cleaning is shown in **Fig. 32**. As the cuttings density increases, cuttings concentration aggravates. In terms of resultant forces acting on the solid particles, the gravity force acting on solid particles (cuttings) aggravates with the increase of particle density that leads to cuttings deposition.

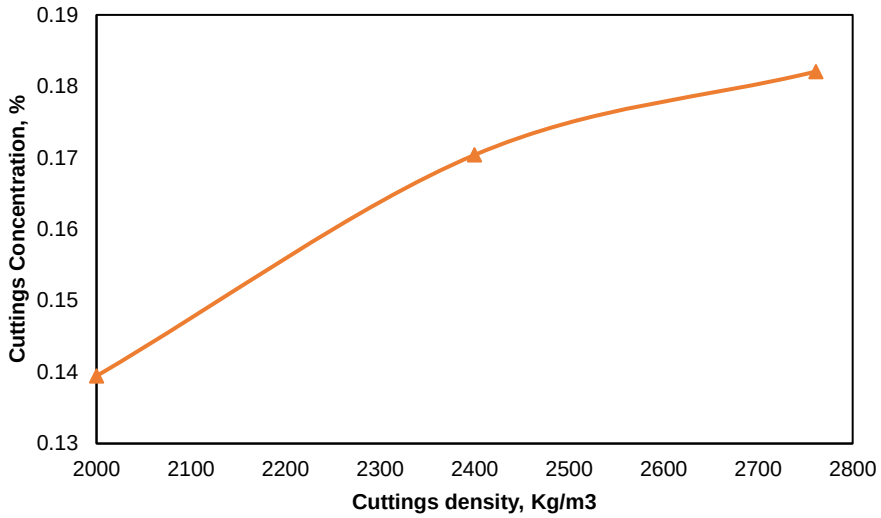

Figure 32 –Effect of cuttings density on cuttings concentration

10. Wellbore Tortuosity

Different researchers show the impact of wellbore tortuosity on the drilling phase by reducing hole size, aggravating drillstring buckling, intensifying drillstring vibration, slowing drilling rate of penetration (ROP), increasing torque and drag, aggravating logging tool reliability, and complicate casing and cement job (Chen et al., 2002; Stuart et al., 2003; Menad, 2013). In addition, Bang et al. (2015) reported that spiral wellbore tortuosity can also affect completion and production phase by reducing the effective

diameter of the wellbore that causes equipment stuck and high bending moments acting on it. Wellbore tortuosity can even lead to wrong calculations of well position (Abughaban, 2017). The impact of wellbore tortuosity on hole cleaning was first investigated by Gyanor et al. (1999), they showed that drilling performance and cuttings lifting efficiency were improved in smooth well profile when it was compared with a tortuous wellbore. Also, Chen et al. (2002) reported that wellbore tortuosity can aggravate cuttings accumulation and bed deposition. Their findings (Gaynor et al., 1999; Chen et al., 2002) contradicted with those reported from other engineering disciplines about the impact of spiral tortuous geometry on fluid flow like blood flow in the human arterial system, heat transfer, and slurry transportation (Pedley, 1980; Berger et al., 1987; Tang et al., 2016). Researchers (Webster, et al., 1999; Yanuar et al., 2016; Tang et al., 2016) observed secondary flow initiations whenever fluid flows in a spiral geometry that increases fluid axial velocity in the flow domain higher than a conventional straight circular pipe. Yanuar et al. (2017) conducted several experiments and developed a computational fluid dynamics model (CFD) to study coal transportation in a spiral pipe. They noted that improvement in slurry transportation when a helical spiral pipe was utilized instead of a straight pipe.

There are many design choices the engineer can make, as well as operational practices, that may reduce the amplitude of spiraling, but awareness is low and practices vary greatly. So the study of how spiraling tortuosity affects cuttings transport is relevant to a great deal of industry footage today. The results may help inspire engineers to cost-justify more of the changes needed to reduce the period length and spiral amplitude, and

operations to change more practices to manage them in real-time. The paper will investigate the impact of spiral tortuous wellbore on cuttings transport by developing a validated computational fluid dynamics model. The CFD model will provide some insight into the dynamics of solid-liquid flows in this complicated geometry under various conditions such as spiral period length, spiral amplitude, flow rate, drillstring rotation, annular eccentricity, drilling rate of penetration (ROP), and cuttings size on cuttings accumulations (average solid volume fraction), annular pressure loss, fluid velocity and cuttings velocity in a spiral tortuous hole.

10.1. Model Development

The annular geometric domain consists of two horizontal helical pipes with a geometry of 2 ft. (0.61 m) period length, 1.5 inches (0.0381 m) spiral amplitude (height), and four spiral turn as shown in **Fig. 33**. The spiral total length (3.1 m) was selected to be longer than hydrodynamic entrance length in all flow conditions and configurations based on the equations proposed by Yunus and Cimbala (2006) as below (see Eqs. 1 and 2). Beger et al. (1983) showed that spiral hydrodynamic length for bending and spiral pipe is less than or equal to what was calculated for normal straight pipe, thus using Yunus and Cimbala (2006) approach for computing hydrodynamic entrance length is considered a good approximation in our case. An eccentric annulus E is considered between these two cylinders to represent the effect of gravity on the drillstring in deviated holes.

The outer wall is always kept stationary, while the inner wall is either kept stationary or had a clockwise rotation to simulate drillstring rotation while drilling.

Drilling fluid and cuttings properties adopted in this model inspired from Iyoho Dissertation (1980) and Okrajni and Azar, 1986. Sauter Mean Diameter (SMD) is utilized to represent the particle size distribution used in the experiment. Drilling fluid is a non-Newtonian fluid that is a mixture of water and bentonite and can be modeled using the power-law model. Simulation input data are summarized in **Table 8**, including geometry, drilling parameters, and fluid rheological properties. Fluid flow is considered to flow in a laminar flow regime, if the drilling fluid Reynold number $Re \leq 3250\text{-}1150\eta$, while the fluid flow is considered in the turbulent regime when $Re \geq 4150\text{-}1150\eta$ (Mitchell and Miska, 2010). The Reynold number calculation used in this study is proposed by A.Busch et al. (2019). These equations selected because the rotational velocity (drillstring rotation) is considered in Reynold number calculation besides the fluid flow linear velocity. It is worth mentioning that all simulations run were conducted in the laminar flow regime.

A mixture of liquid and solid velocity was specified at the inlet and zero gauge pressure at the outlet. No-slip boundary conditions were considered on both walls for both particles and fluid. The drilling rate of penetration (ROP) was computed based on the equations developed by Ozbayoglu et al. (2010). He correlates the solid feed concentration with ROP and porosity. If rock porosity is not provided, Larsen et al. (1997) is utilized. It was assumed that the annular walls are smooth and particle shape won't change due to particle-particle interactions. A value of 0.9 for friction restitution coefficient between particles and walls was utilized.

Table 8 –Simulation input data

Geometry	
Wellbore Length (m)	3.1 m
Hole diameter (m)	0.0739
Pipe diameter (m)	0.047
Wellbore inclination (degrees)	90
Period length (m)	0.61
Spiral amplitude (m)	0.0381
Total number of turns	4
Annular eccentricity, E	0.5
Fluid rheological properties	
Fluid density (kg/m^3)	1018.5
Flow behavior index, n	0.585
Consistency index, k (Pas^n)	0.584
Drilling Parameters	
Drilling fluid velocity (m/s)	0.6
Rate of penetration ROP – m/s / (ft/hr)	0.0085 (100)
Drillpipe rotation (RPM)	0
Particle properties	
Cutting density (kg/m^3)	2619.3
Cutting diameter (m)	0.006
Porosity	0.36

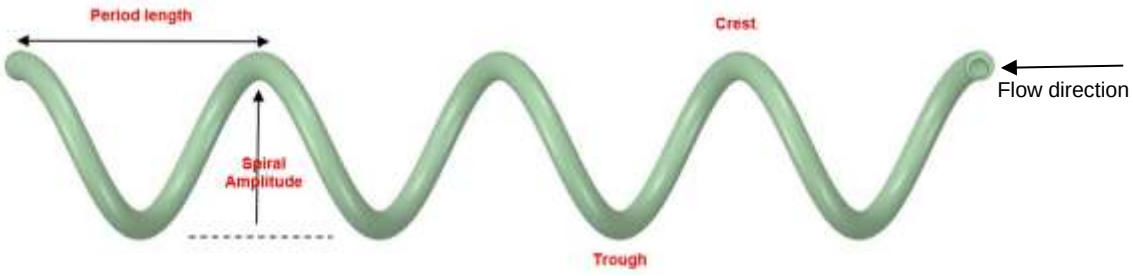

Figure 33 –2D view of the spiral geometry with four spiral turns

10.2. Grid Setup

Khaled et al. (2020a) showed that hexahedral grid (mesh) is an efficient meshing technique for two phase-flow inside the annular geometry of cylindrical bodies because of the fewer cells required for the same number of nodes compared with tetrahedron mesh. However, when hexahedral mesh was implemented for the spiral geometry, it provides a very poor mesh quality, because the hexahedral mesh is not well suited to complex geometries. Thus the tetrahedron mesh and the polyhedral mesh were implemented to get better mesh quality. **Table 9** shows the comparison between the different mesh techniques tested for the spiral geometry. Results proved that polyhedral mesh is the optimum technique for meshing the spiral geometry since it requires a moderate number of cells and provides high mesh quality (mesh minimum orthogonal quality > 0.2 and maximum skewness < 0.95). **Fig. 38** represents the mesh cross section utilized in the simulation with three inflation layers added to the boundaries of the flow domain for accurate results estimation. Then, Grid (mesh) sensitivity analysis was done to determine the optimum number of elements for an accurate solution. The study was conducted by varying element size, then computing the annular pressure loss and

cuttings concentration (average solid volume fraction) as shown in **Table 10**. The mesh choice was done based on results that can show stabilization of the annular pressure loss and cuttings concentration with good mesh property. It was observed from **Fig. 35** and **36** that the annular pressure loss and cuttings concentration stabilized at an element size equals 0.00275 m and a total number of cells equals 701k. This mesh size was adopted in all simulations for accurate computation.

Table 9 –Different meshing technique for the spiral geometry

Mesh type	Number of cells	Minimum orthogonal quality	Maximum skewness
Hexahedral	454,493	0.045	0.95
Tetrahedron	2,604,843	2.9e-8	1
Polyhedral	701031	0.51	0.46

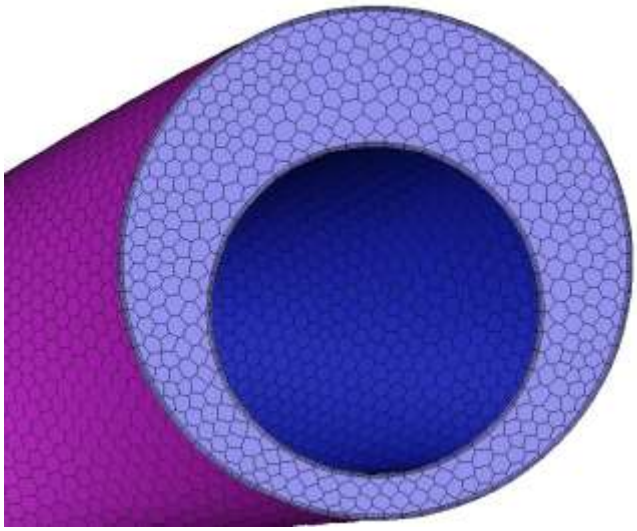

Figure 34 –Polyhedral mesh cross section

Table 10 –Grid independence analysis

Element size, m	Total number of cells	Minimum orthogonal quality	Maximum skewness
0.01	114,979	0.33	0.92
0.008	180,775	0.5	0.43
0.006	241,259	0.54	0.69
0.005	278,380	0.51	0.55
0.004	365,424	0.53	0.42
0.0035	449,925	0.54	0.42
0.003	593,217	0.51	0.39
0.00275	701,031	0.51	0.4
0.00225	1,093,721	0.57	0.46

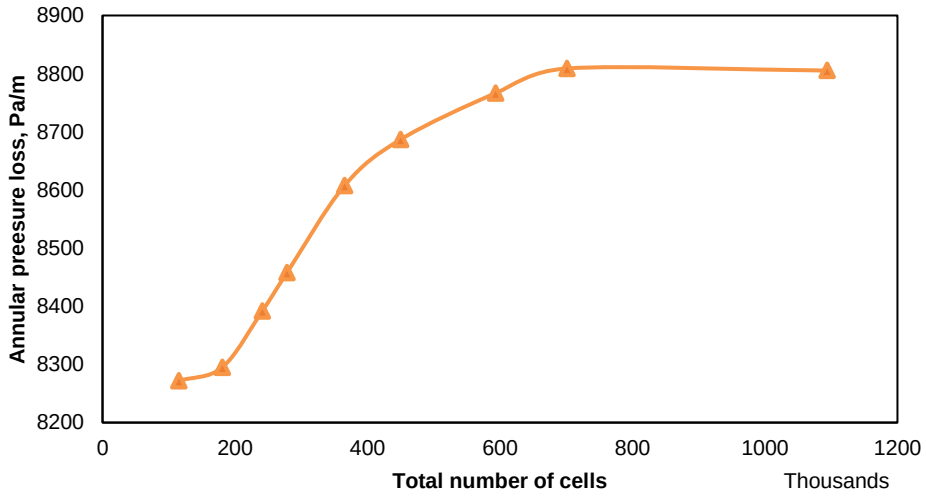

Figure 35 –Mesh sensitivity analysis for annular pressure loss estimation

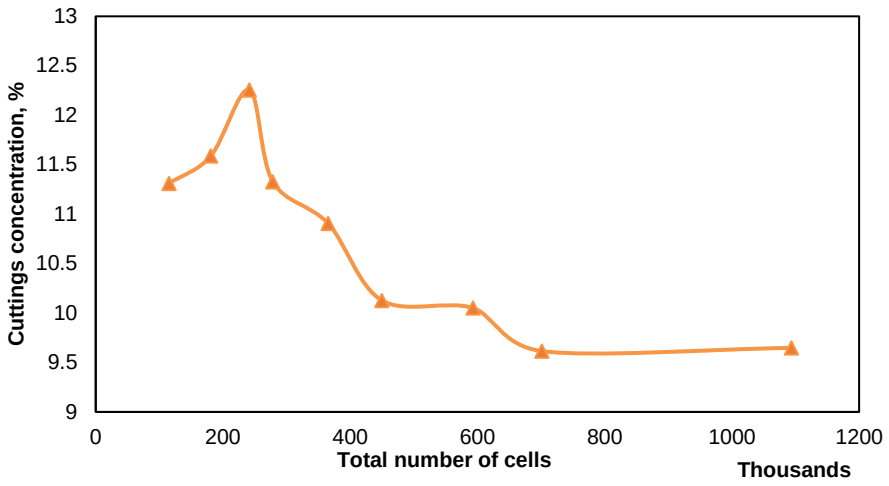

Figure 36 –Mesh sensitivity analysis for cuttings concentration calculations

10.3. Results and Discussion

Wellbore tortuosity occurred in the real case due to an interaction between the bit and the first hard contact point above it in the bottom hole assembly (BHA). This hard contact is usually a stabilizer. The distance between peaks in the spiral will be equal to the distance from the bit to the hard contact point. In motors assembly, the distance between the bit and the motor bent housing (first hard contact point) is known as motor bit to bend distance and are usually 2-4 ft. The height (amplitude) of the spiral is due to a variety of factors but the dominant one is the amount of continuous side force on the bit. Drilling motors with bent housing have enough mass eccentricity due to the bend that when the string is rotated there is a high side force. Also, they tend to develop lateral vibration which greatly amplifies that force (see, **Fig. 37**).

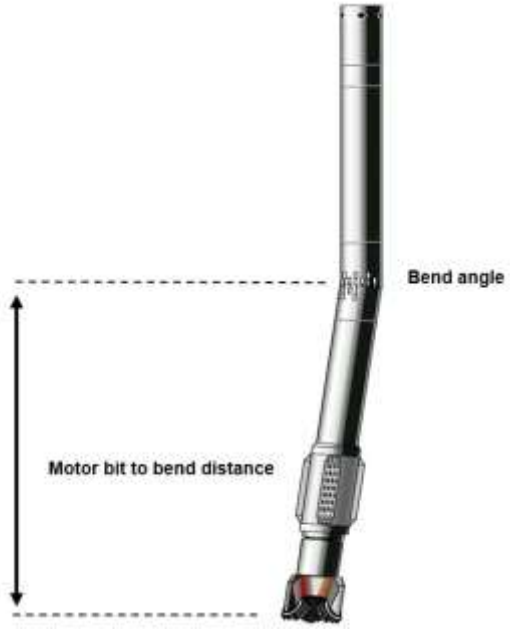

Figure 37 –Drilling motor assembly

The main objective of this study is to investigate the effect of wellbore tortuosity on cuttings transport. Thus, the main output of the simulation will be cuttings concentration (average solid concertation), annular pressure loss, the fluid dynamic force required for hole cleaning, cuttings (solid) velocity, and fluid velocity. Several simulations were conducted to study the impact of different drilling conditions on solid-liquid flow in the spiral hole geometry, such as spiral period length, spiral amplitude, liquid flow rates, drillstring rotation, annular eccentricity, drilling rate of penetration (ROP), and cuttings size.

The impact of wellbore tortuosity on fluid flow, and cuttings transport phenomena in a spiral geometry of 2ft period length and 1.5 inches amplitude were investigated and compared to straight (smooth) horizontal pipe geometry as shown in

Fig. 38. It can be observed that cuttings accumulation was reduced in the spiral geometry over the straight geometry. Reduction in cuttings accumulation from 17.6% inside the straight horizontal pipe to 9.6% cuttings accumulation inside the spiral pipe was observed. Improvement in hole cleaning inside the spiral geometry can be related to the generation of a secondary flow whenever the fluid enters a spiral geometry (Berger et al. 1983). This secondary flow is generated due to the imbalance between the outward centrifugal force and the inward directed-pressure force acting on the fluid (Webester et al., 1993). This makes the spiral geometry has a characteristic of swirling flow and eddy higher than straight circular pipe as reported by Yanouar, et al. (2015). This causes some additional transverse flow that is added to the axial velocity and gives the fluid more velocity that prevents cuttings deposition and improves hole cleaning in a spiral tortuous geometry as shown **Fig. 39**. On the other hand, the annular pressure loss in the annular geometry was observed to be three times more than the straight horizontal pipe. This mainly due to an increase in the friction between high fluid velocity and walls, and an increase in the collision between particles themselves and particles & walls in the spiral geometry as shown in **Fig. 40**. This means that high standup pipe pressure while drilling can be one of the warning signs of wellbore tortuosity occurrence besides excessive torque and drag, and drillstring vibration signs that observed while drilling tortuous hole.

It is worth mentioning that our target while drilling is to completely avoid wellbore tortuosity because the spiral hole can cause many drilling problems like drillstring buckling, drillstring vibration, slow drilling rate of penetration (ROP), high torque and drag, complicated casing and cement job, and wrong calculations of well

position as mentioned before. Therefore, The purpose of this study is not to encourage drilling operators to drill spiral holes for better hole cleaning, but to correct the misconceptions published in the literature about the impact of wellbore tortuosity on hole cleaning and to help engineers in oil and gas companies to optimize bottom hole assembly (BHA) design to prevent the initiation of long spiral period length and long spiral amplitude that will aggravate cuttings deposition as will be presented in next sections.

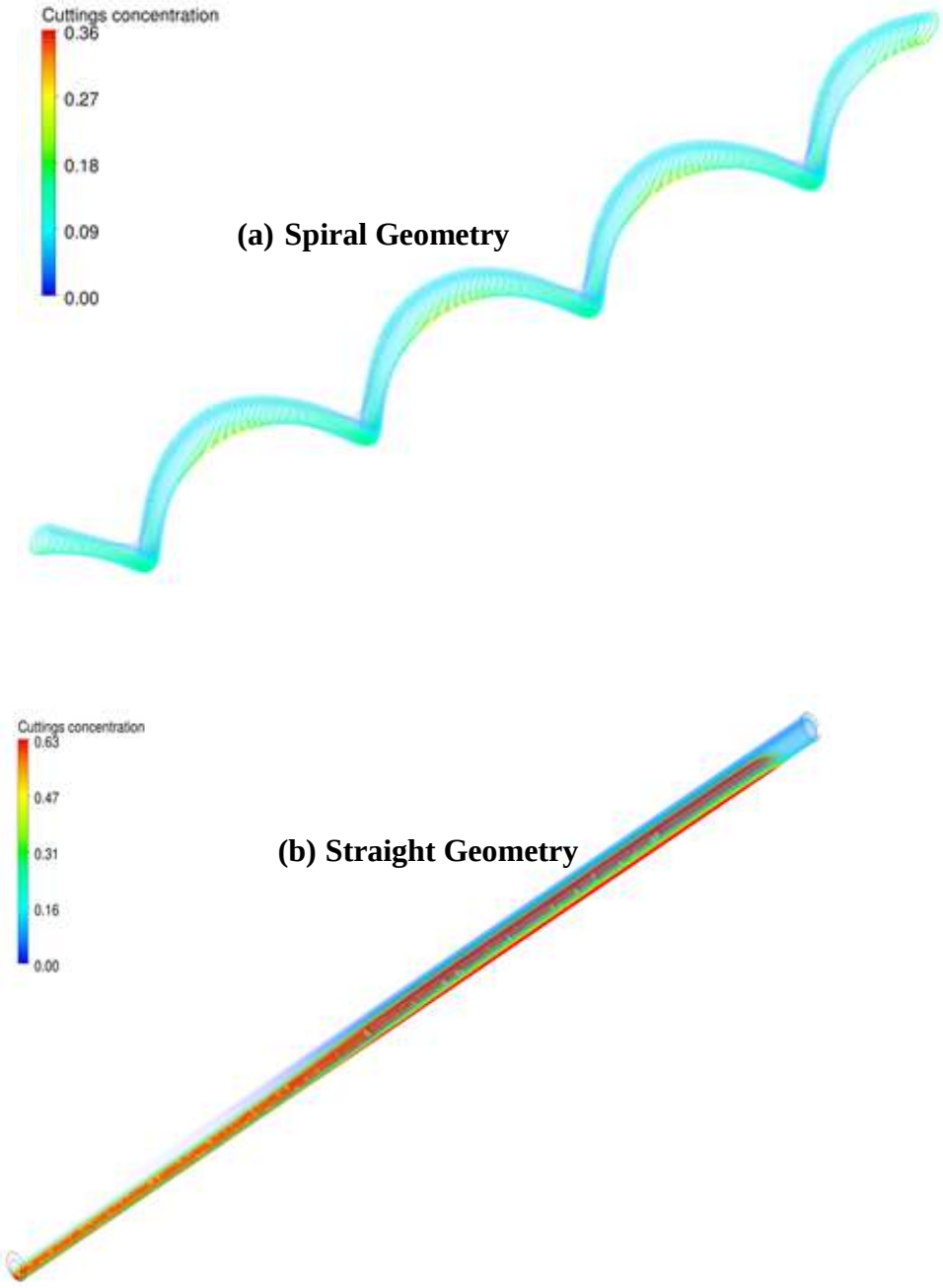

Figure 38 –Cuttings accumulation comparison between spiral and straight hole geometry (3D View)

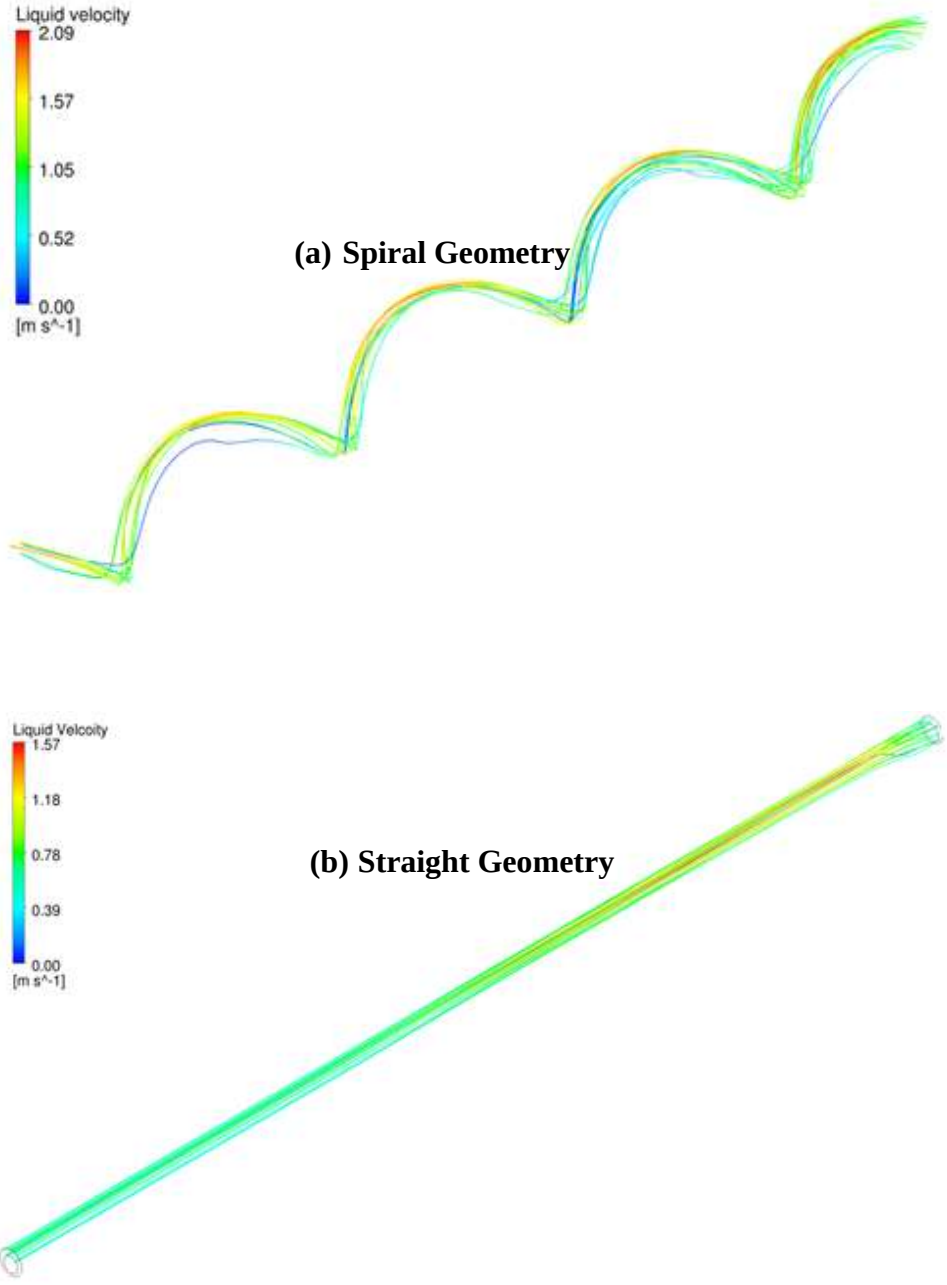

Figure 39 –Fluid streamlines velocity in (a) spiral and (b) straight hole geometry (3D View)

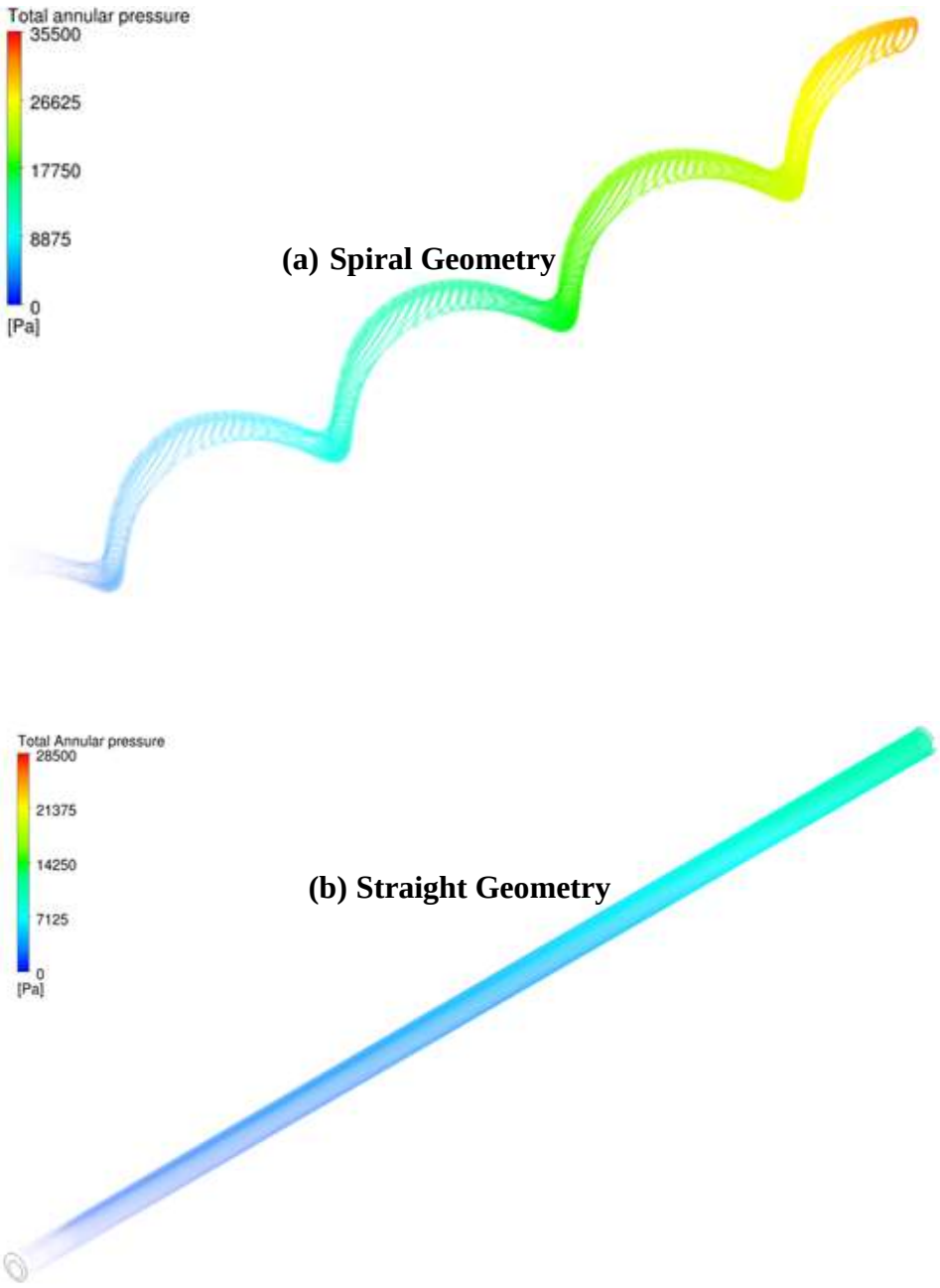

Figure 40 –Total annular pressure loss in (a) spiral Vs (b) straight profile (3D View)

10.3.1. Spiral period length

The impact of varying spiral period lengths from 1-4 ft. (0.3 – 1.22m) on cuttings accumulation was studied as shown in **Fig. 41 & 42**. Cuttings concentration aggravate from 8.3% to 14% for the geometry of 1 ft. and 4 ft. of spiral lengths, respectively. It is also noted that the fluid dynamic force required for cuttings removal is reduced from 433 N to 117 N with the increase in the period length due to the reduction in the spiral swirl effect with a larger period length. Decreasing the fluid dynamic force in the flow domain reduces the fluid carrying capacity for cuttings which leads to poor cuttings transport, and aggravates bed deposition. These results show the importance of selecting drilling motors with a shorter bit to bend distance for drilling lateral sections because cuttings accumulation increases with the increase of the wellbore spiral period length (spiral period length equals to the motor bit to bend distance).

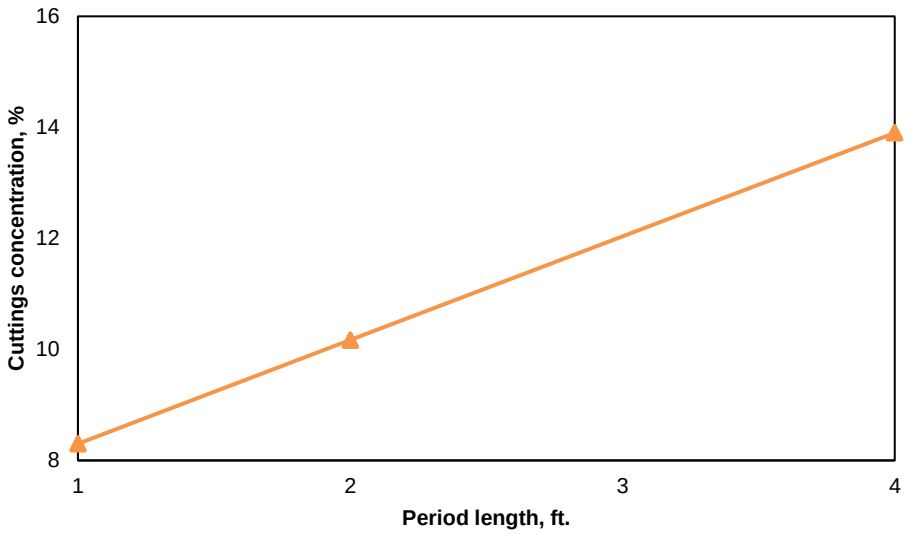

Figure 41 –Impact of spiral period length on cuttings accumulation

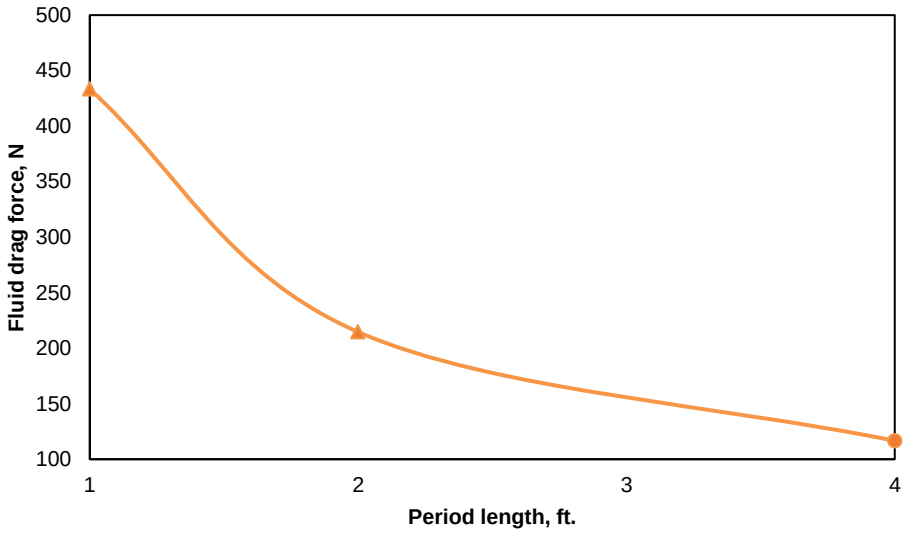

Figure 42 –Impact of spiral period length on fluid drag force

10.3.2. Spiral amplitude (height)

Spiral amplitude was changed from 1.5 inches (0.0381 m) to 6.5 inches (0.1651 m) and its effect on cuttings accumulation was studied. **Fig. 43** demonstrates that cuttings concentration at the crest (top part) and trough (bottom part) of spiral geometries at different spiral amplitudes. It was noted that cuttings deposition in the spiral crest plane is higher than what was in the trough plane as shown in **Fig. 43**. In addition, higher cuttings accumulation was observed as the spiral amplitude increases. This can be related to the change of the flow streamlines while moving in the spiral profile where the particle (cuttings) velocity reduced while moving up along the crest plane due to gravity and friction as shown in **Fig. 44**. Thus cuttings accumulation over the flow domain aggravates with larger spiral amplitude, although minor improvement in hole cleaning along trough planes with larger spiral amplitude was also noted. These results show the importance of using motor bent housing with less bend angle while drilling lateral section because a large bend in the motor assembly will apply a continuous large side force on the bit that can increase the spiral period length and aggravate cuttings deposition.

Based on this analysis, it is important to focus on improving the cuttings transport phenomena along the crest plane for better hole cleaning in a spiral tortuous wellbore with large spiral amplitude. Therefore in the next sections, the impact of different drilling conditions on hole cleaning along the crest plane of a spiral tortuous hole with 2ft period length and 6.5-inch spiral amplitude will be assessed.

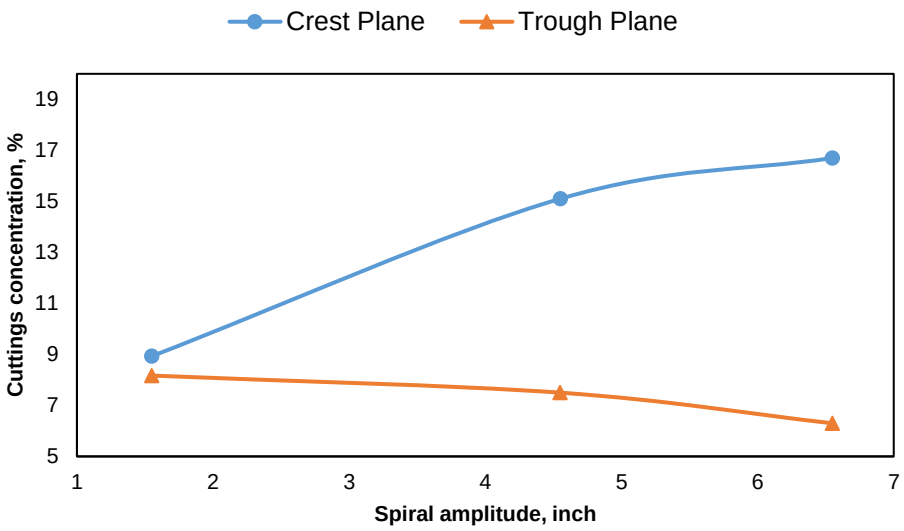

Figure 43 –Cuttings concentration at different spiral amplitudes (height)

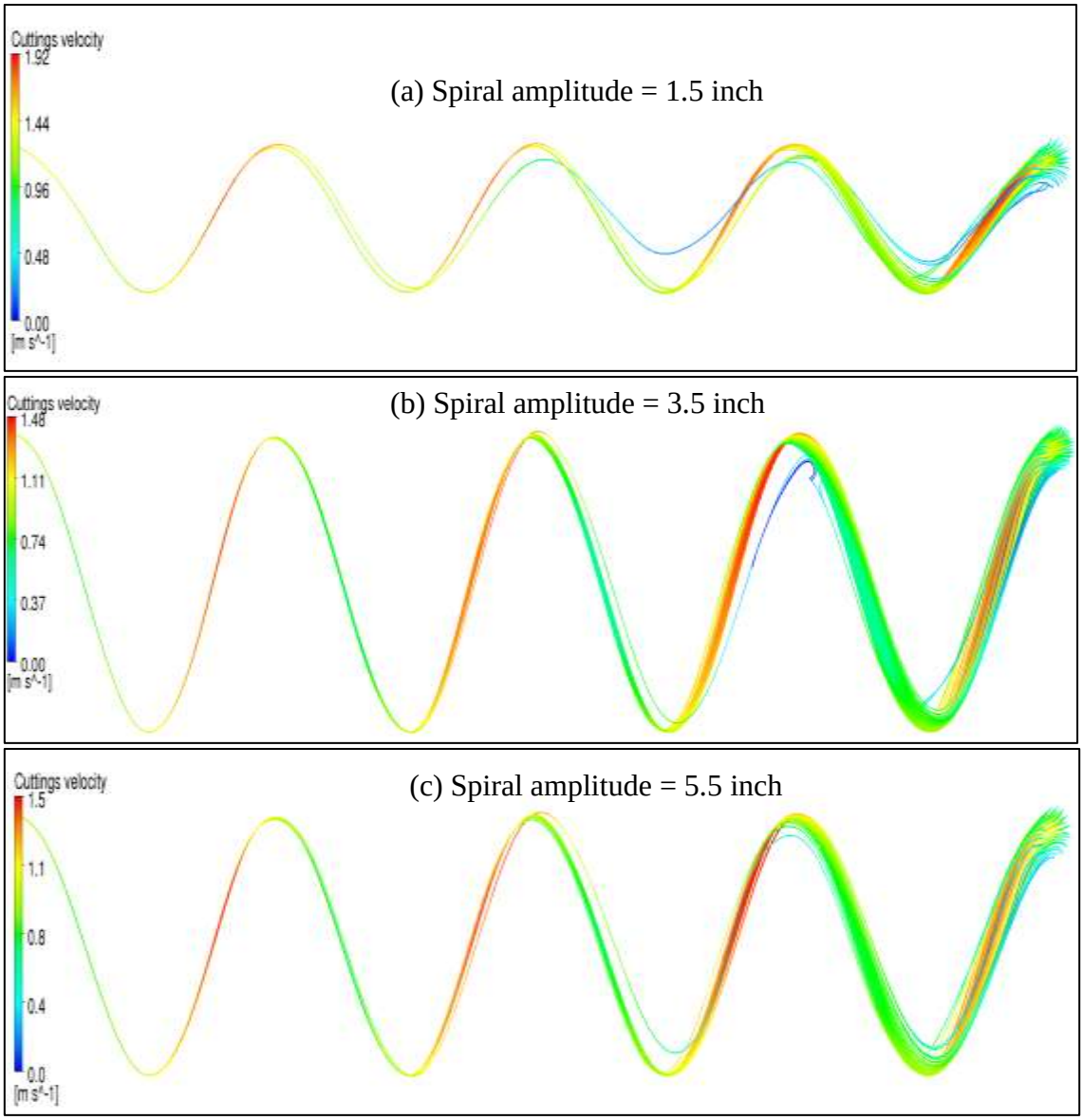

Figure 44 –Cuttings velocity streamlines along spiral geometry of 2ft period length with different amplitude: (a) Spiral amplitude = 1.5 inch; (b) Spiral amplitude = 3.5 inch; and (c) Spiral amplitude = 5.5 inch.

10.3.3. Effect of drilling fluid flow rate

The effects of changing drilling flow rates on cuttings concertation are shown in **Fig. 45**. It was observed that increasing liquid flow rate is an essential parameter for improving cuttings transport in a spiral tortuous hole and for preventing any cuttings deposition in the crest plane. It is clear from the figure that as liquid flow rates increase from 25 GPM to 49 GPM (0.6 – 1.2 m/sec), cuttings concentration decreases from 20% to 3.5%. This can be attributed to the enhancement of the cuttings carrying capacity of the fluid and bed erosion when the liquid flow rate is increased. This observation is similar to the hole cleaning practices utilized for horizontal well with straight lateral section.

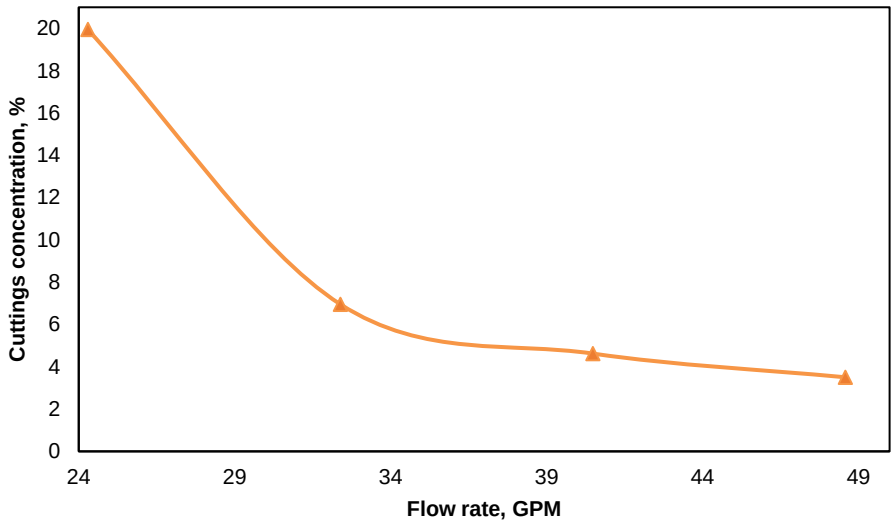

Figure 45 –Impact of drilling flow rate on cuttings concentration in spiral tortuous profile

10.3.4. Effect of drillstring rotation

Fig. 46 shows the impact of the different drillstring rotations per minute (RPM) from 0 to 400 RPM on cuttings concentration in a spiral geometry of 2 ft. period length and 6.5 inches amplitude. As the drillstring rotates, cuttings accumulation decreases significantly even at slow drillstring rotation. This can be related to the centrifugal force acting on the cuttings during rotation which would enhance the erosion effect of the cuttings bed. When drillstring rotates, cuttings are swept from the narrow part to the widest part in the annulus. This helps the cuttings in the lower side of the annulus to be agitated into the liquid and eventually improves the cutting transport to the surface. In addition to that, the friction between the rotating pipe and fluid causes some additional transverse flow that is added to the axial velocity. It gives the fluid more velocity, which allows it to erode the bed to a lower height, which opens up more flow areas above. This proves the necessity for drillstring rotation for efficient cuttings transport in spiral holes and minimizing hole problems in this complex well geometry due to cuttings deposition.

Moreover, there is no much improvement in cuttings concentration when drillstring rotates above 200 RPM. This proves that 0 to 200 RPM is the most critical range for efficient hole cleaning in spiral tortuous profile and increasing RPM above 200 will have a marginal impact on improving cuttings transport.

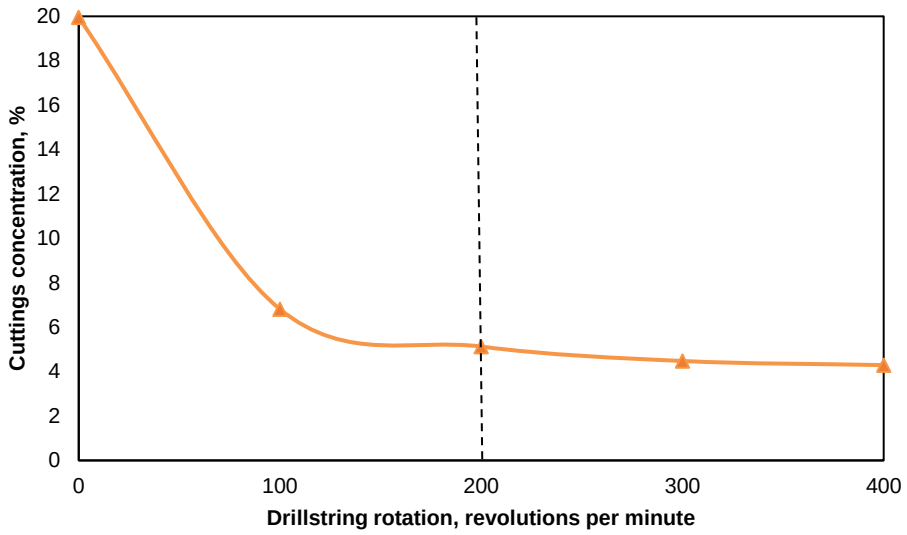

Figure 46 –Effect of drillstring rotation on cuttings concentration in spiral tortuous well

10.3.5. Influence of Drillstring Eccentricity

Since the drillstring in horizontal wells tend to lay down on the wellbore low side due to gravity, the cuttings concentration at different annular eccentricities is demonstrated in **Fig. 47**. It shows that annular eccentricity aggravates cutting deposition similar to what is observed in straight holes. As the drillstring leans downward more (eccentricity increase), it will reduce the flow area available for the cuttings on the wellbore low side, and eventually, cuttings accumulation aggravate.

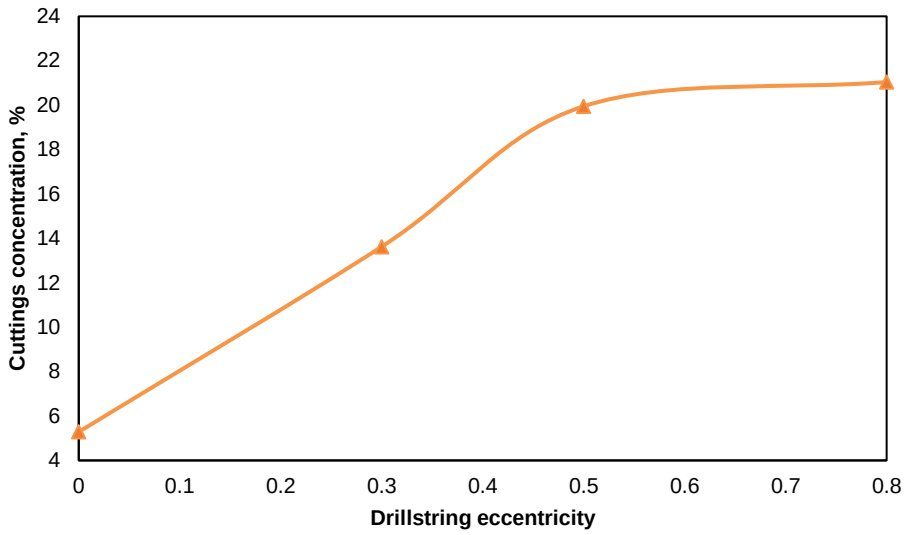

Figure 47 –Impact of drillstring eccentricity in spiral tortuous hole

10.3.6. Impact of Drilling Rate of Penetration

Fig. 48 & 49 depict the impact of drilling rate of penetration (ROP) from 50 to 150 ft. /sec (0.00423 - 0.0127 m/s) on cuttings concentration and cuttings velocity. As the drilling rate increases, more cuttings are generated by drill bits, and frictional forces between the solid particles increases, and drilled cuttings will lose some energy due to collision between each other's & walls, and cuttings kinetic energy will decrease. So cuttings velocity reduces and cuttings accumulation aggravates as a result of the high drilling rate.

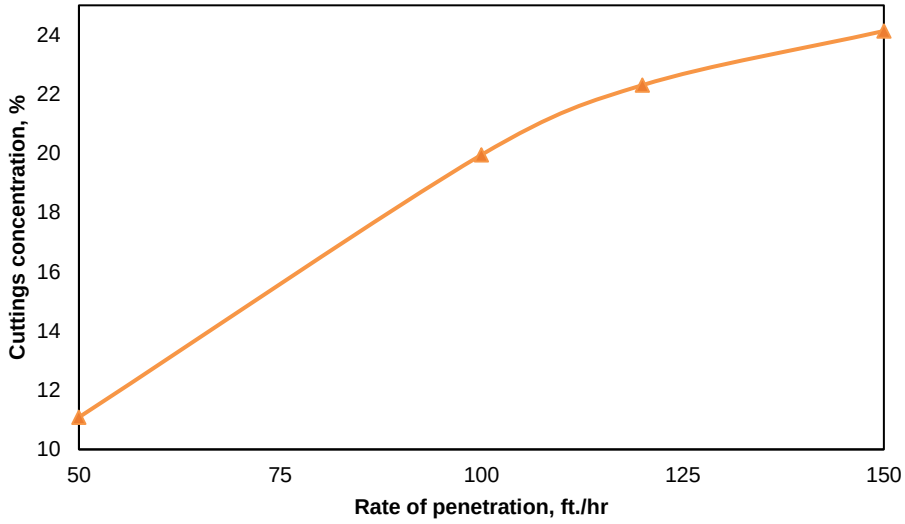

Figure 48 –Impact of drilling rate of penetration on cuttings concentration in spiral tortuous hole

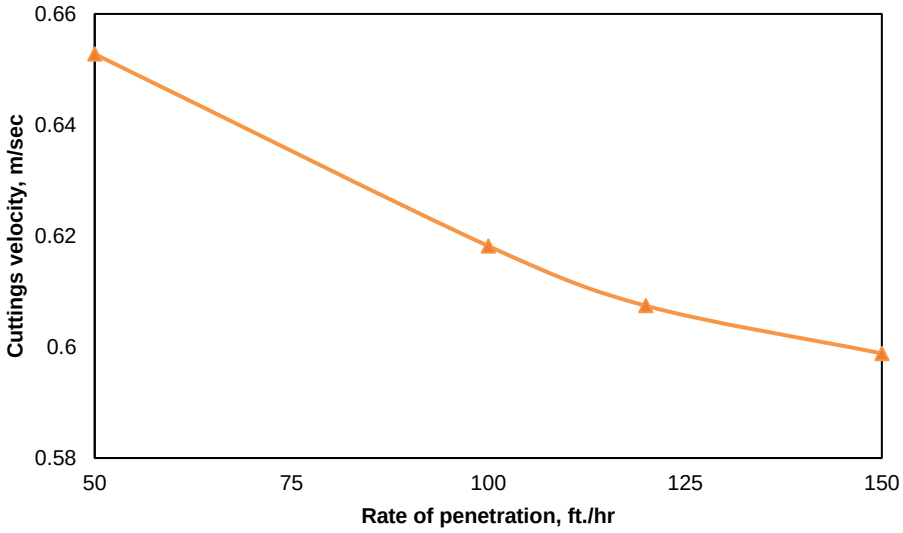

Figure 49 –Impact of drilling rate of penetration on cuttings velocity in spiral tortuous hole

10.3.7. Effect of cuttings size

A wide range of particle sizes were tested from 0.002 to 0.1 m. and represented in **Fig. 50**. It shows that cuttings size between 0.006-0.008 m is considered the critical particle size that is the hardest to be cleaned out. Below this critical particle size, the smaller particle size is easier to clean out than the larger one. On the other hand particles sizes above the critical size, fine particles are harder to be transported. These finding matches with Wilson and Judge (1978) conclusion for slurry flow in a single pipe and Walker and Li (2000) for solids transport for coiled tubing. Ramadan et al. (2003) divided the near-bed velocity profile into four layers: the viscous sublayer, the buffer zone, the logarithmic layer, and the outer layer. They concluded that when the particle size is large and not fully submerged in the viscous layer, it becomes easier for the fluid to drag and lift solid particles, and eventually improve cuttings removal with bigger particles. On the other hand, when the particle sizes are less than the particle critical size and fully submerged in the cuttings viscous layer, a smaller particle will be easier to remove. Because less drag force and shearing action will be required to remove these tiny particles.

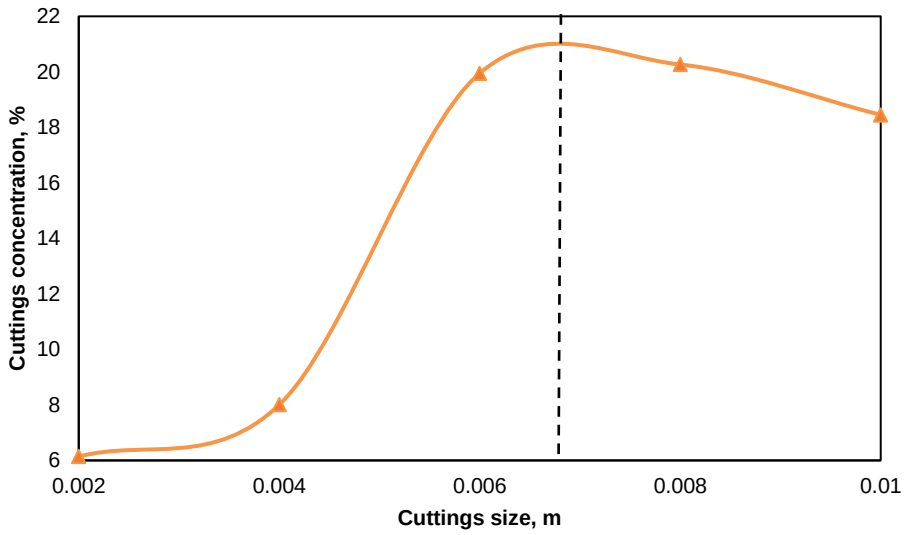

Figure 50 –Impact of cuttings size on cuttings accumulation in spiral tortuous hole

CHAPTER V

CUTTINGS ACCUMULATION AND BED HEIGHT ESTIMATION

In the previous two chapters, a computational fluid dynamics (CFD) model was presented to study cuttings transport phenomena in deviated wells with Herschel Bulkley drilling fluid rheology at different ranges of operating conditions, hydrodynamic scaling, and geometric scaling. The developed CFD model solves numerically the nonlinear partial differential equations of slurry flow using finite volume formulation. Therefore, a computer with high computational capability (super-computer) is required to conduct an investigation related to cuttings transport in an annular geometry of a wellbore. There is always a tradeoff between complexity and computing time in the simulation of complex behaviors. Thus, The developed CFD model will be robust and effective in simulating reality during the planning phase for well design. However, the usage of this model will be very challenging in real-time during the drilling operations and impractical for daily operations due to the shortage of high-speed internet.

Thus, a data driven model was developed for estimating cuttings concentration (average solid volume fraction, CVF) based on statistical techniques. The basic idea of data driven models is to establish relationships between input and output data using statistical/machine learning techniques without worrying too much about physics. The objective of this model was to optimize hole cleaning efficiency during daily drilling operations. A dimensionless analysis was used to develop a global model valid for wide ranges of drilling conditions and to shift correlations results from lab scale to field scale

application. It is worth mentioning the model development followed Busch et al. (2019) approach for generalizing the specific Power Law (PL) case to the Herschel Bulkley (HB) data points using a local power law approximation presented by Metzner and Reed (1955) as shown in **Eqs. 6** and **7**, because the data points utilized in the model varied between Power law (PL) and Herschel Buckley (HB) drilling fluid rheology.

$$n_{PL} = \frac{k_{HB}\ \dot{\gamma}^{n_{HB}}\ n_{HB}}{k_{HB}\ \dot{\gamma}^{n_{HB}} + \tau_{YP}} \quad \text{..... (41)}$$

$$K_{PL} = \dot{\gamma}^{\frac{n_{HB}+\tau_{YP}}{k_{HB}\ \dot{\gamma}^{n_{HB}} + \tau_{YP}}}\ K_{HB} + \dot{\gamma}^{\frac{k_{HB}\ \dot{\gamma}^{n_{HB}}\ n_{HB}}{k_{HB}\ \dot{\gamma}^{n_{HB}} + \tau_{YP}}}\ \tau_{YP} \quad \text{..... (42)}$$

Where n_{PL} is the PL flow behaviour index, k_{PL} is the PL consistency index, $\dot{\gamma}$ is the Newtonian shear rate, n_{HB} is HB flow behaviour index, k_{HB} is the HB consistency index, and τ_{YP} is the fluid yield stress

The data driven models are going to estimate two main parameters for optimizing and evaluating hole cleaning efficiency while drilling:

a- Cuttings concentration (CVF) that represents average solid volume fraction in the flow domain

b- Bed height ratio (BHR) = $\frac{Bed\ height\ thickness}{Hole\ outside\ diameter}$

Based on our experimental results, CFD and other researchers (Larsen et al. 1997; Ozbayoglu et al., 2010; Busch et al., 2020, Ferroudji et al. 2020 Khaled et al., 2021b) observations, the major parameters (independent variables) affecting the dependent variables (CVF and BHR) while drilling can be defined as:

CVF or BHR = Function of (drill pipe rotation (ω), inclination (Θ), eccentricity (e), hydraulic diameter (D_{hyd}), cuttings (solid) diameter (D_c), liquid superficial velocity (v_l), cuttings settling velocity (V_t), drilling rate of penetration (ROP), liquid density (ρ_l), cuttings density (ρ_c), reference shear rate ($\dot{\gamma}$), power law constant (n), power consistency index (k), and acceleration due to gravity (g)). ..... (43)

As shown in **Eq. 43**, 15 physical dimensions are characterizing the problem (dependent and independent variables) = M=15. In addition, there are three fundamentals dimensions [M, L, T] that will be used to fully express all these parameters. Based on Buckingham- Π theorem, an equivalent description of the process will be equal to M-N dimensionless variables equivalent to 12 dimensionless parameters. To get dimensionless numbers with physical meaning, some of the dimensionless parameters observed are manipulated, and the developed dimensionless parameters are as follow:

Π_1 = 2-Θ. ……..……..……/……..…….... (44)

Π_2 = 1-e. ……...…….……..…..…….... (45)

$\Pi_3 = \lambda_c$. ……...…..……..…..…….... (46)

Π_4 = Liquid Reynold Number = RE = $\frac{\rho_l D_h v_l}{\eta_o}$. ……...…….... (47)

Π_5 = Froude number Fr = $\frac{d_h g}{v_l^2}$. ……...…..…..…….... (48)

Π_6 = Archimedes number = Ar = $\frac{(\rho_c - \rho_l)\rho_f g d_s^3}{\eta_o^2}$. ……...…..…….... (49)

Π_7= Taylor Number = Ta = $\frac{\rho_l \omega d_i^{\frac{1}{2}} d_h^{\frac{3}{2}}}{2^{\frac{1}{2}} \eta_o}$. ……...…….... (50)

Π_8 = Reynold number of the terminal settling velocity of a particle =

$\mathrm{Re_p} = \frac{\rho_l D_h v_t}{\eta_o}$. …… (50)

Π_9 = Thuy number = Th = $\left(\frac{v_l g}{v_t^3}\right)^{\frac{1}{3}}$. ……..……..…..……... (51)

Π_{10} = Stokes number = Stk = $\frac{\rho_l D_h v_l}{18\eta_o}$. ……..…..……... (52)

Π_{11} = Shield number = Sh = $\frac{\eta_o \dot{\gamma}_o}{(\rho_p - \rho_l) g d_s}$. ……..……..…..……... (53)

$\Pi_{12} = \frac{v_r}{v_l}$. ……..……...…..……..…..……... (54)

It is worth mentioning that ROP can be related to injected cuttings concentration ($C_{injected}$) by using **Eqs. 37-39**, reference viscosity from **Eq. (30)** and the relation between drillstring rotation and average rotational velocity can be determined by **Eq. 31**, and cuttings (solid) settling velocity (v_t) from **Eq. 55** as proposed by Ruby & Zanke (1977).

$$v_t = \frac{10.V_l}{d_c}\left(\sqrt{1 + \frac{R_{sd}.g.d^3}{100.V_l^2}} - 1\right). \text{……..……..……} \quad (55)$$

$$R_{sd} = \frac{\rho_c - \rho_l}{\rho_l}. \text{……..…….....} \quad (56)$$

Cuttings concentration correlations and bed height ratio correlations were developed based on more than 1300 data gathered from our experimental data from TAMQ flow loop, our CFD model results, and data adapted from open literature (Iyoho, 1980; Tomren et al., 1986; Jalukar, 1993; Bassal, 1995; Duan et al., 2006; Han et al., 2010; and Osgouei, 2010). The global empirical correlations developed were trained with 80% of the collected data sets and validated with the remaining 20% using the

nonlinear least square method for estimating cuttings accumulations and the multilinear regression method for estimating of bed height ratio while drilling. The developed models were validated and trained for wellbore inclination between 20 to 90 degrees.

1. Models (Correlations) Development

The developed models (correlations) are optimized by keeping:

a) Largest Adjusted R^2:

$Total\ sum\ of\ squares: SS(Total) = \sum_{i=1}^{n}\left(Y_i - \overline{Y}\right)^2 = \sum Y_i^2 - (\sum Y_i)^2/n$ ..... (57)

Error sum of squares: SS (Residual) = $\sum_{i=1}^{n} e_i^2 = \sum_{i=1}^{n}\left(Y_i - \hat{Y}_i\right)^2 = \sum_{i=1}^{n}\left[Y_i - \left(\hat{\beta}_0 + \hat{\beta}_1 x_{i1} + \cdots \hat{\beta}_k x_{ik}\right)\right]^2$ ..... (58)

Regression sum of squares: SS(Regression) = $\sum_{i=1}^{n}\left(\hat{Y}_i - \overline{Y}\right)^2 = SS(Total) - SS(Residual)$ ..... (59)

Coefficient of determination: $R^2 = \frac{SS(Regression)}{SS(Total)} = 1 - \frac{SS(Residual)}{SS(Total)}$ ..... (60)

The Adjusted R^2 accounts for the number of predictors and the sample size:

Adjusted $R^2 = \frac{(n-1)R^2-k}{n-1-k}$ ..... (61)

Where Y_i accounts for the observed dependent variable, $\hat{Y}_i$ is the predicated dependent variable based on the developed correlation, x is the independent variables, n is the number of points in the data sample (sample size) and k is the number of independent variables (predicators).

b) Smallest Root Mean Square Error (RMSE):

RMSE is used to measure of the differences between values predicted by the correlation (model) and the actual values observed.

$$\text{RMSE} = \sqrt{\frac{\sum_{i=1}^{n}(\hat{Y}_i - Y_i)^2}{n}} \quad \text{……………………………………………..……..…….. (62)}$$

c) Mallow's C_p:

C_p is based on normalized error of estimation and is kept equal to p (p= k +1) or smaller and the goal is to find the best model involving a subset of these predictors.

$$C_p = \frac{SS(Residual)_k}{s_\varepsilon^2} + 2p - n \quad \text{………………………………………………..…. (63)}$$

d) Smallest Corrected Akaike Information Criterion (AIC_C):

AIC_C to penalize more predicators the corrected Akaike's information criterion adjusts the value of AIC to reduce the bias when the sample size is small or the number of parameters is a moderate to large fraction.

of the sample size.

$$AIC_{C,k} = AIC_k + \frac{2(k+2)(k+3)}{n-k-1} \quad \text{………………………………………………………….. (64)}$$

$$AIC_k = n\log_e(SS(Residual/n) + 2k \quad \text{……………………………………..……. (65)}$$

e) Smallest Bayes Information Criterion (BIC):

BIC is an alternative measure that places a larger penalty on overfitting the model.

$$BIC_k = n\log_e(SS(Residual/n) + 2k\log_e(n) \quad \text{..... (66)}$$

f) Smallest PRESS statistics:

PRESS statistic provides a measure of how well the model will predict new data. Each observed response compared to what a model fitted without the corresponding observation would predict.

$$PRESS = \sum_{i=1}^{n}\left(Y_i - \hat{Y}_i^*\right)^2 \quad \text{..... (67)}$$

Where $\hat{Y}_i^*$ is the predicted value for the i[th] response based on a regression model fitted from the other n-1 observations.

g) Cook's distance:

It is a diagnostic for identifying influential observations and measuring the change in the estimated coefficients when deleting an observation. If an observations have large value of Cook's distance (above 1), it should be examined to determine whether there are problems with the observations.

$$D_i = \frac{e_i^2}{(k+1)\hat{\sigma}^2}\frac{h_{ii}}{(1-h_{ii})^2} \quad \text{..... (68)}$$

Where $\hat{\sigma}$ is the mean square error for regression and h_{ii} is is known as the leverage of the i-th observation.

The gathered data is divided into two parts, a training sample - 80% of the collected data - and a validation sample - 20% of the remaining data. Models are trained

and validated for wellbore inclination between 20 to 90 degrees. JMP Statistics Software is utilized to check relation between independent variables and optimize variable selection as shown in below tables. **Table 11** shows that the best way to predict the cuttings concentration is to use the Twelve dimensionless number discussed before (2-Θ, 1-e, λ_c, RE, Fr^2, Ar, Ta, Solid Re, Thuy number, Stokes number, Shield number, $\frac{u_r}{v_l}$). On the other hand, **Table 12** shows that the best way to predict the cuttings bed height ratio is to only use the ten dimensionless number (2-Θ, 1-e, λ_c, RE, Fr^2, Ar, Ta, Solid Re, Stokes number, and Shield number).

Table 11 –Variable selection for cuttings concentration correlation

Model	Number	RSquare	RMSE	AICc	BIC	Cp
2-Θ	1	0.1273	0.1171	-1207.1	-1192.9	340.2394
1-e	1	0.1102	0.1182	-1190.9	-1176.7	363.1878
Fr	1	0.0486	0.1222	-1135.0	-1120.9	445.7990
Shield Number	1	0.0285	0.1235	-1117.6	-1103.4	472.7881
2-Θ,Fr	2	0.2096	0.1115	-1287.7	-1268.8	231.8826
2-Θ,1-e	2	0.1902	0.1128	-1267.4	-1248.6	257.9030
1-e,Fr	2	0.1829	0.1133	-1259.9	-1241.1	267.6984
1-e,λc	2	0.1481	0.1157	-1225.1	-1206.3	314.3929
2-Θ,1-e,Fr	3	0.2888	0.1058	-1373.7	-1350.1	127.7265
2-Θ,1-e,λc	3	0.2328	0.1099	-1310.5	-1286.9	202.7489
1-e,λc,Fr	3	0.2273	0.1103	-1304.6	-1281.0	210.0942
2-Θ,λc,Fr	3	0.2208	0.1107	-1297.6	-1274.0	218.8184
2-Θ,1-e,λc,Fr	4	0.3405	0.1019	-1434.6	-1406.4	60.3297
2-Θ,1-e,Solid Re,Stokes Number	4	0.3002	0.1050	-1385.2	-1356.9	114.3333
2-Θ,1-e,Fr,Stokes Number	4	0.2978	0.1052	-1382.3	-1354.1	117.5515
2-Θ,1-e,RE,Fr	4	0.2959	0.1053	-1380.1	-1351.8	120.1142
2-Θ,1-e,λc,Fr,Shield Number	5	0.3464	0.1016	-1440.1	-1407.1	54.4476
2-Θ,1-e,λc,Fr,Thuy Number	5	0.3442	0.1017	-1437.3	-1404.4	57.3433
2-Θ,1-e,λc,Fr,Solid Re	5	0.3441	0.1017	-1437.1	-1404.2	57.5306
2-Θ,1-e,λc,Fr,Ur/Vl	5	0.3439	0.1018	-1436.9	-1403.9	57.8253
2-Θ,1-e,λc,Fr,Solid Re,Stokes Number	6	0.3617	0.1004	-1457.8	-1420.1	35.9261
2-Θ,1-e,λc,Fr,Ar,Solid Re	6	0.3575	0.1007	-1452.3	-1414.7	41.5341
2-Θ,1-e,λc,RE,Fr,Solid Re	6	0.3520	0.1012	-1445.2	-1407.5	48.9889
2-Θ,1-e,λc,Fr,Shield Number,Ur/Vl	6	0.3495	0.1014	-1441.9	-1404.3	52.3336
2-Θ,1-e,λc,Fr,Ar,Solid Re,Stokes Number	7	0.3723	0.0996	-1469.7	-1427.4	23.6694
2-Θ,1-e,λc,Fr,Solid Re,Stokes Number,Shield Number	7	0.3684	0.1000	-1464.5	-1422.2	28.9808
2-Θ,1-e,λc,Fr,Solid Re,Thuy Number,Stokes Number	7	0.3671	0.1001	-1462.8	-1420.5	30.6917
2-Θ,1-e,λc,Fr,Solid Re,Stokes Number,Ur/Vl	7	0.3660	0.1001	-1461.4	-1419.0	32.1819
2-Θ,1-e,λc,Fr,Ar,Solid Re,Stokes Number,Shield Number	8	0.3772	0.0993	-1474.2	-1427.2	19.1442
2-Θ,1-e,λc,Fr,Ar,Solid Re,Thuy Number,Stokes Number	8	0.3765	0.0994	-1473.2	-1426.2	20.1357
2-Θ,1-e,λc,Fr,Ar,Solid Re,Stokes Number,Ur/Vl	8	0.3759	0.0994	-1472.4	-1425.4	20.9317
2-Θ,1-e,λc,Fr,Ar,Ta,Solid Re,Stokes Number	8	0.3735	0.0996	-1469.2	-1422.2	24.1644
2-Θ,1-e,λc,Fr,Ar,Solid Re,Stokes Number,Shield Number,Ur/Vl	9	0.3806	0.0991	-1476.7	-1425.0	16.6041
2-Θ,1-e,λc,RE,Fr,Ar,Solid Re,Thuy Number,Stokes Number	9	0.3805	0.0991	-1476.6	-1424.9	16.6738
2-Θ,1-e,λc,Fr,Ar,Ta,Solid Re,Stokes Number,Ur/Vl	9	0.3796	0.0992	-1475.4	-1423.7	17.8722
2-Θ,1-e,λc,Fr,Ar,Solid Re,Thuy Number,Stokes Number,Ur/Vl	9	0.3796	0.0992	-1475.4	-1423.7	17.9234
2-Θ,1-e,λc,Fr,Ar,Ta,Solid Re,Thuy Number,Stokes Number,Ur/Vl	10	0.3852	0.0988	-1480.8	-1424.5	12.4439
2-Θ,1-e,λc,Fr,Ar,Ta,Solid Re,Stokes Number,Shield Number,Ur/Vl	10	0.3836	0.0989	-1478.7	-1422.4	14.5271
2-Θ,1-e,λc,RE,Fr,Ar,Solid Re,Thuy Number,Stokes Number,Ur/Vl	10	0.3835	0.0989	-1478.6	-1422.3	14.6642
2-Θ,1-e,λc,RE,Fr,Ar,Solid Re,Thuy Number,Stokes Number,Shield Number	10	0.3824	0.0990	-1477.1	-1420.8	16.1502
2-Θ,1-e,λc,Fr,Ar,Ta,Solid Re,Thuy Number,Stokes Number,Shield Number,Ur/Vl	11	0.3868	0.0987	-1480.9	-1419.9	12.3290
2-Θ,1-e,λc,RE,Fr,Ar,Ta,Solid Re,Thuy Number,Stokes Number,Ur/Vl	11	0.3864	0.0988	-1480.4	-1419.4	12.8568
2-Θ,1-e,λc,RE,Fr,Ar,Solid Re,Thuy Number,Stokes Number,Shield Number,Ur/Vl	11	0.3854	0.0988	-1479.1	-1418.1	14.1259
2-Θ,1-e,λc,RE,Fr,Ar,Ta,Solid Re,Stokes Number,Shield Number,Ur/Vl	11	0.3837	0.0990	-1476.7	-1415.7	16.4486
2-Θ,1-e,λc,RE,Fr,Ar,Ta,Solid Re,Thuy Number,Stokes Number,Shield Number,Ur/Vl	12	0.3877	0.0987	-1480.2	-1414.5	13.0000

Table 12 –Variable selection for bed height ratio correlation

Model	Number	RSquare	RMSE	AICc	BIC	Cp
λc	1	0.3945	0.1199	-681.18	-668.65	345.5732
Fr	1	0.3752	0.1218	-665.91	-653.39	371.9331
W	1	0.1719	0.1402	-528.44	-515.92	650.4302
1-e	1	0.1652	0.1408	-524.51	-511.99	659.6119
1-e,Fr	2	0.5128	0.1077	-785.29	-768.61	185.4076
1-e,λc	2	0.5023	0.1088	-774.81	-758.13	199.8905
λc,Fr	2	0.4932	0.1098	-765.97	-749.29	212.3625
λc,W	2	0.4420	0.1152	-719.07	-702.39	282.3987
1-e,λc,Fr	3	0.6043	0.0971	-884.77	-863.95	62.0459
1-e,λc,Solid Re	3	0.5283	0.1060	-799.01	-778.19	166.1876
1-e,Fr,Shield Number	3	0.5244	0.1065	-794.94	-774.11	171.6056
1-e,λc,W	3	0.5213	0.1068	-791.80	-770.97	175.8155
1-e,λc,RE,Fr	4	0.6111	0.0964	-891.18	-866.21	54.7348
1-e,λc,Fr,Ar	4	0.6109	0.0964	-890.86	-865.90	55.0795
1-e,λc,Fr,Stokes Number	4	0.6107	0.0964	-890.59	-865.63	55.3760
1-e,λc,Fr,Solid Re	4	0.6103	0.0965	-890.15	-865.18	55.8605
1-e,λc,RE,Fr,Shield Number	5	0.6415	0.0926	-928.81	-899.71	15.1200
1-e,λc,Fr,Stokes Number,Shield Number	5	0.6361	0.0933	-921.46	-892.36	22.5797
1-e,λc,Fr,Ar,Shield Number	5	0.6336	0.0937	-918.11	-889.01	26.0116
1-e,λc,Fr,Solid Re,Shield Number	5	0.6268	0.0945	-909.14	-880.04	35.3222
2-Θ,1-e,λc,RE,Fr,Shield Number	6	0.6442	0.0924	-930.43	-897.21	13.4246
1-e,λc,RE,Fr,Solid Re,Shield Number	6	0.6437	0.0925	-929.78	-896.55	14.0791
1-e,λc,RE,Fr,Ar,Shield Number	6	0.6425	0.0926	-928.07	-894.85	15.7910
1-e,λc,RE,Fr,Ta,Shield Number	6	0.6421	0.0927	-927.49	-894.27	16.3706
2-Θ,1-e,λc,RE,Fr,Solid Re,Shield Number	7	0.6466	0.0922	-931.61	-894.27	12.1886
2-Θ,1-e,λc,RE,Fr,Ar,Shield Number	7	0.6456	0.0923	-930.21	-892.87	13.5755
1-e,λc,RE,Fr,Ta,Solid Re,Shield Number	7	0.6452	0.0924	-929.76	-892.42	14.0244
2-Θ,1-e,λc,RE,Fr,Stokes Number,Shield Number	7	0.6450	0.0924	-929.43	-892.09	14.3554
2-Θ,1-e,λc,RE,Fr,Ta,Solid Re,Shield Number	8	0.6481	0.0921	-931.68	-890.24	12.0513
2-Θ,1-e,λc,Fr,Ar,Solid Re,Stokes Number,Shield Number	8	0.6473	0.0922	-930.50	-889.06	13.2174
1-e,λc,RE,Fr,Ar,Solid Re,Stokes Number,Shield Number	8	0.6470	0.0922	-930.10	-888.65	13.6184
2-Θ,1-e,λc,RE,Fr,Solid Re,Shield Number,W	8	0.6469	0.0922	-929.98	-888.54	13.7358
2-Θ,1-e,λc,RE,Fr,Ar,Solid Re,Stokes Number,Shield Number	9	0.6499	0.0919	-932.01	-886.47	11.6673
2-Θ,1-e,λc,Fr,Ar,Solid Re,Thuy Number,Stokes Number,Shield Number	9	0.6494	0.0920	-931.38	-885.84	12.2858
2-Θ,1-e,λc,RE,Fr,Ta,Solid Re,Shield Number,W	9	0.6493	0.0920	-931.17	-885.64	12.4853
~~1-e,λc,RE,Fr,Ar,Ta,Solid Re,Stokes Number,Shield Number~~	~~9~~	~~0.6493~~	~~0.0920~~	~~-931.16~~	~~-885.62~~	~~12.4992~~
2-Θ,1-e,λc,RE,Fr,Ar,Ta,Solid Re,Stokes Number,Shield Number	10	0.6522	0.0917	-933.12	-883.49	10.5205
2-Θ,1-e,λc,RE,Fr,Ar,Solid Re,Stokes Number,Shield Number,W	10	0.6508	0.0919	-931.24	-881.61	12.3539
2-Θ,1-e,λc,Fr,Ar,Ta,Solid Re,Thuy Number,Stokes Number,Shield Number	10	0.6508	0.0919	-931.23	-881.60	12.3645
2-Θ,1-e,λc,RE,Fr,Ar,Solid Re,Thuy Number,Stokes Number,Shield Number	10	0.6506	0.0919	-930.95	-881.32	12.6441
2-Θ,1-e,λc,RE,Fr,Ar,Ta,Solid Re,Thuy Number,Stokes Number,Shield Number	11	0.6528	0.0918	-931.82	-878.11	11.7255
2-Θ,1-e,λc,RE,Fr,Ar,Ta,Solid Re,Stokes Number,Shield Number,W	11	0.6527	0.0918	-931.76	-878.05	11.7857
2-Θ,1-e,λc,RE,Fr,Ar,Solid Re,Thuy Number,Stokes Number,Shield Number,W	11	0.6515	0.0919	-930.05	-876.34	13.4565
2-Θ,1-e,λc,Fr,Ar,Ta,Solid Re,Thuy Number,Stokes Number,Shield Number,W	11	0.6508	0.0920	-929.12	-875.41	14.3644
2-Θ,1-e,λc,RE,Fr,Ar,Ta,Solid Re,Thuy Number,Stokes Number,Shield Number,W	12	0.6533	0.0918	-930.44	-872.67	13.0000

2. Cuttings Concentration (CVF) Correlation

The developed model utilized 526 data points gathered from our experimental data From TAMQ flow loop, our CFD model results, and data adapted from open literature (Iyoho, 1980; Okranji et al., 1986; Tomren et al., 1986; Duan et al., 2006; Han et al., 2010; and Osgouei, 2010), and covering a wide range of drilling conditions as shown in **Table 13** and **14**. The model was trained with 80% of the collected data and validated with the remaining 20% using the nonlinear least square method for estimating cuttings accumulations in wellbore inclination (from vertical) between 20 to 90 degrees. **Eq. 69** shows the global correlation developed by our model for estimating cuttings concentration. The correlation coefficients are shown in **Table 15**. As shown in **Fig. 51**, Correlation shows good accuracy in estimating cuttings concentration, predicated (calculated) points from the trained data sets lay in between 20% error margin in most cases. The proposed relation between calculated and measured cuttings concentration has an adjusted R^2= 0.85 and with an average absolute error equals 29%.

$$\boldsymbol{CVF = a_0 \pi_1^{a_1} \pi_2^{a_2} \pi_3^{a_3} \pi_4^{a_4} \pi_5^{a_5} \pi_6^{a_6} \pi_7^{a_7} \pi_8^{a_8} \pi_9^{a_9} \pi_{10}^{a_{10}} \pi_{11}^{a_{11}} \pi_{12}^{a_{12}}} \quad \text{..... (69)}$$

Table 13 –Trained data sets utilized for data-driven model

	TAMUQ Exp.	Tomren et al., 1986	Okranji et al., 1986	Duan et al., 2006	Osgouei, 2010	Han et al., 2010	CFD Model
Data Points	44	11	79	51	66	118	22
Geometry							
Hole diameter (m)	0.1143	0.127	0.127	0.2032	0.0739	0.044	0.0739
Pipe diameter (m)	0.0508	0.0482	0.048	0.1143	0.047	0.03	0.047
Fluid Properties							
Fluid type	Water, polymer mud	Water, bentonite mud	Water, bentonite mud	Water, Polanionic Cellulose solutions	Water	Water, 0.4% CMC, and 5% bentonite	water, carboxymethyl cellulose (CMC)
Density (kg/m^3)	997, 999, 1001	998.7, 1012.5	995, 1013, 1019	999, 1040	998.5	997, 999, 1041	1020
Fluid Yield Stress, τ_0 ($Pa.sec^n$)	-, 0.229, 0.269	-	-	-	0	-	3.8
Flow behaviour index, n	1, 0.878, 0.557	1, 0.64	1, 0.585, 0.736	1, 0.72	1	1, 0.73, 0.75	0.88
Consistency index, K (Pas^n)	-, 0.005, 0.064	-, 0.2828	-, 0.0881, 0.1757, 0.293	-, 0.0254	-	-, 0.15, 0.055	0.0429
Particle properties							
Cutting density (kg/m^3)	2550	2619.3	2619.3	2650	2761.4	2550	2400, 2600, 2761
Cutting Diameter (m)	0.0025	0.0064	0.0064	0.00045, 0.0014	0.00201	0.001	0.002, 0.004, 0.006, 0.008

Cont. Table 13 –Trained data sets utilized for data-driven model

Drilling Parameters							
Drilling fluid velocity (m/sec)	0.39 - 0.81	0.29 - 1	0.58 - 1.2	0.57 - 1.1	0.45 – 2.74	0.32 – 0.89	0.8 – 1.5
Drillpipe Rotation (RPM)	0, 40, 80, 120	50	50	0, 40, 80	0, 60, 80, 120	0, 200, 400, 600	0, 100, 200, 300, 400, 500
Hole eccentricity, E	0.3	0.5	0.5	0.2	0.623	0	0, 0.3, 0.6, 0.8
Inclination (degrees)	90	20, 80	40, 50, 60, 70, 90	90	90	0, 30, 45, 60	30, 50, 70, 90

Table 14 –Validation data sets utilized for data-driven model

	TAMUQ Exp.	**Iyoho, 1986**
Data Points	64	71
Geometry		
Hole diameter (m)	0.1143	0.127
Pipe diameter (m)	0.0508	0.0482
Fluid Properties		
Fluid type	Water, polymer mud	Water, bentonite mud
Density (kg/m^3)	997, 999, 1001	998.7, 1012.5
Fluid Yield Stress, τ_0 ($Pa.sec^n$)	-, 0.229, 0.269	-
Flow behaviour index, n	1, 0.878, 0.557	1, 0.64
Consistency index, K (Pas^n)	-, 0.005, 0.064	-, 0.2828
Particle properties		
Cutting density (kg/m^3)	2550	2619.3
Cutting Diameter (m)	0.0025	0.0064
Drilling Parameters		
Drilling fluid velocity (m/sec)	0.39 - 0.81	0.29 - 1
Drillpipe Rotation (RPM)	0, 40, 80, 120	0, 50, 100
Hole eccentricity, E	0	0, 0.5, 0.99
Inclination (degrees)	90	20, 40, 60, 80, 90

Table 15 –Cuttings concentration correlation coefficients

a_0	a_1	a_2	a_3	a_4	a_5	a_6
0.01	-0.35	-1.12	-0.03	13.09	-1.58	-0.87
a_7	a_8	a_9	a_{10}	a_{11}	a_{12}	
-2.43	-21.2	-19.542	-2.36	-8.18	2.43	

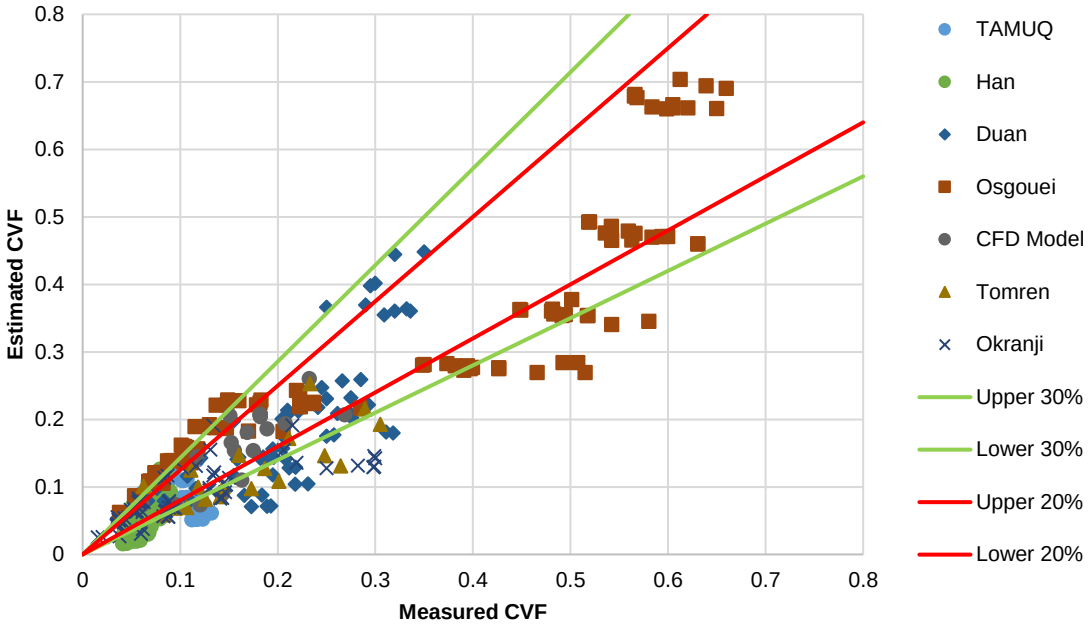

Figure 51 –Comparison of measured and estimated cuttings concertation for trained data sets

After the cuttings concentration correlation was developed, a simplification approach was implemented to reduce the number of the model's predictors (variables). The objective of this approach was to come up with a simplified correlation for easier implementation in oil fields and without scarifying a lot with accuracy. The variables of low coefficient values were neglected and a new dimensionless number was developed by combining three variables together as shown in **Eqs. 71-73** and **Table 16**. It was observed that the new correlation for CVF estimation has an adjusted R^2= 0.9 and can predict with an error ± 20 in most cases as shown in **Figure 52**.

$$\pi_{13} = \pi_2 \times \pi_4 \times \pi_8 = (1-e) \times \left(\frac{\rho_l D_h v_l}{\eta_o}\right) \times \left(\frac{\rho_l D_h v_t}{\eta_o}\right) = (1-e).\left(\frac{{\rho_l}^2 {D_h}^2 (v_l.v_t)}{{\eta_o}^2}\right). \ldots\ldots (71)$$

For simplification, we take a square root of Eq. 71

$$\pi_{13} = \left(\frac{\rho_l D_h}{\eta_o}\right).\sqrt{\left(v_l v_t (1-e)\right)}. \ldots\ldots (72)$$

$$CVF = a_0 \pi_1^{a_1} \pi_3^{a_2} \pi_5^{a_3} \pi_7^{a_4} \pi_{11}^{5} \pi_{13}^{6} \ldots\ldots (73)$$

Table 16 –Final cuttings concentration correlation coefficients

a_0	a_1	a_2	a_3	a_4	a_5	a_6
0.003	-0.4	-0.08	1	0.002	-3	-2.8

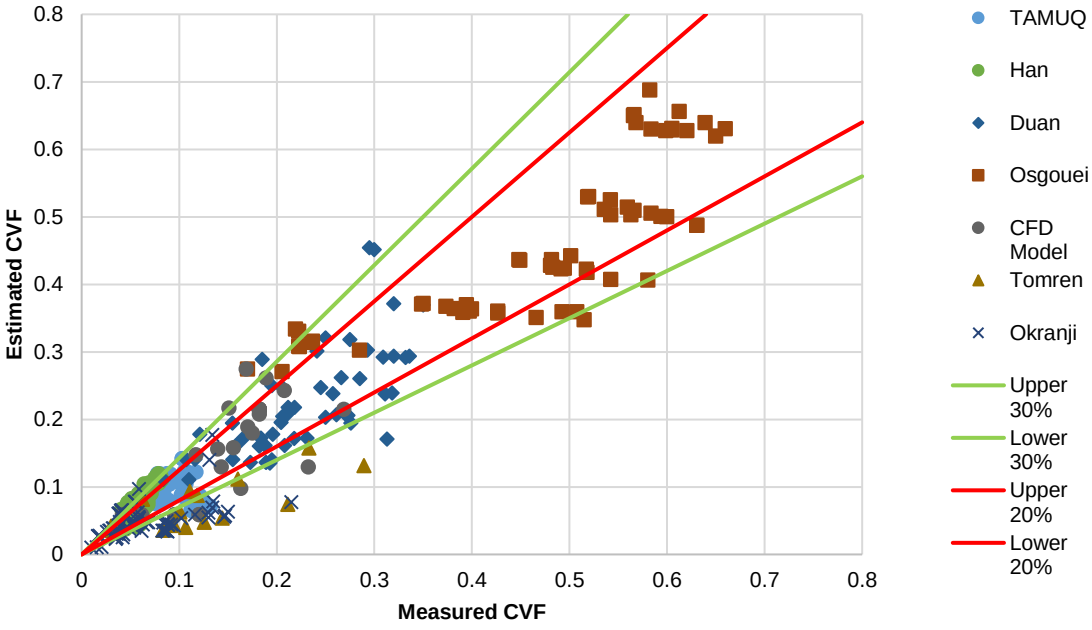

Figure 52 –Comparison of measured and estimated cuttings concertation for trained data sets after correlation simplification

To evaluate the performance of the developed model on evaluating and optimizing hole cleaning efficiency, two distinct experimental data sets (validation data sets). In addition, a comparison between our model and Duan model was conducted to check model accuracy on estimating cuttings concentration in deviated wells (see **Figures 53 & 54**). It is worth mentioning that Duan model was selected for this comparison because this model was developed for Newtonian and Non-Newtonian fluid, involved different drilling parameters in their model, and showed good accuracy on cuttings concentration estimation (Duan et al., 2006). More information about Duan model for calculating cuttings concentration can be found below. Results show that our model has a good estimation of cuttings concentration, has an adjusted R^2= 0.6, and predicts with an error ± 20 in most cases even after using two distinct experimental results. Since the presented data-driven model was developed from wide range of different drilling conditions, and utilized dimensionless parameters for scale-up application, and accurate estimation. On the other hand, Duan model has a very poor estimation of cuttings concentration with an ABE huge error. This can be attributed to the limited application of Duan model outside their experimental conditions, and setup, and henceforth cannot apply to all drilling cases.

Duan presented two correlations for estimating cuttings concentration for Newtonian and Non-Newtonian drilling fluids as below

Eq. 74 estimates cuttings concentration for water, where Fr is Froude number, is wellbore inclination in radians, D_c is the cuttings diameter, D_h is the hydraulic diameter and Ta is the Taylor number (see, **Table 17**)

$$CVF = a_0 Fr^{a_1} \theta^{a_2} \left(\frac{D_c}{D_h}\right)^{a_3} \tanh(1 + a_4 Ta) \quad \text{..... (74)}$$

Table 17 –Duan cuttings concentration correlation coefficients for water base mud

a_0	a_1	a_2	a_3	a_4
0.24	-0.715	-0.146	-0.065	-9e-6

While **Eq. 75** estimates cuttings concentration for non-Newtonian fluid (polyanionic Cellulose – PAC solutions) and cuttings concentration 0.45 mm. (i.e., **Table 18**)

$$\boldsymbol{CVF = a_0 Fr^{a_1} \theta^{a_2} \tanh(1 + a_3 Ta)} \quad \text{..... (75)}$$

Eq. 55 estimates cuttings concentration for non-Newtonian fluid (polyanionic Cellulose – PAC solutions) and cuttings concentration 0.45 mm.

Table 18 –Duan cuttings concentration correlation coefficients for Non-Newtonian Fluid and 0.45 mm cuttings size

$\boldsymbol{a_0}$	$\boldsymbol{a_1}$	$\boldsymbol{a_2}$	$\boldsymbol{a_3}$
0.18	-1.05	0.69	-3.61e-4

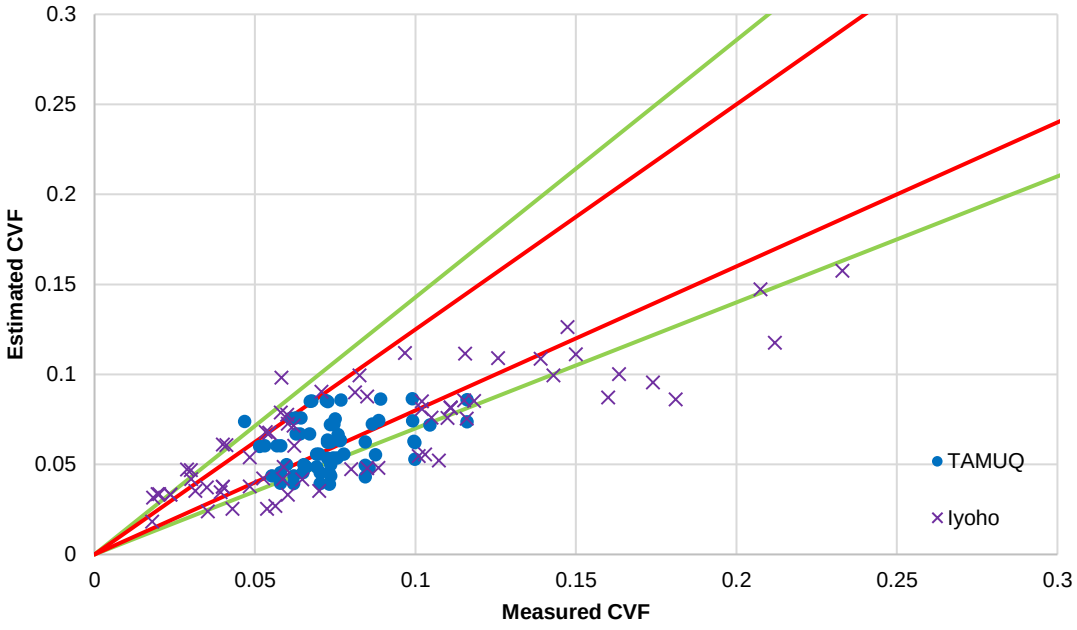

Figure 53 –Model estimation of cuttings concentration for the validation data sets

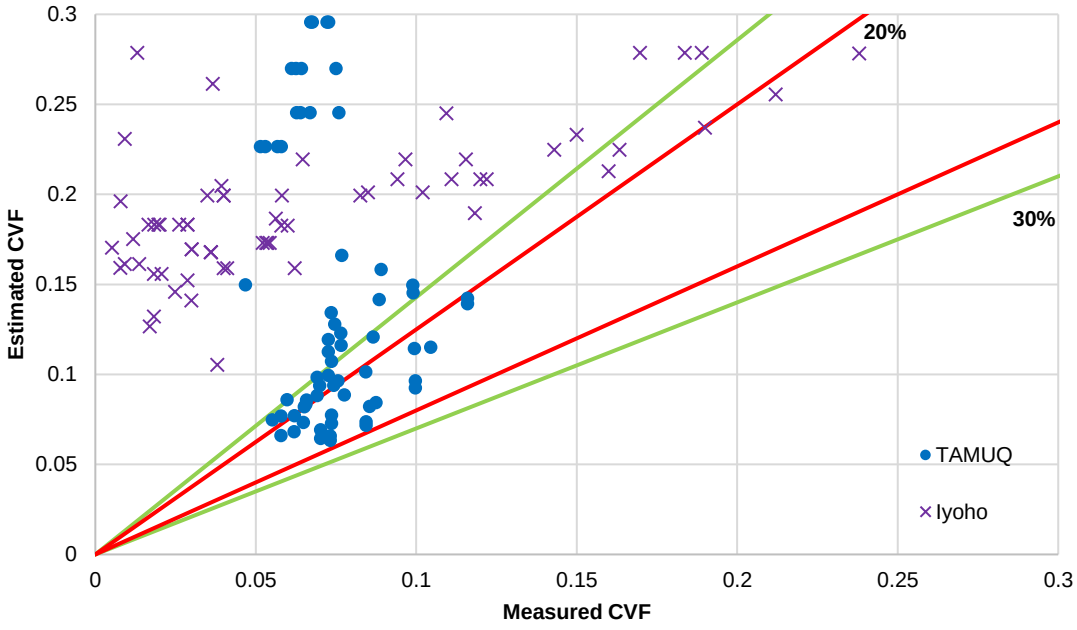

Figure 54 –Duan model for estimating cuttings concentration for the validation data sets

3. Bed Height Ratio (BHR) Correlation

Using the database developed from the open literature (more than 500 points), it was concluded that the best way to estimate bed height thickness is to use multi-linear regression statistical method. The gathered data is divided into two parts, a training sample, 80% of the collected data (Tomren et al., 1986; Duan et al., 2006; Jalukar, 1993; and Osgouei, 2010) and a validation sample, 20% of the remaining data (Iyoho, 1980; and Bassal, 1995). **Eq. 76** shows the global correlation developed by our model for estimating bed height ratio (BHR). The correlation coefficients are shown in **Table 19**. As shown in **Fig. 55**, Correlation shows good accuracy in estimating cuttings bed thickness, estimated (calculated) points from the trained data sets lay in between 10% error margin in most cases. The proposed relation between calculated and measured cuttings concentration has an adjusted R^2= 0.7 and with an average absolute error equals 9%.

$$C_{AVF} = a_0 \pi_1^{a_1} \pi_2^{a_2} \pi_3^{a_3} \pi_4^{a_4} \pi_5^{a_5} \pi_6^{a_6} \pi_7^{a_7} \pi_8^{a_8} \pi_{10}^{a_9} \pi_{11}^{a_{10}} \quad \text{.....} \quad (76)$$

Table 19 –Bed height ratio correlation coefficients

a_0	a_1	a_2	a_3	a_4	a_5
0.66	0.05	-0.33	5.07	-8.1e-6	-0.32
a_6	a_7	a_8	a_9	a_{10}	
-7.5e-8	-1.2e-6	0.04	0.001	0.88	

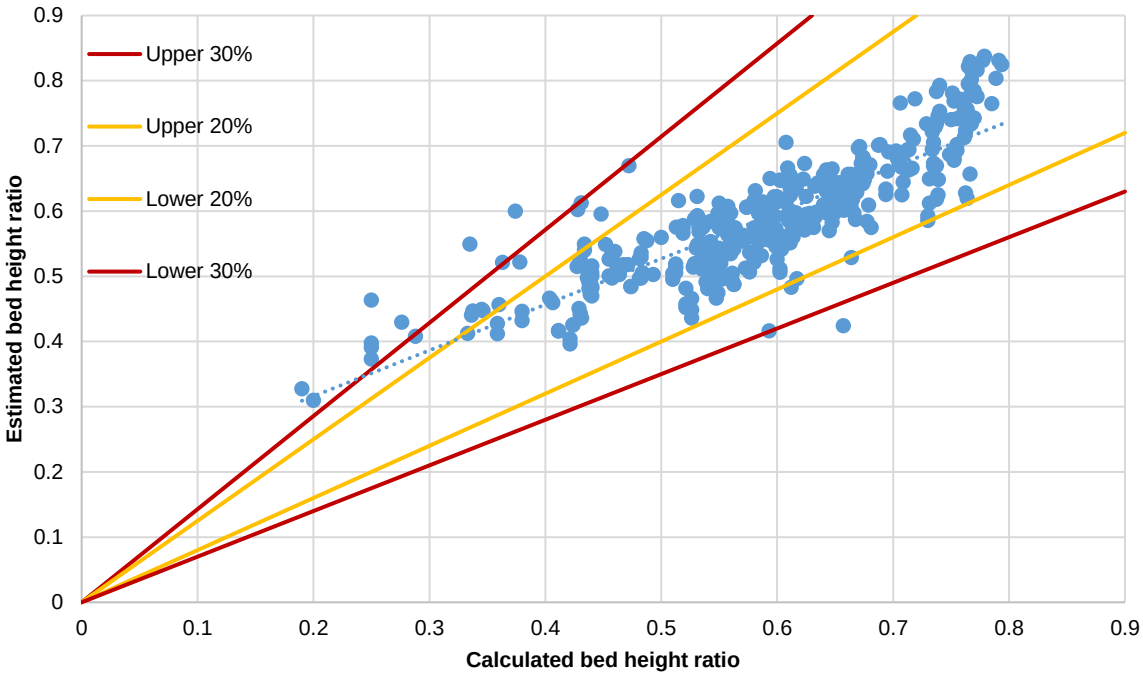

Figure 55 –Comparison of measured and estimated bed height ratio for trained data sets

After the bed height ratio correlation was developed and validated with the trained data sets, we also tried to simplify the BHR correlation for easier implementation in oil fields by neglecting variables of low coefficients value and combining between variables as shown in **Eq. 77** and **Table 20**. It was observed that the new correlation for BHR estimation has an adjusted R^2= 0.71 and with an average absolute error equals 10% as shown in **Fig. 56.**

$$\mathbf{BHR} = a_0(\pi_1\pi_8)^{a_1}(\pi_2\pi_5)^{a_2}\pi_3^{a_3}\pi_7^{a_4} \quad \text{..... (77)}$$

Table 20 –Final bed height ratio correlation coefficients

a_0	a_1	a_2	a_3	a_4
0.66	0.05	-0.33	5.07	-8.1e-6

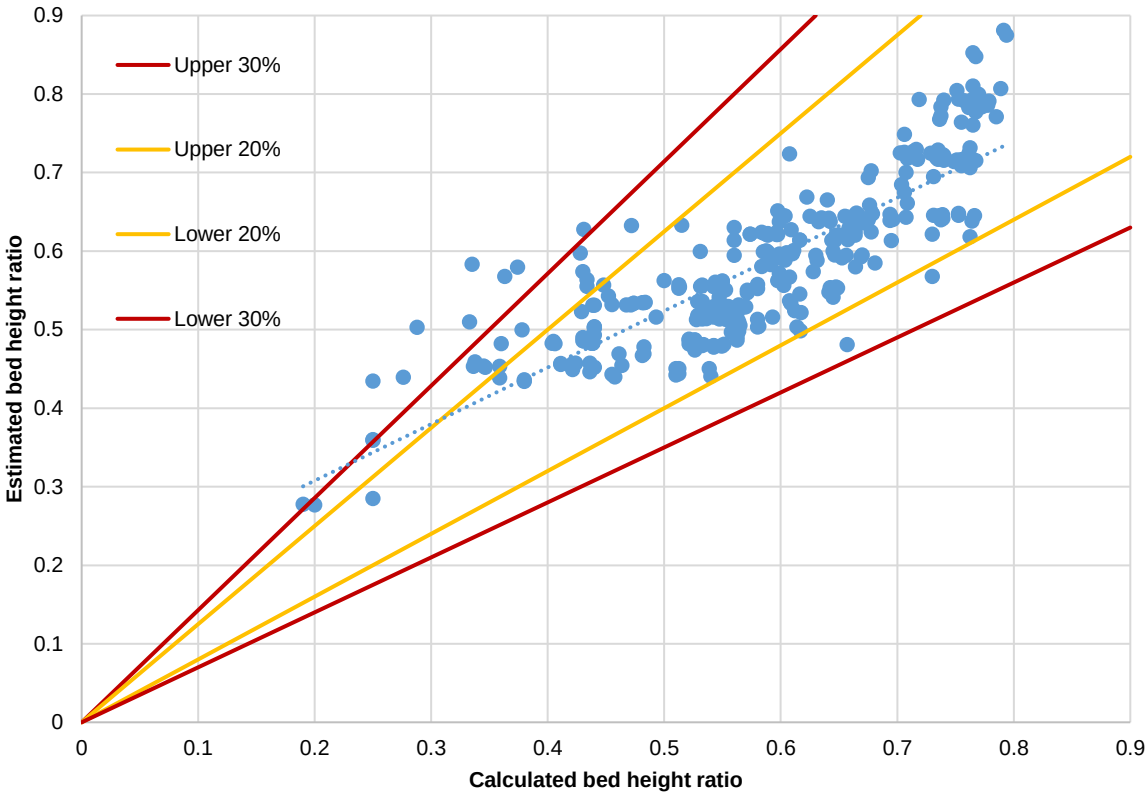

Figure 56 –Comparison of measured and estimated bed height ratio for trained data sets based on the final correlation developed after simplification

The final correlation presented in **Eq. 77** for estimating bed height thickness was validated with distinct data sets (validation data sets) as shown in **Fig. 57.** Results show that the global BHR correlation for the validation data sets has an adjusted R^2= 0.61 and with an average absolute error equals 20%.

To show the effectiveness of the developed correlation for optimizing the hole cleaning efficiency, Duan correlation (Duan, et al., 2006) for estimating cuttings bed height deposition was used to estimate bed height ratio for the validation data sets (**Eq. 78 & 79**). **Fig. 58** shows that the correlation developed by Duan has a very poor estimation of bed height ratio with an ABE = 90% and R^2 equals 0.02%. This can be attributed to the established correlations by Duan are limited to their experimental data range, and setup and henceforth cannot apply to all drilling cases.

$$\boldsymbol{BHR = a_0(a_1 + a_2 Fr)\,(1 + a_3 Ta)^{a_4} \frac{D_c}{D_h}^{a_5}} \quad \text{..... (78)}$$

Eq. 78 estimates cuttings concentration for water, where Fr is Froude number, D_c is the cuttings diameter, D_h is the hydraulic diameter and Ta is the Taylor number

Table 21 –Duan bed height ratio correlation coefficients for water base mud

a_0	a_1	a_2	a_3	a_4	a_5
0.82	1.24	-0.44	1.782e-4	-0.326	0.006

$$BHR = a_0(a_1 + a_2 Fr)\,(1 + a_3 Ta)^{a_4} \frac{D_c}{D_h}^{a_5} \quad \text{……..(79)}$$

Eq. 79 estimates cuttings concentration for non-Newtonian fluid (polyanionic Cellulose – PAC solutions).

Table 22 –Duan bed height ratio correlation coefficients for Non-Newtonian Fluid

a_0	a_1	a_2	a_3	a_4	a_5
5.1	0.31	-0.13	4.513e-3	-0.329	0.089

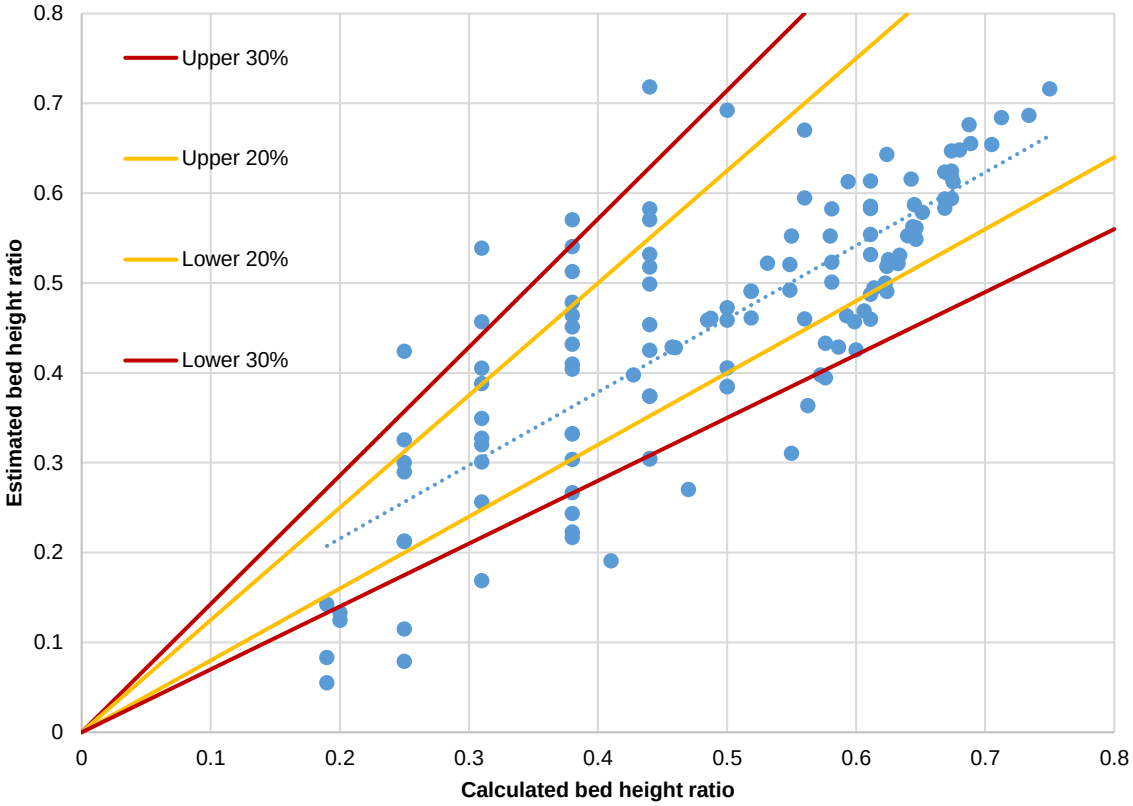

Figure 57 –Comparison of measured and estimated bed height ratio for the validation data sets (Eq. 59 correlation)

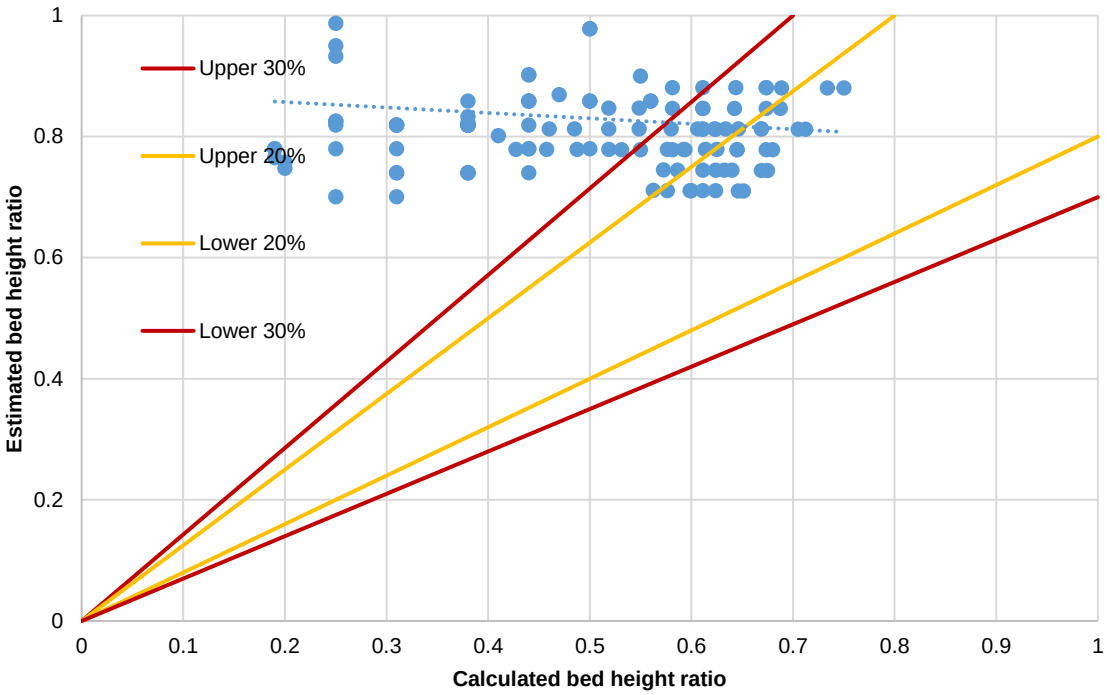

Figure 58 –Comparison of measured and estimated bed height ratio for the validation data sets based on Duan correlation

CHAPTER VI

CONCLUSIONS AND FUTURE WORK

1. Conclusions

In this study, a computational fluid dynamics (CFD) model was developed to study cuttings transport phenomena in deviated wells with Herschel Bulkley drilling fluid rheology at different ranges of operating parameters (flow rate, penetration rate, drillstring rotation, and eccentricity), wellbore configuration (hole size, wellbore inclination, and wellbore tortuosity), fluid parameters (density and rheology), and cuttings parameters (cuttings density, and size).The developed CFD model was validated with different experimental data sets and used to examine other phenomena that were not tested in our horizontal flow loop in TAMUQ flow loop. Then, data-driven models were presented for estimating cuttings concentration and stationary bed height in deviated wells based and optimizing hole cleaning efficiency during daily operations, In summary, we can conclude that:

- A reliable CFD model is a good approach to understand the fundamentals of cuttings transport under different geometric, hydrodynamic, and operating conditions and proved to be an alternative solution of conventional multiphase flow metering.
- The developed CFD code is a robust tool for optimizing hole cleaning efficiency in deviated and horizontal wells during well planning phase
- The developed models can be used as a reliable tool for simulating cuttings transport in real-time, monitoring cuttings accumulation, avoiding Non-Productive Time (NPT)

related to hole cleaning issues, and optimizing hole cleaning efficiency and drilling efficiency during daily operations. Models utilized dimensionless analysis to shift model results from lab scale to field scale, and a new dimensionless number was introduced.

- The developed data driven models were tested for different fluid rheology (Newtonian and Non-Newtonian) in well inclination (from vertical) 20-90 degrees and shows a good accuracy in estimating cuttings concentration and bed height ratio in deviated wells (estimated data points lay in between 20% error margin).
- Polyhedral mesh is an optimum meshing technique for complex geometry like spiral tortuous profile since it requires a moderate number of cells and provides high mesh quality. However, the hexahedral mesh is an optimum meshing technique for simple geometry like straight (smooth) well profile.
- Low viscosity fluids are advisable for hole cleaning in deviated holes due to the chaotic movements of turbulent flow in the annulus that enhances bed erosion and solids pick up than laminar flow. It was observed that the best approach to cleanout horizontal wells flowing under a turbulent flow regime is to keep n/K value high. In this study, in this study when fluid with n/K value approaches 15 or more shows a good cleaning effect. However, for laminar flow it is advisable to increase YP/PV ratio or decrease fluid effective viscosity for efficient hole cleaning. In this study drilling fluid with YP/PV ratio of 2 was good enough to minimize solid bed accumulation.

- The cuttings particle size of 0.004 m was determined as the critical particle size for solid-liquid flow in smooth (straight) well. A smaller particle size is easier for clean out than the larger one when the particle size is below 0.004m. On the other hand, smaller particles size is harder to clean out when the particle size is larger than 0.004m.
- Wellbore tortuosity with a small period length (2 ft.) and small spiral amplitude (1.5 inch) will not aggravate cuttings accumulation due to the generation of a secondary flow whenever the fluid entered in the spiral geometry that increases fluid velocity and prevents cuttings deposition.
- Solid-liquid flow in the spiral geometry is accompanied by high annular pressure loss due to the friction between high-velocity fluid and walls and an increase in the collision between particles themselves and particles & walls in the spiral geometry.
- The shorter motor bit to bend distance is preferred in drilling lateral sections since cuttings accumulation aggravates with the increase of the spiral period length due to reduction in the spiral swirl effect and reduction in the fluid dynamic force required to circulate cuttings outside the wellbore.
- Higher cuttings accumulation was observed in the crest plane of the spiral profile compared to the trough plane in the same geometry.
- It is recommended to use motors bent housing with less bend angle while drilling lateral sections because a large bend in the motor assembly will apply a continuous large side force on the bit that can increase the spiral period length and aggravate cuttings deposition.

- It was observed that drillstring rotation from 0-200 RPM is the most critical range for efficient hole cleaning in straight and spiral tortuous profile and increasing RPM above 200 will have a marginal impact on improving cuttings transport.
- Drilling flow rate and drillstring rotation are the major factors that enhance hole cleaning and bed erosion in straight and/or spiral hole profile. On the other hand, holely enlargement has a huge adverse effect on the fluid carrying capacity due to reduction of fluid velocity in the enlarge section and cuttings concentrate.
- The annular eccentricity has a negative impact on cuttings removal in spiral holes, because it reduces the mixture velocity in the narrow parts and narrows the flow area available for cuttings transportation.
- Cuttings deposition aggravates with high drilling rate of penetration due to reduction in cuttings kinetic energy and the inability of mud to circulate cuttings outside the hole.
- Poor hole cleaning signs were observed with increasing cuttings density and wellbore inclination between 50-70 degrees
- In this study, cuttings size between 0.006-0.008 m is considered the critical particle size that is the hardest to be cleaned out in the spiral profile. Below this critical particle size, the smaller particle size is easier to clean out than the larger one. On the other hand particles sizes above the critical size, fine particles are harder to be transported.

2. Future Work

The possibilities of future work are seemingly limitless with this topic. Thus, the author encourages future researchers:

1. To extend the application of the presented CFD model to foam drilling application (air, liquid, and gas flow), and high-pressure high temperature (HPHT) drilling fluids for deep wells. Cuttings transport by gas and liquid flow (three-phase flow) or under HPHT drilling fluids is expected to be different from solid-liquid two-phase flow discussed in this dissertation.
2. To assess different data-driven models such as statistical regression techniques, machine learning algorithms such as neural network, support vector mechanisms,…etc. and to select the optimum technique for estimating cuttings concentration and bed height deposition that can optimize hole cleaning efficiency and simulate reality.
3. Although a lot of research was conducted on investigating the fundamentals of cuttings (solid) transport in drilling fluids (liquid), limited research was published to investigate the dirtiest hole possible concept (Dupriest et al., 2010). Drilling operators aim to drill the well with the maximum rate of penetration and equilibrium bed height that will not result in ECD or pack-offs above well integrity. Thus, the objective is not to drill the cleanest hole (as always published by literature) but to drill with the dirtiest hole possible. Researchers can use different techniques such as experimental work and different modeling techniques to investigate this concept at different drilling conditions and help in redesigning the drilling process. Identifying

the dirtiest hole possible points at different drilling conditions will help the drilling operators to accurately estimate the time required for cleaning the wellbore with an equilibrium cuttings bed height below well integrity, will enable a faster drilling penetration rate, and will save a lot of drilling cost.

4. To develop a hybrid model combining physics-based model (mechanistic model and CFD) and data-driven models (regression and machine learning techniques) using a rule-based stochastic decision-making algorithm to prevent the disadvantages of using purely data-driven or mechanistic models and provide a robust model for accurate prediction of cuttings transport phenomena and hole cleaning related issues.

REFERENCES

1. Abughaban, Mahmoud, 2017. Extending the reach of drilling: better wellbore trajectory and torque & drag models. Doctoral dissertation. University of Colorado School of Mines, USA.
2. Akhshik, S., Behzad, M., & Rajabi, M. 2015. CFD–DEM approach to investigate the effect of drill pipe rotation on cuttings transport behavior. Journal of Petroleum Science and Engineering, 127, 229-244.
3. Adaze, E., Al-Sarkhi, A., Badr, H.M., 2019. Current status of CFD modeling of liquid loading phenomena in gas wells: a literature review. J Petrol Explor Prod Technol 9, 1397–1411.
4. Azar, J.J. and R.A., Sanchez. 1997. Important Issues in Cuttings Transport for Drilling Direction Wells. SPE-39020-MS presented at the Fifth Latin American and Caribbean Petroleum Engineering Conference and Exhibition, Rio de Janeiro, Brazil, 30 August – 3 September.
5. Bang, J., Jegbefume, O., Ledroz, A., & Thompson, J., 2015. Wellbore Tortuosity Analysed by a Novel Method May Help to Improve Drilling, Completion, and Production Operations. SPE-173103-MS presented at the SPE/IADC Drilling Conference and Exhibition, London, United Kingdom, 17-19 March.
6. Bellay, G., Al-Waheed, H., and Audah, T., 1996. Cyclic borehole effects in deviated wells. SPE 36288-MS presented at the 7th Abu Dhabi International Petroleum Exhibition and Conference, Abu Dhabi, UAE, 13-16 October.

7. Berger, SA & Talbot, L & Yao, L. (2003). Flow in Curved Pipes. Annual Review of Fluid Mechanics. Vol. 15. 461-512.
8. Busch, A., Werner, B., & Johansen, S. T. 2020. Cuttings Transport Modeling-Part 2: Dimensional Analysis and Scaling. SPE-198907-PA. SPE Drilling and Completion Journal. March
9. Chen, D. C.-K., Gaynor, T., Comeaux, B., & Glass, K., 2002. Hole Quality: Gateway to Efficient Drilling. OTC-14277-MS presented at Offshore Technology Conference, Houston, Texas, USA, 6-9 May.
10. Dupriest, F. E., Elks, W. C., Ottesen, S., Pastusek, P. E., Zook, J. R., & Aphale, C., 2010. Borehole Quality Design and Practices to Maximize Drill Rate Performance. SPE-134580-MS presented at SPE Annual Technical Conference and Exhibition in Florence, Italy, 19-22 September.
11. Emmanuel I. Epelle, Dimitrios I. Gerogiorgis. 2017. A multiparametric CFD analysis of multiphase annular flows for oil and gas drilling applications. Journal of Computers & Chemical Engineering. V. 106, 645-661.
12. Emmanuel I. Epelle, Dimitrios I. Gerogiorgis. 2018. CFD modelling and simulation of drill cuttings transport efficiency in annular bends: Effect of particle sphericity. Journal of Petroleum Science and Engineering. V.170, 992-1004.
13. Ford, J. T., Peden, J. M., Oyeneyin, M. B., Gao, E., & Zarrough, R., 1990. Experimental Investigation of Drilled Cuttings Transport in Inclined Boreholes. SPE-20421-MS presented at SPE Annul Technical Conference and Exhibition. New Orleans, LA, September 23-26.

14. Gaynor, T. M., Irvine, G. T., Boulton, R., Gilchrist, D. A., & Lane, I., 1999. Step Change in Drilling Efficiency in Mature North Sea Fields From New Motor and Bit Drilling System. SPE-56936-MS presented at the Offshore Europe Oil and Gas Exhibition and Conference held in Aberdeen, United Kingdom, 7-10 September.
15. Gaynor, T., Chen, D. C.-K., Maranuk, C., & Pruitt, J., 2000. An Improved Steerable System: Working Principles, Modeling, and Testing. SPE-63248-MS presented at the SPE Annual Technical Conference and Exhibition held, Dallas, Texas, 1–4 October.
16. Gaynor, T. M., Chen, D. C.-K., Stuart, D., & Comeaux, B., 2001. Tortuosity versus Micro-Tortuosity - Why Little Things Mean a Lot. SPE-67818-MS presented at IADC/SPE Drilling Conference in Amsterdam, The Netherlands, 27 February- 1 March.
17. Gaynor, T., Hamer, D., Chen, D. C.-K., & Stuart, D., 2002. Quantifying Tortuosities by Friction Factors in Torque and Drag Model. SPE-77617-MS presented at the SPE Annual Technical Conference and Exhibition, San Antonio, Texas, 29 September -2 October.
18. Gidaspow, D., (1994). Multiphase Flow And Fluidization: Continuum and Kinetic Theory Descriptions. Academic Press, New York.
19. Hemphill, T., & Larsen, T. I., 1996. Hole-Cleaning Capabilities of Water- and Oil-Based Drilling Fluids. A Comparative Experimental Study. SPE-26328-PA. SPE Drilling and Completion. December.

20. Hicham, F., Ahmed, H., Mohammad Azizur, R., Ibrahim, H., Titus, N. O., & Ahmed, H. (2020). The Impact of Orbital Motion of Drill Pipe on Pressure Drop of Non-Newtonian Fluids in Eccentric Annulus. Journal of Advanced Research in Fluid Mechanics and Thermal Sciences, 65(1), 94-108.
21. Hopkins, C.J., and R.A. Leicksenring, 1999. Reducing the Risk of Stuck Pipe in The Netherlands. SPE-29422-MS Paper presented at the SPE/IADC Drilling Conference, Amsterdam, Netherlands, 28 February-2 March.
22. Hussein, M.M., Al-Sarkhi, A., Badr, H.M., 2019. CFD modeling of liquid film reversal of two-phase flow in vertical pipes. J Petrol Explor Prod Technol 9, 3039–3070.
23. Iyoho Aniekan, 1980. Drilled-Cuttings Transport by Non-Newtonian Drilling Fluids through Inclined, Eccentric Annuli. Doctor dissertation, University of Tulsa, USA.
24. Janwadkar, S. S., Hummes, O., Peter, A., Freeman, M. A., Privott, S. A., Greene, D. M., & Loesel, C. W., 2011. Overcoming Challenges for Drilling High-Dogleg-Severity Curves. SPE-139773-MS presented at SPE/IADC Drilling Conference and Exhibition in Amsterdam, Netherlands, 1-3 March.
25. Kamyab, M., & Rasouli, V. 2016. Experimental and numerical simulation of cuttings transportation in coiled tubing drilling. Journal of Natural Gas Science and Engineering, 29, 284-302
26. Khaled Mohamed, Rahman Aziz, Hassan Ibrahim, Sultan Rasel, and Hasan Rashid, 2020a. Computational Fluid Dynamics Simulation of the Transient Behavior of

Liquid Loading in Gas Wells. OMAE 2020-18220 presented at the 39th International Conference on Ocean, Offshore and Arctic Engineering, Virtual, Online, August 3-7.

27. Khaled Mohamed, Hasan Rashid, Rahman Aziz, Hassan Ibrahim, and Priyank Maheshwari, 2020b. CFD Approach to Investigate the Effect of Mud Rheology on Cuttings Removal in Horizontal Wells. AADE-20-FTCE-SPP-08 presented at the 2020 AADE Fluids Technical Conference and Exhibition, Houston, Texas, April 14-15.
28. Larsen, T.I., 1990. A Study of the Critical Fluid Velocity in Cuttings Transport. MS thesis, University of Tulsa, Tulsa, Oklahoma,USA., 1990.
29. Larsen, T., Pilehvari, A., & Azar, J., 1997. Development of a new cuttings-transport model for high angle wellbores including horizontal wells. SPE Drilling & Completion. V.12 No.02, 129-136.
30. Lubinski, A., and Woods H. B., 1953. Factors affecting the angle of Inclination and Dog-Legging in Rotary Bore Holes., API-53-222 presented at the spring meeting of the Mid-Continent District, Division of Production, Tulsa, March.
31. Mason, C. J., & Chen, D. C.-K., 2005. The Perfect Wellbore! SPE-95279-MS presented at SPE Annual Technical Conference and Exhibition in Dallas, Texas, USA, 9-12.
32. MacDonald, G. C., Lubinski, 1951. A. Smooth-Hole Drilling in Crooked-Hole Country. Drilling and Production Practice, API 1951.
33. Madlener K, Frey B, Ciezki HK, 2009.Generalized Reynolds number for non-Newtonian fluids.” Prog Propuls Phys, V.1, 237–250.

34. Marck, Julien, 2015. A Nonlinear Dynamical Model of Borehole Spiraling. Doctoral dissertation. University of Minnesota, USA.

35. Martins, A. L., Sa, C. H. M., Lourenco, A. M. F., & Campos, W. 1996. Optimizing Cuttings Circulation in Horizontal Drilling , SPE-35341-MS presented at the international Petroleum Conference and Exhibition of Mexico, Villahemosa, Mexico, March 5-7.

36. Mei, R., Klausner, J., 1994. Shear lift force on spherical bubbles. Int. J. Heat Fluid Flow 15 (1), 62–65

37. Mitchell, Robert F., and Miska, Stefan Z., 2010. Fundamentals of Drilling Engineering. Society of Petroleum Engineers (SPE) book. Richardson, Texas, United States, PP-555-557.

38. Mohammadzadeh, K., Hashemabadi, S. H., & Akbari, S. 2016. CFD simulation of viscosity modifier effect on cutting transport by oil based drilling fluid in wellbore. Journal of Natural Gas Science and Engineering, 29, 355-364

39. Monterrosa, L. C., Rego, M. F., Zegarra, E., & Lowdon, R., 2016. Statistical Analysis Between Different Surveying Instruments to Understand the Reliability of MWD/RSS High Resolution Surveys and its Effect in Well Trajectory Characterization. SPE-178830-MS presented at IADC/SPE Drilling Conference and Exhibition in Fort Worth, Texas, USA, 1-3 March.

40. Moraga, F., Bonetto, F., Lahey, R., 1999. Lateral forces on spheres in turbulent uniform shear flow. Int. J. Multiphase Flow 25 (6), 1321–1372.

41. Ofei, T. N., Irawan, S., & Pao, W. 2014. CFD method for predicting annular pressure losses and cuttings concentration in eccentric horizontal wells. Journal of Petroleum Engineering, 2014.
42. Ofei, T.N. and Alhemyari,S.A. 2015. Computational fluid dynamics simulation of the effect of drill pipe rotation on cuttings transport in horizontal wellbores using a Newtonian fluid, in: International Field Exploration and Development Conference (IFEDC 2015), IET, 2015.
43. Okrajni, S., & Azar, J. J., 1986. The Effects of Mud Rheology on Annular Hole Cleaning in Directional Wells. SPE-14178-PA. SPE Drilling Engineering, August 1986.
44. Osgouei, R., 2010. Determination of cuttings transport properties of gasified drilling fluids. Doctoral dissertation, Middle East Technical University, Turkey.
45. Ozbayoglu, M.E., Saasen, A., Sorgun, M., Svanes, K., 2008. Effect of pipe rotation on hole cleaning for water-based drilling fluids in horizontal and deviated wells. SPE- 114965-MS presented at the IADC/SPE Asia Pacific Drilling Technology Conference and Exhibition. Jakarta, Indonesia, 25–27 August.
46. Ozbayoglu, M.E., Saasen, A., Sorgun, M., Svanes, K., 2010. Critical Fluid Velocities for Removing Cuttings Bed Inside Horizontal and Deviated Wells. Petroleum Science and Technology. V.28:6, 594-602
47. Omid Heydari, Eghbal Sahraei, Pål Skalle, 2017. Investigating the impact of drillpipe's rotation and eccentricity on cuttings transport phenomenon in various

horizontal annuluses using computational fluid dynamics (CFD). Journal of Petroleum Science and Engineering V. 156, 801-813.

48. Pang, B., Wang, S., Liu, G., Jiang, X., Lu, H., Li, Z., 2018. Numerical prediction of flow behavior of cuttings carried by Herschel-Bulkley fluids in horizontal well using kinetic theory of granular flow. Powder Technol. V.329, 386–398.
49. Patankar, S.V., Spalding, D.B., 1972. A calculation procedure for heat, mass and momentum transfer in three-dimensional parabolic flows. Int. J. heat mass Transf. 15 (10), 1787–1806.
50. Peden, J.M., Ford, J.T., Oyeneyin, M.B., 1990. Comprehensive experimental investigation of drilled cuttings transport in inclined wells including the effects of rotation and eccentricity. SPE-20925-MS presented at the European Petroleum Conference. Hague, Netherlands, 22-24 October, 1990.
51. Pedley, T. J. 1980. The Fluid Mechanics of Large Blood Vessels, Chap. 4, pp. 160-234. Cambridge Univ. Press.
52. Piroozian, Ali, Ismail, Issham, Yaacob, Zulkefli, Babakhani, Parham, Ismail, Ahmad Shamsul Izwan, 2012. Impact of drilling fluid viscosity, velocity and hole inclination on cuttings transport in horizontal and highly deviated wells. Journal of Petroleum Exploration and Production Technology. V.2, 149-156.
53. S. Menand, 2013. Borehole Tortuosity Effect on Maximum Horizontal Drilling Length Based on Advanced Buckling Modeling. AADE-13-FTCE-21 presented at AADE National Technical Conference and Exhibition, Cox Convention Center, Oklahoma City, USA, February 26-27.

54. Saffman, P., 1965. The lift on a small sphere in a slow shear flow. J. Fluid Mech. 22 (02), 385–400.

55. Sang-Mok Han, Young-Kyu Hwang, Nam-Sub Woo, Young-Ju Kim, 2010. Solid–liquid hydrodynamics in a slim hole drilling annulus. Journal of Petroleum Science and Engineering. V.70, issue (3-4), 308-319.

56. Shih, T. H., Liou, W. W., Shabbir, A., Yang, Z., & Zhu, J. (1995). A new k-ϵ eddy viscosity model for high reynolds number turbulent flows. Computers & fluids, 24(3), 227-238

57. Sorgun Mehmet, 2010. Modeling of Newtonian Fluids and Cuttings Transport Analysis in High Inclination Wellbores with Pipe Rotation. Doctor dissertation. Middle East Technical University, Turkey, August.

58. Stuart, D., Hamer, C. D., Henderson, C., Gaynor, T., & Chen, D.-K., 2003. New Drilling Technology Reduces Torque and Drag by Drilling a Smooth and Smooth Wellbore. SPE-79919-MS presented at SPE/IADC Drilling Conference, Amsterdam, Netherlands, 19–21 February.

59. T.-H. Shih,W.W. Liou, A. Shabbir, Z. Yang, and J. Zhu. 1995. A New κ-ε Eddy-Viscosity Model for High Reynolds Number Turbulent Flows - Model Development and Validation. Computers Fluids. 24(3). 227–238.

60. Tang, Lingdi & Tang, Yue & Parameswaran, Siva. (2016). A numerical study of flow characteristics in a helical pipe. Advances in Mechanical Engineering, Vol. 8.

61. Sun, X., Wang, K., Yan, T., Shao, S., & Jiao, J. (2014). Effect of drillpipe rotation on cuttings transport using computational fluid dynamics (CFD) in complex structure wells. Journal of Petroleum Exploration and Production Technology, 4(3), 255-261
62. A Ramadan, P Skalle, S.T Johansen. 2003. A mechanistic model to determine the critical flow velocity required to initiate the movement of spherical bed particles in inclined channels. Chemical Engineering Science. Vol. 5(10), 2153-2163.
63. Rasul, G., Qureshi, M. F., Ferroudji, H., Butt, S., Hasan, R., Hassan, I., & Rahman, M. A. 2020. Analysis of Cuttings Transport and Flow Pattern in Nearly Horizontal Extended Reach Well. 71 (2), 69 – 86
64. Rubiandini R.S., Rudi. 1999. Equation for Estimating Mud Minimum Rate for Cuttings Transport in an Inclined-Until-Horizontal Well. SPE-57541-MS presented at the SPE/IADC Middle East Drilling Technology Conference, Abu Dhabi, United Arab Emirates, 8-10 November.
65. Tobenna, U.C., 2010. Hole Cleaning and Hydraulics, Master Degree Thesis, University of Stavanger, Norway.
66. Tomren, P. H., Iyoho, A. W., & Azar, J. J., 1986. Experimental Study of Cuttings Transport in Directional Wells. SPE-12123-PA. SPE Drilling and Completion, February 1.
67. Van Wachem, B.G.M., Almstedt, A.E., 2003. Methods for multiphase computational fluid dynamics. Chem. Eng. J. 96 (1), 81–98

68. Walker, S., & Li, J., 2000. The Effects of Particle Size, Fluid Rheology, and Pipe Eccentricity on Cuttings Transport. SPE-60755-MS presented at the SPE/ICoTA Coiled Tubing Round table, Houston, Texas, 5–6 April.

69. Webster, D. R., and Humphrey, J. A. C. 1993. "Experimental Observations of Flow Instability in a Helical Coil (Data Bank Contribution)." ASME. J. Fluids Eng. September 1993; 115(3): 436–443.

70. Wilson, K. C. and J. K. P. Tse., 1984. Deposition Limit for Coarse-Particle Transport in Inclined Pipes, Paper D1, Hydro transport9 presented at the 9th International Conference on the Hydraulic Transport of Solids in Pipes, Rome, Italy, October 17-19.

71. Yan, T., Wang, K., Sun, X., Luan, S., & Shao, S. (2014). State-of-the-art cuttings transport with aerated liquid and foam in complex structure wells. Renewable and Sustainable Energy Reviews, 37, 560-568.

72. Yanuar, Yanuar & Waskito, Kurniawan & Gunawan, Gunawan & Budiarso, Budiarso.(2015. Drag Reduction and Velocity Profiles Distribution of Crude Oil Flow in Spiral Pipes. International Review of Mechanical Engineering (IREME), Vol 9.

73. Yanuar, Yanuar & Waskito, Kurniawan & Mau, Sealtial & Wulandari, Winda & Sari, Sri. 2017. Helical twisted effect of spiral pipe in generating swirl flow for coal slurries conveyance. Jurnal Teknologi, Vol. 79 No. 7-3

74. Yeu, W. J., Katende, A., Sagala, F., & Ismail, I. (2019). Improving hole cleaning using low density polyethylene beads at different mud circulation rates in different hole angles. Journal of Natural Gas Science and Engineering, 61, 333-343
75. Yunus AC, Cimbala JM, 2006. Fluid mechanics fundamentals and applications, International edn. McGraw Hill Publication, NewYork.
76. Massie, G. W., Castle-Smith, J., Lee, J. W., & Ramsey, M. S. (1995). Amocos training initiative reduces wellsite drilling problems. Petroleum Engineer International, 67(3).
77. Sun, X., Wang, K., Yan, T., Shao, S., & Jiao, J. (2014). Effect of drillpipe rotation on cuttings transport using computational fluid dynamics (CFD) in complex structure wells. Journal of Petroleum Exploration and Production Technology, 4(3), 255-261.
78. Ozbayoglu, M. E., Saasen, A., Sorgun, M., & Svanes, K. (2008, January). Effect of pipe rotation on hole cleaning for water-based drilling fluids in horizontal and deviated wells. In IADC/SPE Asia Pacific Drilling Technology Conference and Exhibition. Society of Petroleum Engineers.
79. Li, J., & Luft, B. (2014, December). Overview solids transport study and application in oil-gas industry-theoretical work. In International petroleum technology conference. International Petroleum Technology Conference.
80. Shao, B., Yan, Y., Yan, X., & Xu, Z. (2019). A study on non-spherical cuttings transport in CBM well drilling by coupled CFD-DEM. Engineering Applications of Computational Fluid Mechanics, 13(1), 579-590.

81. Awad, A. M., Hussein, I. A., Nasser, M. S., Karami, H., & Ahmed, R. (2021). CFD modeling of particle settling in drilling fluids: Impact of fluid rheology and particle characteristics. Journal of Petroleum Science and Engineering, 199, 108326.
82. Ferroudji, H., Hadjadj, A., Haddad, A., & Ofei, T. N. (2019). Numerical study of parameters affecting pressure drop of power-law fluid in horizontal annulus for laminar and turbulent flows. Journal of Petroleum Exploration and Production Technology, 9(4), 3091-3101.
83. Pang, B., Wang, S., Jiang, X., & Lu, H. (2019). Effect of orbital motion of drill pipe on the transport of non-Newtonian fluid-cuttings mixture in horizontal drilling annulus. Journal of Petroleum Science and Engineering, 174, 201-215.
84. Ferroudji, H., Hadjadj, A., Ofei, T. N., & Rahman, M. A. (2020). The effect of orbital motion and eccentricity of drill pipe on pressure gradient in eccentric annulus flow with Newtonian and non-Newtonian fluids. Progress in Computational Fluid Dynamics, an International Journal, 20(4), 238-247.
85. Sanchez, R. A., Azar, J. J., Bassal, A. A., & Martins, A. L. (1997, January). The effect of drillpipe rotation on hole cleaning during directional well drilling. In SPE/IADC drilling conference. Society of Petroleum Engineers.
86. Duan, M., Miska, S. Z., Yu, M., Takach, N. E., Ahmed, R. M., & Zettner, C. M. (2006, January). Transport of small cuttings in extended reach drilling. In International Oil & Gas Conference and Exhibition in China. Society of Petroleum Engineers.

87. Chen, Z., Ahmed, R. M., Miska, S. Z., Takach, N. E., Yu, M., Pickell, M. B., & Hallman, J. H. (2007). Experimental study on cuttings transport with foam under simulated horizontal downhole conditions. SPE Drilling & Completion, 22(04), 304-312.
88. Bilgesu, H. I., Mishra, N., & Ameri, S. (2007, October). Understanding the effect of drilling parameters on hole cleaning in horizontal and deviated wellbores using computational fluid dynamics. In Eastern Regional Meeting. OnePetro.
89. Mohammadzadeh, K., Hashemabadi, S. H., & Akbari, S. (2016). CFD simulation of viscosity modifier effect on cutting transport by oil based drilling fluid in wellbore. Journal of Natural Gas Science and Engineering, 29, 355-364.
90. Epelle, E. I., & Gerogiorgis, D. I. (2017). A multiparametric CFD analysis of multiphase annular flows for oil and gas drilling applications. Computers & Chemical Engineering, 106, 645-661.
91. Hakim, H., Katende, A., Sagala, F., Ismail, I., & Nsamba, H. (2018). Performance of polyethylene and polypropylene beads towards drill cuttings transportation in horizontal wellbore. Journal of Petroleum Science and Engineering, 165, 962-969.
92. Rasul, G., Qureshi, M. F., Ferroudji, H., Butt, S., Hasan, R., Hassan, I., & Rahman, M. A. (2020). Analysis of Cuttings Transport and Flow Pattern in Nearly Horizontal Extended Reach Well. Journal of Advanced Research in Fluid Mechanics and Thermal Sciences, 71, 69-86.
93. Qureshi, M. F., Ali, M. H., Ferroudji, H., Rasul, G., Khan, M. S., Rahman, M. A., ... & Hassan, I. (2021). Measuring solid cuttings transport in Newtonian fluid across

horizontal annulus using electrical resistance tomography (ERT). Flow Measurement and Instrumentation, 77, 101841.

94. Martins, A. L., & Santana, C. C. (1992, January). Evaluation of cuttings transport in horizontal and near horizontal wells-A dimensionless approach. In SPE Latin America Petroleum Engineering Conference. Society of Petroleum Engineers.
95. Kamp, A. M., & Rivero, M. (1999, January). Layer modeling for cuttings transport in highly inclined wellbores. In Latin American and Caribbean Petroleum Engineering Conference. Society of Petroleum Engineers.
96. Cho, H., Shah, S. N., & Osisanya, S. O. (2000, January). A three-layer modeling for cuttings transport with coiled tubing horizontal drilling. In SPE Annual technical conference and exhibition. Society of Petroleum Engineers.
97. Li, Y., Bjorndalen, N., & Kuru, E. O. (2004, January). Numerical modelling of cuttings transport in horizontal wells using conventional drilling fluids. In Canadian International Petroleum Conference. Petroleum Society of Canada.
98. Sun, X., Wang, K., Yan, T., Shao, S., & Jiao, J. (2014). Effect of drillpipe rotation on cuttings transport using computational fluid dynamics (CFD) in complex structure wells. Journal of Petroleum Exploration and Production Technology, 4(3), 255-261.
99. Song, X., Xu, Z., Wang, M., Li, G., Shah, S. N., & Pang, Z. (2017). Experimental study on the wellbore-cleaning efficiency of microhole-horizontal-well drilling. SPE Journal, 22(04), 1-189.

100. Pandya, S., Ahmed, R., & Shah, S. (2020). Wellbore Cleanout in Inclined and Horizontal Wellbores: The Effects of Flow Rate, Fluid Rheology, and Solids Density. SPE Drilling & Completion, 35(01), 48-68.

101. Erge, O., & van Oort, E. (2020). Modeling the effects of drillstring eccentricity, pipe rotation and annular blockage on cuttings transport in deviated wells. Journal of Natural Gas Science and Engineering, 79, 103221.

102. Zhu, X., Shen, K., & Li, B. (2021). Investigation: Cutting Transport Mechanism in Inclined Well Section under Pulsed Drilling Fluid Action. Energies, 14(8), 2141.

103. Yeo, L., Feng, Y., Seibi, A., Temani, A., & Liu, N. (2021). Optimization of hole cleaning in horizontal and inclined wellbores: A study with computational fluid dynamics. Journal of Petroleum Science and Engineering, 108993.

104. Ozbayoglu, E., Ozbayoglu, M., Ozdilli, B. G., & Erge, O. (2021). Optimization of Flow Rate and Pipe Rotation Speed Considering Effective Cuttings Transport Using Data-Driven Models. Energies, 14(5), 1484.

105. Huque, Mohammad Mojammel, Imtiaz, Syed, Zendehboudi, Sohrab, Butt, Stephen, Rahman, Mohammad Azizur, and Priyank Maheshwari. (2021). Experimental Study of Cuttings Transport with Non-Newtonian Fluid in an Inclined Well Using Visualization and Electrical Resistance Tomography Techniques. SPE Drill & Compl (2021).